UNIVERSITY OF BIRMINGHAM

The Fabrication of Aluminium-Carbon Nanotube Metal Matrix Composites

Thesis submitted in accordance with the requirements of the University of Birmingham for the degree of Master of Philosophy

In

School of Metallurgy and Materials

By

Adam Powell

July 2013

Dedication

To my family

Acknowledgements

First and foremost, I would like to express my sincere gratitude to my supervisor Dr. Bill Griffiths for his support, patience and guidance during my study. His knowledge and experience have been of great benefit and help. I would also like to thank Dr. KeeHyun Kim for his advice.

In addition, I am grateful to Mr. Nick Harrison for his assistance and advice during my study and his help during my laboratory experiments.

Finally I would like to thank my family for their continued support.

Abstract

A range of multi-walled carbon nanotubes of various purities were used to produce aluminium-carbon nanotube metal matrix composite specimens. Composite preform powders were prepared by multi-axial mixing, known as turbula mixing, for 8 hours and high energy ball milling for 1 hour and for 4 hours, mixing methods were compared to derive differences. Composite specimens were then prepared using a number of techniques: cold compaction, sintering and casting. These processing techniques were contrasted in an attempt to define optimum processing route. Equal Channel Angular Pressing (ECAP) was also investigated as a means of fabricating composite specimens and achieving uniform carbon nanotube distribution. Specimens from all methods were tested for density and hardness in order to determine effects of processing route on carbon nanotube distribution within the final composite. They were also examined using scanning electron microscopy. It was found that high grade carbon nanotubes produced the best density and hardness properties, and that high energy ball milling was superior to turbula mixing for preparation of composite preforms. Ball milling for 4 hours produced the most consistent composite properties. Equal Channel Angular Pressing (ECAP) was found to produce a consistent improvement in both hardness and density of composite samples compared to cold compaction. Results from sintered specimens showed further improvement and these specimens showed the highest hardness and most densification of all samples investigated in this report. An attempt to produce cast composite specimens showed numerous issues with distribution in the melt. Composite castings did not achieve comparable properties to other processing techniques.

Contents

List of Figures

List of Tables

List of Equations

Chapter 1

Introduction

1.1 Overview of Composite Theory and Carbon Nanotubes

Composite materials combine a ductile formable matrix with a high strength, high stiffness reinforcement filler phase. These materials can achieve mechanical properties comparable to wrought alloys whilst also providing a significant reduction in weight and increased formability. Carbon Nanotubes (CNTs) are graphene tubes with high strength and stiffness properties as well as good thermal and electrical conductivity (Agarwal et al., 2011). These materials have the potential to produce formable, high strength composite structures. Possible future application areas for these materials include the aerospace and automotive industries.

Currently there are a number of challenges associated with production of composites using carbon nanotubes, including achieving a satisfactory dispersion of carbon nanotubes whilst maintaining a cost effective processing route. Liquid processing is an attractive method for manufacture of these composites as it is capable of producing near net shape components quickly and relatively cheaply. However overcoming challenges with carbon nanotube wetting and agglomeration have thus far prevented effective processing of carbon nanotube composites via this method.

Carbon nanotube introduction into a composite system can be effectively assessed by numerous techniques ranging from simple hardness and density measurements to X-Ray Diffraction (XRD) and Raman Spectroscopy.

A number of preforms, matrix media and processing techniques have been investigated to date. A range of processing techniques for aluminium-carbon nanotube metal matrix

composites are explored and compared in this report. Properties of the resultant composite samples are evaluated and production problems are highlighted as well as possible improvements.

Chapter 2

Literature Review

2.1 Composite Materials

Composite materials consist of a matrix material combined with one or more distinct reinforcement phases distributed within the matrix. The reinforcement phase is added with the aim of achieving specific improved properties, for example strength, stiffness, toughness, thermal conductivity, electrical conductivity, coefficient of thermal expansion, electromagnetic shielding, damping and wear resistance. (Agarwal et al., 2011).

The primary role of fibres however is to provide strength and stiffness to a weaker, less stiff matrix. The addition of reinforcement has been seen to produce great improvements in properties such as strength-to-weight and stiffness-to-weight ratios relative to monolithic materials (Agarwal et al., 2011). Applications of composite materials are varied, from aerospace and automotive applications to sports equipment.

2.2 Development of Carbon Fibres and Carbon Nanotubes

The discovery of carbon fibres is attributed to Bacon (Bacon, 1960) who observed stalagmite-like structures formed as a result of the evaporation of carbon during an arc discharge process in a high-pressure inert gas. This was the first instance of the synthesis of fibres, which had up to 20GPa tensile strength and 700GPa Young's modulus. Bacon also proposed a scroll-like structure for the carbon fibres (Bacon, 1960).

During the 1960s and 70s the development and fabrication of high strength carbon fibres made them the most popular choice for reinforcement of composites which were used in rocket and missile nose cones and re-entry heat shields. Since 1970, carbon fibre composites have been used extensively in applications such as military and commercial aerospace, the space industry and sporting goods. Currently carbon fibre composites use polymeric matrices to provide lightweight, formable structures.

Iijima discovered that they were made up of seamless, concentric tubes as opposed to the scroll structure which Bacon had proposed (Iijima, 1991). These types of nanotube structures became known as Multi-Walled Carbon Nanotubes (MWNT). Single-Walled Carbon Nanotubes (SWNT) were discovered by both (Iijima and Ichihashi, 1993) and (Bethune et al., 1993). (Agarwal et.al., 2011) reported that a seamless Single Wall Carbon Nanotube (SWNT) can be produced by rolling a sheet of graphene. In practice this can be achieved in numerous ways, as shown by Figure 1.

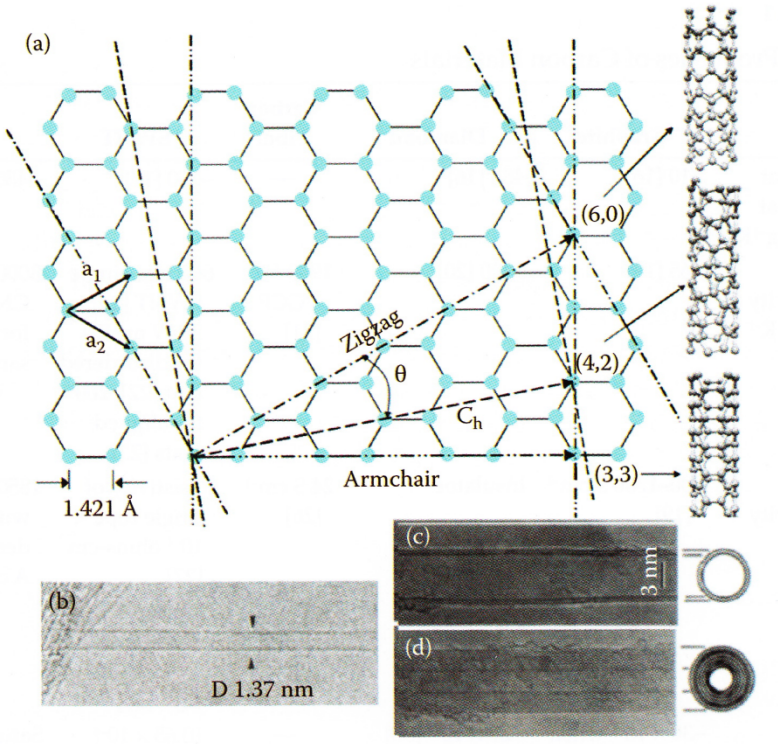

Figure 1: (a) Schematic showing the formation of an SWNT by rolling along different chiral vectors C_h and the resulting SWNTs, and (b), (c) and (d) high resolution TEM images showing a single, double and seven-walled nanotube, respectively. (Agarwal et al., 2011)

When the graphene sheet is rolled along the chiral axis C_h , i.e. an axis that is not superimposable on its mirror image, the resultant nanotube would have a circumference equal to the length of the chiral axis.

The chiral axis can be represented by the integers n and m where $C_h = na_1 + ma_2$.

a_1 and a_2 are lattice translation vectors as shown in figure 1. In this case the diameter of the resultant nanotube would depend on n and m. The diameter of a SWNT is given by equation 1:

$$diameter = a(\sqrt{n^2 + m^2 + nm})/\pi \qquad \text{Equation 1}$$

where a refers to the lattice vector and equals 2.46Å. When n = m, ‘armchair’ nanotubes are formed which are metallic, and when n or m = 0, ‘zigzag’ nanotubes are the result which are semiconducting (Agarwal et al., 2011). The terms ‘armchair’ and ‘zig-zag’ refer to the arrangement of hexagons around the circumference. ‘Armchair’ nanotubes are formed along the same axis as the hexagons, whereas ‘zig-zag’ nanotubes are formed along a diagonal axis through the hexagons, giving a spiral arrangement of hexagons.

Multi-Walled Carbon Nanotubes (MWNTs) consisting of 2-50 concentric tubes can be obtained by methods including Chemical Vapour Deposition (CVD) and Physical Vapour Deposition (PVD). CNTs have outstanding mechanical properties due to the isotropic nature of their atomic structure. They have been shown, depending on the method of measurement, to produce Young’s modulus values of up to 4TPa and tensile strengths of up to 63GPa (Agarwal et al., 2011). SWNTs have been found to possess superior mechanical properties than MWNTs, which can be attributed to the presence of defects within the MWNTs.

2.3 Carbon Nanotube-Metal Matrix Composites

There are numerous issues surrounding the fabrication of metal matrix composites reinforced with carbon nanotubes, the most important of which is achieving a uniform distribution of carbon nanotubes within the metal matrix material. Carbon nanotubes tend to agglomerate into clusters due to Van der Waal's forces, as a result of their high specific surface area (up to $200 m^2.g^{-1}$).

In order to successfully use the properties of CNTs as a reinforcement phase, a good dispersion within the metal matrix is necessary. Carbon nanotube clusters both reduce strength and increase the porosity of the final composite, detrimental features within the microstructure.

2.4 Mechanics of Metal-Carbon Nanotube Systems

The mechanical behaviour of metal matrix-carbon nanotube systems can be described at several length scales:

At the macro scale (>1mm) composite behaviour can be summarised by models such as Hooke's Law (Agarwal et al., 2011). Properties of the material at this scale are a mean.

Between 1mm and 1μm (micro scale), interest is in stresses around pores and inclusions as well as crack initiation/propagation. To model these phenomena, micromechanical models, dislocation plasticity and fracture mechanics are used (Agarwal et al., 2011).

At the nano scale length molecular dynamics are employed to study the interaction between carbon nanotubes and metal matrix material at an atomic level (Agarwal et al., 2011).

2.5 Strengthening Mechanisms in Metal Matrix-Carbon Nanotube Composites

The aim of the addition of carbon nanotubes as a reinforcement phase within metal-matrix composites is to utilize their high tensile strength to improve the overall strength of the composite material; tensile strength values can be, for example, of the order of 200-400MPa (Agarwal et al., 2011). Carbon nanotubes have a higher elastic modulus relative to the metal matrix materials; because of this CNTs can bear a greater share of the load at a finite strain thus increasing the strength of the overall composite. There are a number of models that can be used to predict the strength of MM-CNT composites (Agarwal et al., 2011).

2.5.1 Shear Lag Models

Shear lag models (Agarwal et al., 2011) use the theory of load transfer from the matrix material to the fibres through an interfacial shear stress to predict the final overall strength of the composite.

Tensile load transfer to the fibre reinforcement varies along the length of the fibre; the tensile load is zero at the ends of the fibre, increasing to its maximum value at the centre

of the fibre assuming the fibre is fully wetted. The maximum force that can be transferred to a fibre increases with increasing fibre length and therefore the efficiency of fibre property utilization also increases with fibre length.

At the critical fibre length (l_c), the maximum load at the centre of the fibre is equal to its fracture strength; it is therefore desirable to have fibres of length greater than l_c in order to take full advantage of the load transfer effect.

(Choi et al., 2008) used a shear lag model where the fibre length was lower than the critical fibre length ($l < l_c$) in order to calculate the strength of an Al-4 vol. % CNT composite. The overall strength of the composite was defined by equation 2:

$$\sigma_c = \sigma_f V_f \left(\frac{l}{l_c}\right) + \sigma_m (1 - V_f) \qquad \text{Equation 2}$$

where:

$l_c = \frac{\sigma_f d}{2\tau_m}$ = Critical Fibre Length

V_f = Volume Fraction of Fibres

l = Average carbon nanotube length

d = Carbon nanotube diameter

σ_m = Yield strength of Matrix Material

τ_m = Matrix shear strength, obtained from $\sigma_m/2$

σ_f = Yield strength of carbon nanotubes

(Choi et al., 2008) applied this model to Al-4 vol. % CNT composites and used X-Ray Diffraction (XRD) to estimate two mean grain sizes of 72nm and 200nm respectively. Experimental tensile strength values of approximately 403MPa for 70nm grain size and

323MPa for 200nm grain size were measured. When compared to calculated values of 434MPa and 391MPa for 70nm and 200nm grain sizes respectively, a reasonable agreement between experimental and computed tensile strength data was seen.

This was investigated further when (Choi et al., 2009) applied the model to 1.5, 3 and 4.5% volume fractions of CNT reinforcement and saw continued agreement between experimental and computational data up to 4.5 vol.% CNT. This data is shown in figure 2.

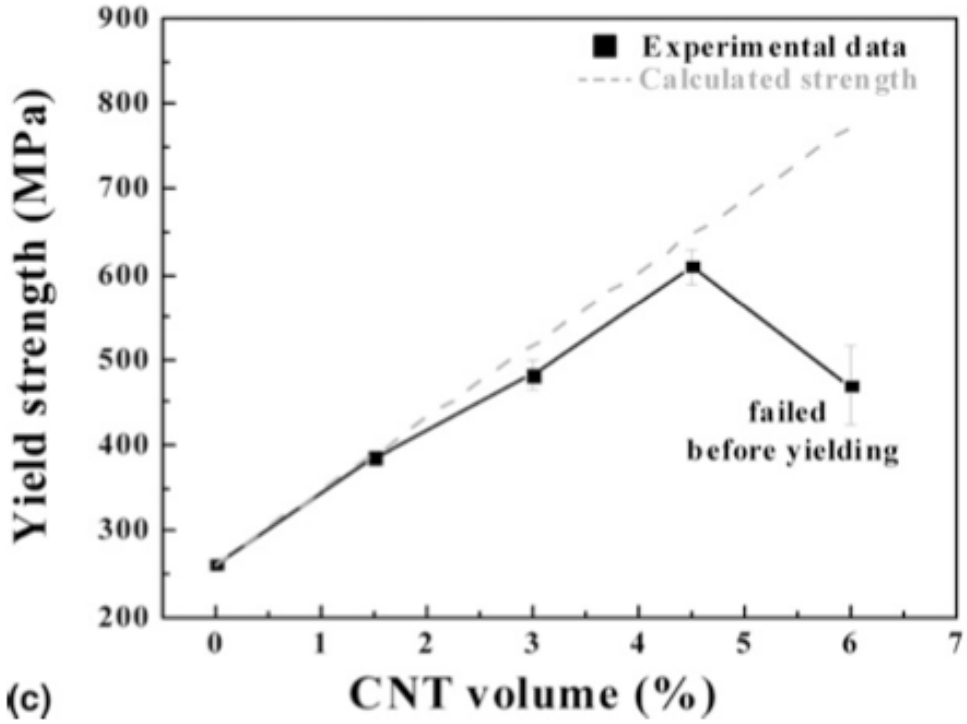

Figure 2: Yield strength as a function of the volume fraction of the MWNTs (Choi et al.,2009)

Further strengthening is expected when the fibre length is greater than the critical fibre length ($l > l_c$). (Kuzumaki et al., 1998) applied the Kelly-Tyson formula (equation 2.1) for calculating the strength of short fibre composites to Al-CNT composites.

$$\sigma_c = \sigma_f V_f \left(1 - \frac{l_c}{2l}\right) + \sigma_m^f (1 - V_f) \qquad \text{Equation 2.1}$$

where:

σ_c = Composite Fracture Strength

σ_f = Fibre Fracture Strength

σ_m^f = Failure Strength of Matrix at the Failure Strain of the Composite

V_f = Volume fraction of CNTs

l_c = Critical length of the CNTs

l = Average CNT length

(Kuzumaki et al., 1998) produced strength values that were significantly lower than theoretical values. (Kuzuamaki et al., 1998) calculated a theoretical strength value of the composite of 270MPa, however, it can be seen from figure 2.1 that the measured tensile strength values (~40-80MPa) were significantly below this value. This was attributed to CNT clustering.

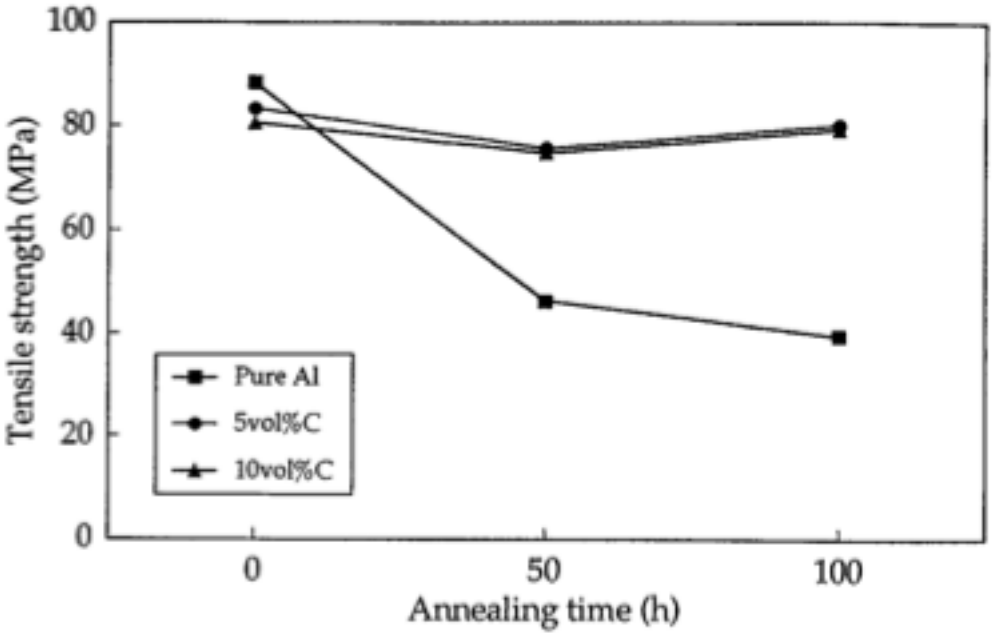

Figure 2.1: Tensile strength as a function of annealing time at 873K (Kuzumaki et al.,1998)

2.5.2 Strengthening by interfacial phase between matrix and CNTs

During processing, reactions can cause products to occur at the metal/CNT interface. The shear strength of this interfacial compound then becomes the limiting factor for the strength of the overall composite. Production of high strength interfacial phases could aid load transfer from the matrix to the CNT reinforcement. A model was proposed by (Coleman et al., 2004) in order to predict the shear strength of a composite (σ_c) with an interfacial compound present:

$$\sigma_c = \left(1 + \frac{2b}{D}\right)\left[\sigma_{shear}\, l/D - \left(1 + \frac{2b}{D}\right)\sigma_m\right]V_f + \sigma_m \qquad \text{Equation 2.2}$$

where:

σ_{shear} = Shear strength of the interface

b = Width of the interfacial compound

D = Diameter of CNT

$\sigma_m = Shear\ strength\ of\ matrix$

$V_f = Volume\ fraction\ of\ CNTs$

For metal matrix-carbon nanotube composites (MM-CNT), reactions between the matrix and carbon nanotubes may lead to carbide formation at the interface (Agarwal et al., 2011). In this case, the shear strength of the carbide phase becomes the limiting factor for the transfer of stress from the matrix to the carbon nanotubes.

(Laha et al., 2009) applied equation 2.2 above to aluminium-carbon nanotube composite systems in order to predict their strength. However the calculated value of the tensile strength (226MPa) was in disagreement with the experimentally determined strength of the composites (83.1MPa). This was attributed by the authors to poor distribution and agglomeration of nanotubes within the composite structure.

2.5.3 Strengthening by carbon nanotube clusters

Carbon nanotube clusters can, however, improve the strength of metal matrix-carbon nanotube composites. For this to occur, two criteria must be satisfied:

(1) CNT clusters must be well infiltrated by the metal matrix material and

(2) There must be sufficient transfer of load from the matrix to the carbon nanotube cluster.

Should these criteria be fulfilled, CNT clusters can have high strength and improve the mechanical properties of the final composite (Agarwal et al., 2011).

(Ryu et al., 2003) proposed a modified shear lag model in order to assess load transfer efficiency in whisker fibre reinforced metal-matrix composites. The model considered both shape and alignment of the reinforcement phase. This model could be applied to elongated CNT clusters and is given by equation 2.3.

$$\sigma_{y,1} = \frac{V_f \sigma_m}{2} S_{eff} + \sigma_m \qquad \text{Equation 2.3}$$

where $\sigma_{y,1}$ is the yield point of the matrix, V_f is the volume fraction of fibres, σ_m is the matrix strength and S_{eff} is the parameter defined as the effective aspect ratio of an elongated CNT cluster oriented at an angle θ to the loading direction.

(Kim et al., 2008) produced copper-carbon nanotube composites by spark plasma sintering of ball-milled powders, which was followed by cold rolling. The composites were analysed using SEM microscopy and tensile testing. Micrographs showed fibrous

Cu/CNT regions within the microstructure which confirmed the presence of CNT clusters. The stress/strain data for Cu-5vol.% CNT and Cu-10vol.% CNT systems showed two yield points, designated $\sigma_{y,1}$ and $\sigma_{y,2}$.

$\sigma_{y,1}$ represented the matrix yield point and can be calculated by equation 2.3. $\sigma_{y,2}$ represented the CNT cluster yield point that can be expressed by equation 2.4, which is a modified rule of mixtures formula.

$$\sigma_{y,2} = \sigma_{y,1}(1 - V_f) + \sigma_f V_f \qquad \text{Equation 2.4}$$

The study used the model proposed by (Ryu et al., 2003) to calculate theoretical $\sigma_{y,1}$ and $\sigma_{y,2}$values, which were calculated to occur at 151MPa and 167MPa respectively, for the Cu-5vol.% CNT system, and which were in agreement with experimental values of 149MPa and 180MPa.

Similarly, for Cu-10vol.% CNT, the calculated $\sigma_{y,1}$and $\sigma_{y,2}$values were 180MPa and 256MPa respectively. These were also in close agreement with experimental values obtained which were 180MPa and 240MPa.

This study shows an agreement between the model proposed by (Ryu et al., 2003) and the experimentally observed yield points of CNT cluster containing composites. The study, however, only investigated 5 and 10vol.% CNT compositions, no investigation was conducted to explore if the relationship between calculation and experiment broke down at higher CNT additions. In addition, the model used in this study was modified

for whisker fibre reinforced metal matrix composites. The model may not be applicable to particulate reinforcement metal matrix systems.

2.5.4 Halpin-Tsai Equations

Halpin-Tsai equations (Agarwal et al., 2011) are mathematical models used to predict both elastic moduli and strength of fibre-reinforced composite materials. (Yeh et al., 2006) applied a modified Halpin-Tsai model to a PF-650 phenolic resin-MWNT system at varying nanotube loadings between 0 and 4wt.% with both dispersed and agglomerated MWNTs and found good agreement between the model and experimentally measured tensile strength values. The distribution of MWNTs was not thoroughly evaluated.

The Halpin-Tsai model can also be applied to metal matrix-carbon nanotube composite systems and the model is shown in equation 2.5:

$$\sigma_c = \frac{1+\varepsilon\eta V_f}{1-\eta V_f}\sigma_m \qquad \text{Equation 2.5}$$

where:

σ_c= composite strength

V_f= volume fraction of fibres

σ_m= matrix strength

$\varepsilon' = strain\ rate$

η depends on the ratio of fibre strength to matrix strength (σ_f/σ_m):

$$\eta = \frac{\alpha\left(\frac{\sigma_f}{\sigma_m}\right)-1}{\alpha\left(\frac{\sigma_f}{\sigma_m}\right)+\varepsilon\prime} \qquad \text{Equation 2.6}$$

The coefficients α and ε are influenced by the dispersion of carbon nanotubes within the matrix material. If the sample thickness is much greater than the fibre length (as with CNTs), the fibres are assumed to be randomly orientated in three dimensions with $\alpha = 1/6$ and $\varepsilon = 2(\frac{l}{d})$, where l and d represent fibre length and diameter respectively.

(Coleman., 2006) also applied Halpin-Tsai equations to polymer-CNT composites and found good correlations between predicted strength values and experimentally determined values at low CNT concentrations (<10wt.%).

2.5.5 Strengthening by Dislocations

When metal matrix-carbon nanotube composites are processed via deformation techniques, dislocations can be piled up and pinned against CNTs which can cause a strengthening effect.

(Lahiri et al., 2009) studied the strengthening effects of CNTs in roll-bonded Al-CNT composite systems produced by spraying CNTs onto aluminium foil layers, followed by rolling layers of foil together. Results from this study showed that at low CNT additions of 2 vol.%, well-dispersed carbon nanotubes produced an improvement in the modulus

of elasticity of the composite, while at higher CNT additions, the presence of carbon nanotube clusters was increased.

These clusters were shown to behave as precipitates and produced no improvement in modulus; they did however improve the tensile strength of the composite system by inhibiting the movement of dislocations and therefore increasing dislocation density. Strain hardening then caused a strength increase in the composites. The strength of the composite can be expressed quantitatively using the Taylor expression:

$$\sigma = \sigma_0 + \alpha M^T G b \rho^{\frac{1}{2}} \qquad \text{Equation 2.7}$$

where:

$\sigma =$ Flow Stress

$\sigma_0 =$ Internal Frictional Stress

$\alpha =$ Constant $= 1/3$

$M^T =$ Taylor Factor, given a value of 3 for untextured polycrystalline materials

$G =$ Shear Modulus

$b =$ Burgers Vector of dislocations

$\rho =$ Dislocation density

The dislocation density within a composite can increase due to other factors, for example, due to a mismatch in thermal expansion between the metal matrix and CNTs. (George et al., 2005) investigated the effect of thermal mismatch on dislocation density in aluminium-carbon nanotube systems using equation 2.8:

$$\rho_{th} = \frac{10 V_f \epsilon}{bt(1 - V_f)} \qquad \text{Equation 2.8}$$

where:

ρ_{th}= Dislocation density due to thermal mismatch

V_f = Volume fraction of CNTs,

ϵ = Thermal strain,

b = Burgers vector

t = Diameter of CNTs

However differences were seen between measured yield strength values and theoretical values using the thermal mismatch equation 2.8.

Three MWNT systems were investigated:

0.5% MWNT volume fraction

0.5% volume fraction of MWNT plus K_2ZrF_6

2% MWNT volume fraction

Three SWNT systems were also investigated:

1% SWNT volume fraction

1% volume fraction of SWNT plus K_2ZrF_6

2% MWNT volume fraction

The strengths of these samples are shown in tables 1 and 2 respectively, where a weak correlation between experimental and theoretical values for MWNT systems was apparent. However there was no correlation between experimental and theoretical values for SWNT systems.

(George et al., 2005) also investigated the mechanism of Orowan strengthening within Al-CNT composite systems. Orowan strengthening occurs when CNTs act as precipitates and impede motion of dislocations. As dislocations pass through the CNT, they leave behind dislocation loops, which in turn create a back-stress which then repels dislocation motion.

(George et al., 2005) compared yield strength values obtained both experimentally and by the Orowan looping mechanism given by equation 2.9.

$$\Delta\tau = \frac{A}{r\ln(\frac{2r}{r_0})} Gbf^{\frac{1}{2}}$$ Equation 2.9

where:

$\Delta\tau$ = Increment in shear strength

A = Constant (0.093 for an edge dislocation and 0.14 for a screw dislocation)

r_0 = Radius of the dislocation core

r = Volume equivalent radius for CNT

G = Shear modulus

b = Burgers vector

f = Dislocation density

These values are shown for MWNT and SWNT systems in tables 3 and 4 respectively. Table 3 shows a close correlation between measured yield strength values and yield strength values for Orowan looping strengthening mechanism models. A large degree of variation is seen between the same values for SWNT systems, as shown in table 4. For all data it was observed that experimental values were lower than those calculated by

models. This is because not all strengthening mechanisms may contribute, or may be less pertinent than predicted by the model. Defects such as porosity, CNT clusters which are not infiltrated by matrix material and poor CNT dispersion can also affect experimental strength values (Agarwal et al., 2011).

MWNT% volume fraction	Experimental yield strength (MPa)	Thermal mismatch yield strength (MPa)
0.5	86	117.346
0.5 + K_2ZrF_6	93	117.346
2	99	197.346

Table 1: Comparison of theoretical thermal mismatch and experimental data for MWNT/Al composite (George et al., 2005)

SWNT% volume fraction	Experimental yield strength (MPa)	Thermal mismatch yield strength (MPa)
1	79.8	471.403
1 + K_2ZrF_6	98.7	471.403
2	90.8	636.344

Table 2: Comparison of theoretical thermal mismatch and experimental data for SWNT/Al composite (George et al., 2005)

MWNT% volume fraction	Experimental yield strength (MPa)	Orowan looping yield strength (MPa)
0.5	86	90.573
0.5 + K_2ZrF_6	93	90.573
2	99	101.145

Table 3: Comparison of theoretical Orowan looping and experimental data for MWNT/Al composite (George et al., 2005)

SWNT% volume fraction	Experimental yield strength (MPa)	Orowan looping yield strength (MPa)
1	79.8	184.203
1 + K_2ZrF_6	98.7	184.203
2	90.8	227.365

Table 4: Comparison of theoretical Orowan looping and experimental data for SWNT/Al composite (George et al., 2005)

2.5.6 Strengthening by Grain Refinement

This is a common strengthening mechanism amongst metallic systems and can also be applied to metal matrix composites. Carbon nanotubes can cause a number of phenomena that result in grain refinement.

Firstly, the addition of CNTs to a metal matrix increases both work hardening of the matrix and thermal conductivity of the composite (Agarwal et al., 2011). In addition carbon nanotubes can act as secondary particles within the matrix, CNTs could react with matrix phase e.g. titanium to forma carbide compound, which cause grain refinement as a result of grain boundary pinning. All of these factors contribute to increased nucleation rates during recrystallization processes.

Both (Choi et al., 2008) and (Li et al., 2009) attempted to quantify the grain refinement effect within metal matrix-carbon nanotube composites. (Choi et al., 2008) prepared powders of Al-5wt.% Si alloy reinforced with 3 vol.% CNTs by ball milling and hot rolling at 480^{o}C. It was found that as a result of both grain refinement and CNT reinforcement, 520MPa yield strength and 5% strain to failure were achieved.

Similarly, (Li et al., 2009) observed an increase in micro hardness as a result of reduced grain size in nanostructured Cu-CNT composite systems prepared by ball milling followed by high-pressure torsion. (Li et al., 2009) also observed that the increase in micro hardness was greater than that predicted by a reduction in grain size alone. This seems to suggest that although grain refinement has been seen within MM-CNT

systems, the strengthening of the final composite is greater than should be achieved by grain refinement alone.

2.6 Fabrication methods for Carbon Nanotube-Metal Matrix Composites

The method of processing carbon nanotube-metal matrix composites can be significantly influential on the final properties of the composite. The objective of successful processing for MM-CNT composites is to achieve a uniform carbon nanotube dispersion within the metal matrix. Processing methods can be subject to limitations in order to ensure CNTs remain intact. CNTs may be exposed to elevated temperatures or concentrated stress during processing, which could lead to, for example, chemical reactions between CNT and matrix material leading to carbide formation. These carbides could have a detrimental of favourable effect on the final properties of the structure (Agarwal et al., 2011). A number of processing methods for MM-CNT composites are outlined in the following sections.

2.6.1 Powder Metallurgy

Powder metallurgy processing routes have the advantage that, unlike liquid metal processing, almost any composition of material can be processed. Material wastage is also kept to a minimum due to the minimal need for machining of components (Agarwal et al., 2011).

Powder metallurgy is a useful method for processing composite materials. Two phases can easily be mixed and dispersed in the solid state. Mechanical alloying techniques involve placing powder constituents in a rotating chamber along with either hardened steel or ceramic balls. They are then mixed by the mechanism of the balls impacting the powders causing deformation and fracture of particles. These techniques have been widely used for the preparation of composites. (Suryanarayana., 2001) described the mechanism and variables in the process of mechanical alloying and discussed recent advances in the technology.

(Esawi et al., 2007) studied the capability of ball milling to effectively distribute carbon nanotubes in aluminium matrices at up to 48 hours, examining the powder morphology and dispersion of the nanotubes. It was concluded that ball milling was an effective means of distributing carbon nanotubes, and at longer milling times, CNTs are assumed to reside between cold welded aluminium powder particles.

Similarly, (Morsi et al., 2007) investigated the effect of milling times of up to 48 hours on particle size and morphology, comparing results of two concentration loadings of carbon nanotubes. Results from both studies were similar concluding that milling time has an effect on particle morphology and that ball milling is an effective means of dispersing carbon nanotubes within an aluminium matrix. Neither study attempted to quantify the distribution of carbon nanotubes.

In order to produce composite specimens, consolidation and densification has to take place following mechanical alloying. There are a number of ways in which densification

can be achieved, the most common being: sintering, deformation processing and melt processing (Agarwal et al., 2011).

2.6.2 Conventional Sintering

This is the most conventional form of densification, powders must first be blended and compacted before sintering. Due to the potential of metallic constituents to oxidise, sintering must either take place under vacuum or in an inert atmosphere. Aluminium and copper carbon nanotube composites are the most common systems to be produced in this way. No further dispersion of carbon nanotubes will occur during sintering so pre-dispersion is required through mechanical alloying and blending (Agarwal et al., 2011).

Some studies, such as those conducted by (C.He et al., 2007) have explored the possibility of increasing the distribution of carbon nanotubes within a metal matrix by growing CNTs directly onto prepared metal powder. Aluminium powder was prepared by precipitation of $Ni(OH)_2$ catalytic nanoparticles onto the surface of aluminium powder particles. The particles were then put through a drying and calcination process at 200^{o}C for 4 hours. The effect of this is to form NiO-Al, which is then reduced by H_2 at 400^{o}C for 2 hours to Ni-Al. Ni particles of size order 5-20 nm in diameter were observed on the surface of the aluminium powder particles.

Carbon nanotubes were then grown in situ within the matrix by catalytic decomposition of CH_4-N_2-H_2 at 630^{o}C. The composite was prepared via a powder press at 600MPa, followed by a sintering stage at 640^{o}C under vacuum.

Following sintering, composite discs were subjected to a further pressure of 2GPa to improve density. Composite samples were also prepared via ball milled powders.

Tensile tests were performed on composite samples from each processing route. Ball milled powders produced a tensile strength of 213MPa compared to 398MPa for composites prepared by in situ CNT growth. These results highlighted the importance of carbon nanotube distribution in prepared powders before processing.

2.6.3 Deformation Processing: Equal Channel Angular Pressing (ECAP)

The ECAP technique involves material being extruded through a die where the extrusion ratio is 1. Material is passed through an angled region in the die which induces shear deformation into the material microstructure.

(Valiev et al., 2006) outlined the principles of the process, including induced strain, slip systems and shearing patterns, as well as die geometry and pressing methods. It was concluded that all of these parameters have an effect on the properties of the final pressed metal/alloy or metal matrix composite. It was stated that to achieve improved mechanical properties after ECAP requires control of numerous variables such as grain boundary misorientation and distribution of any secondary phases.

(Derakhshandeh et al., 2011) performed a capability study on the ECAP process to consolidate both pure aluminium powders and aluminium with varying concentrations of nano alumina particles. Results found that pressing by ECAP at 200^{o}C was effective in consolidating: pure aluminium, Al-5-vol% Al_2O_3 and Al-10 vol.% Al_2O_3 powders, to near theoretical density. It was also noted that the ECAP process eliminated and distributed Al_2O_3 agglomerates after a maximum of four passes.

Subsequently to this, a study was done by (Derakhshandeh et al., 2011) comparing ECAP at 200^{o}C and conventional extrusion as consolidation techniques for pure aluminium and Al-5 vol.% Al_2O_3 powders. It was found that three ECAP passes consolidated composite powders to 99.29% of theoretical density, whereas conventional extrusion only produced samples that were 98.5% dense. Hardness measurements performed on samples showed that ECAP produced 1.7 and 1.2 times greater hardness in composite and pure aluminium samples respectively compared to conventional extrusion. Compressive strength tests showed higher bond strength in ECAP composite samples compared to conventional extrusion. ECAP samples also demonstrated improved wear resistance in a pin on ring test in comparison with extrusion.

There has been a limited amount of investigation into the application of ECAP to the consolidation of aluminium-carbon nanotube composites. (Kollo et al., 2012) conducted a study investigating hot consolidation of aluminium powders and aluminium nano-reinforced metal matrix composite powders by ECAP. Powders containing nano SiC particles and carbon nanotubes as well as pure aluminium were consolidated using ECAP. Results showed a 60% increase in hardness for ECAP aluminium powder

relative to conventional extrusion. Composite samples were reported to be brittle after ECAP due to the lack of back pressure during pressing. Hardness values from both Al-6 vol.% CNT and Al-1 vol.% nanoSiC increased compared to values achieved by other processing routes. This was attributed to matrix grain refinement during ECAP.

(Quang et al.,2007) investigated ECAP as a method of compaction for Cu-CNT composite samples and concluded that ECAP is a viable method for producing fully dense composite samples. Samples were produced by being passed through the ECAP die one, four and eight times. It was reported that after one pass, pores and carbon nanotube agglomerates were still observed; this was not evident in samples processed with multiple passes. This was attributed to the hydrostatic pressure within the die, and the shear deformation induced on the microstructure by multiple passes. It was also calculated that Cu-CNT ECAP samples achieved 97% of their relative density. A reduction in grain size was seen for two ECAP passes, after which the grain size was concluded to be constant. However no data was provided for this analysis. Hardness test data showed an improvement of more than twice the hardness between initial ECAP Cu-powders and ECAP 1% CNT/Cu powders.

2.6.4 Melt Processing: Casting

In order to successfully cast metal matrix-carbon nanotube composite materials, carbon nanotubes must be effectively distributed within the melt. This is challenging due to the low density of carbon nanotubes. Also, in order to disperse carbon nanotubes within liquid metal, nanotubes must be wetted, with the molten matrix. This can be achieved if

a contact angle of less than 90^{o} is produced, using a force balance as shown in equation 3:

$$\cos\theta = \frac{\gamma SV - \gamma LS}{\gamma LV} \qquad \text{Equation 3}$$

where:

L = Liquid i.e. molten metal

S = Surface of carbon nanotube

γ = Surface tension

(Dujardin et al., 1994) conducted a study investigating the capillarity and wetting of carbon nanotubes. Experimental results showed that carbon nanotubes could be fully wetted by substances with a low surface tension. Substances such as sulfur, selenium and caesium were shown to successfully wet carbon nanotubes. An upper limit of less than 200 mNm^{-1} for surface tension in order to fill the 'bore' of carbon nanotubes by capillary action has been suggested.

These results are significant as they imply that most pure molten metals will not wet carbon nanotubes under capillary action. Therefore some alterations to alloying or processing are needed to induce wetting.

Table 5 shows some common elements and their surface tension values as quoted by (Dujardin et al., 1994).

Element	Surface Tension (mN/m)	Wetting with CNT
S	61	Yes
Cs	67	Yes
Rb	77	Yes
Se	97	Yes
Te	190	No
Pb	470	No
Hg	490	No
Ga	710	No
Al	860 at 750^{o}C	No

Table 5: Common molten elements and their surface tension characteristics (Dujardin et al., 1994)

Limited investigations have been done into liquid processing of metal matrix-carbon nanotube composite materials.

(Abbasipour et al., 2010) investigated a novel method known as compocasting as a possible fabrication route and compared this to stir casting. To improve the wettability of the carbon nanotubes in the melt, CNTs coated with aluminium were injected into the molten matrix and gradually melted. In order to coat the CNTs, Ni-P electroless deposition was used. Following this aluminium particles were coated to form Ni-P-CNTs. Composite samples were then cast by being heated to a temperature of 700^{o}C whilst being isothermally stirred.

During this stage, a mass fraction of 1% Mg was added in order to improve wettability between reinforcement and matrix phases. Following injection of CNTs into the melt, cast samples were cast into a steel die sitting below the furnace, at a temperature of 700^{o}C.

The composite samples were evaluated by optical and SEM analysis and hardness measurements. Results showed complete interaction between CNTs and the Ni-P coating. No agglomeration of CNTs was reported from the microstructural evaluation. This was attributed to the slow co-deposition of Ni-P and CNTs on the aluminium particles. Cast specimens of both monolithic A356 aluminium alloy and A356-2 vol.% CNT composites with 0, 15 and 30% solid fractions were analysed by optical microscopy and by SEM. Results showed dendritic structures in A356 castings produced from a fully molten state, i.e. 0% solid fraction. Castings produced within semi-solid temperature ranges (15 and 30% solid fractions) produced non-dendritic microstructures. Results showed that the microstructure of A356-2 vol.% CNT composite castings was significantly finer than those of monolithic A356.

Analysis of equivalent circle diameter/grain size of α-Al particles within semi solid microstructures for both composite and monolithic samples showed that composite samples have smaller α-Al equivalent circle diameter particles than equivalent monolithic specimens. It was noted that the composite casting produced at the lowest temperature produced the smallest α-Al particles. The study attributed this grain refinement to the Ni-P coating on the CNTs acting as heterogeneous nucleation sites, but did not provide any elaboration or evidence of this theory. The density of the composite specimens was reported to be lower than monolithic samples; this was attributed mainly to the presence of low density CNTs, but also increased porosity. The study did not provide any extensive porosity comparison between composite and monolithic samples. It was also noted that densities of both monolithic and composite samples cast in the semi-solid state were higher than those cast in the fully liquid state.

Hardness data produced by (Abbasipour et al., 2010) showed an increase in hardness due the addition of CNTs, this was attributed in part to the grain refinement of the A356 matrix.

(Uozumi et al., 2007) investigated a different method, squeeze casting, as a possible means for producing aluminium or magnesium carbon nanotube reinforced composites. A wettability study of graphite was first performed using molten aluminium and magnesium, the technique used was the sessile drop method, as shown in figure 3. This method uses the contact angle to measure wettability of the substrate in molten metal.

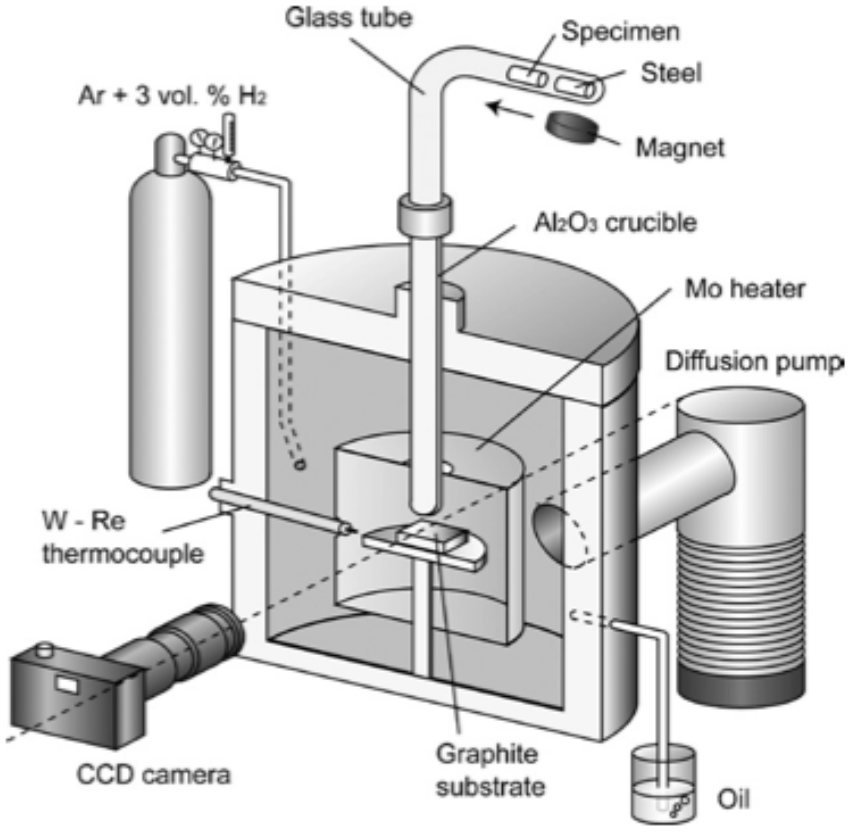

Figure 3: Apparatus for sessile drop experiment (Uozumi et al., 2007)

Results from wettability experiments in this study showed that, for magnesium, the contact angle between the basal plane of graphite and molten magnesium was larger than 90^o for 200 seconds after molten magnesium was dropped onto the graphite substrate. This indicated that magnesium would not spontaneously infiltrate porous graphite.

Results were similar for molten aluminium. When the contact angle is larger than 90^o, external force is necessary to induce wetting of substrate. (Uozumi et al., 2008) used Young's equation (equation 3.1) to estimate the work required per unit area of external force to induce wetting.

$$W = \gamma_{SL} - \gamma_{SV} = -\gamma_{LV} \cos\theta \qquad \text{Equation 3.1}$$

Calculations showed that less work is required to induce wetting of magnesium onto a graphite substrate in comparison with aluminium, therefore fabrication of composites using magnesium matrix material should, in theory, be easier.

Final composite samples produced by (Uozumi et al., 2007) using pure aluminium, Al-12Si-Cu-Ni-Mg and Mg-5Al-2Ca matrices produced by squeeze casting were reported to be fully infiltrated, i.e. the molten matrix had fully wetted MWCNT preforms. However this was only quantified through microscopy.

Other investigations into melt processing techniques include friction stir processing. (Lim et al., 2009) synthesized aluminium-CNT composite samples via the friction stir process using multi-walled carbon nanotubes. A base plate of 7075 aluminium was used

and covered by a plate of 6111 aluminium containing a groove into which CNTs were stirred. SEM and TEM showed that nanotubes were embedded in the aluminium matrix. This analysis also proved that the multi-walled nanotube structure survived the friction stirring process. Applying an increase in tool rotation speed and penetration depth was found to improve the homogeneity of the carbon nanotubes within the aluminium matrix. When using tangled multi-walled nanotubes it was observed that full dispersion of nanotubes within the stir zone could not be achieved.

Micro hardness measurements showed that, for both rotation speeds and penetration depths investigated, the addition of CNTs improved the hardness in the stirred region. Regions adjacent to the stirred region and the thermo-mechanically affected zone (TMAZ) showed higher than average hardness. This could indicate a non-uniform dispersion of CNTs. Segregation of the solidified structure within the weld or work hardening of the surrounding material could also account for the change in hardness.
Based on other work (Lim et al., 2009) theorized that a more uniform distribution of CNTs could be achieved by using multiple stir passes without significantly degrading the multi-walled structure of the CNTs, although this was not investigated further.

(Liu et al., 2011) also investigated the possibility of fabricating aluminium-carbon nanotube composites via friction stir processing, using powder metallurgy to produce the preform. This study built on the work of (Lim et al., 2009). CNTs were mixed with a 2xxx series aluminium-copper alloy powder using a rotary mixer. This was followed by cold compaction and hot forging before friction stir processing using either one or four-passes. After friction stir processing, the samples were solutionized, quenched and

naturally aged. Reported results from the study were that the process zone of the friction stir process was only seen to be uniform after four passes. Carbon nanotube clusters were observed extensively in forged composite specimens. However in friction stirred samples, after one pass, large CNT clusters were significantly reduced and after four passes CNT clusters were reported to be absent (analysed using optical imaging and SEM). This indicated that the friction stir process was effective in distributing carbon nanotubes within the matrix material. Problems with wetting of CNTs by the aluminium matrix were also noted in forged and one-pass friction stir processed specimens. The carbon nanotubes in the composite samples were seen to be shorter than unprocessed nanotubes. CNTs were shortened from several microns down to ~400nm.

Raman spectroscopy revealed that damage to the CNT structure was minimal. Some aluminium carbide Al_4C_3 was observed either attached to CNTs or near CNTs in the matrix material. Despite this it was reported that the layered structure of CNTs was retained however only one example of this was shown by microscopy. A grain refinement effect was also reported in friction stirred aluminium-carbon nanotube specimens relative to friction stirred aluminium alloy specimens. This was not investigated by (Lim et al., 2009).

The yield strength of friction stirred Al/CNT specimens was shown to improve relative to friction stirred Al samples. An increase in carbon nanotube concentration from 0 to 3 wt.% was shown to improve yield strength. In terms of Ultimate Tensile Strength (UTS), it was reported that an increase in CNT concentration from 0 to 1 wt.% resulted in an improvement in UTS of 50-60MPa. UTS began to deteriorate as CNT percentage was further increased up to 3wt.%.

Furthermore (Liu et al., 2011) proposed a yield strength equation based on load transfer and grain refinement. Results from this equation were in good agreement with experimental values, which indicated strongly that the increase in yield strength of the Al/CNT composites could be attributed to the load transfer effect from matrix to carbon nanotubes, and also to the grain refinement effect.

Other investigations into melt processing of metal matrix-carbon nanotube composites include (Li et al., 2009) who investigated a two-step process to fabricate MMCs. Firstly, carbon nanotubes were dispersed onto magnesium alloy chips using a polymer. The chips were then melted, poured into a cylindrical mould and mechanically stirred at 370rpm for 30 minutes. Results from microscopy on pre-dispersed Mg alloy chips revealed that CNTs were evenly distributed on Mg alloy chips.

Raman spectroscopy was carried out and confirmed that the CNT structures were intact and had survived the dispersion process. Composite specimens were examined for grain refinement and no significant change was observed. This disagreed with other work done by (Liu et al., 2011) who reported grain refinement effects when investigating the fabrication of aluminium-carbon nanotube composite specimens.

This study took a different approach to mechanical property evaluation than other studies detailed in this report; compressive mechanical properties were investigated rather than tensile. However (Li et al., 2009) reported that mechanical properties of melt stirred Mg-CNT composite specimens, namely compression at failure (36% improvement), compressive yield strength (10% improvement) and ultimate

compressive strength (20% improvement), were all enhanced by the addition of 0.1 wt.% CNTs.

The thermal stability of CNTs is another factor to be considered in the melt processing of MM-CNT composites. The stability of CNTs is high due to the near perfect nature of their structure. In-plane sigma bonds between carbon atoms give rise to high mechanical strength, whilst out-of-plane orbital bonds lead to high thermal and electrical conductivity. Carbide formation during contact of matrix material with the side of the carbon nanotube is not favourable due to the stable nature of the stable nature of basal plane within the graphene sheet. Contact of matrix material with the end of a carbon nanotube however can lead to significant interaction leading to carbide formation at the interface between CNT and matrix material (Agarwal et al., 2011).

2.7 Summary

In summary, a review of the existing literature on metal matrix-carbon nanotube composites showed that most studies focused on just one preparation method for fabrication and limited studies have been done comparing mixing methods. There was general agreement that addition of carbon nanotubes improves mechanical properties compared to conventional metals/alloys. There was disagreement whether CNTs cause a grain refinement effect. A variety of fabrication techniques have been investigated with the issue of CNT dispersion being consistently highlighted as a key factor during processing. The application of novel techniques such as the ECAP process to the fabrication of MMCs has, to date, been limited.

The objective of this report is to select several processing techniques involving powder metallurgy, sintering and melt processing, as well as the ECAP process, and to compare and contrast these processes in terms of final composite properties.

In addition the effect of powder metallurgy processing parameters such as powder mixing speed and mixing time will be investigated and compared.

Chapter 3

Experimental Procedure

3.1 Raw Materials

Pure Aluminium powder with a particle size of 10µm 99.97% purity was supplied by the Aluminium Powder Company (ALPOCO). 3 types of Multi-walled carbon nanotube (MWNTs) were used and are shown in table 6 below:

Nanotube type	Length	Outer diameter	Inner diameter	Purity	Supplier
Industrial Grade (IGMWNTs)	10-30µm	10-30nm	5-10nm	90wt.%	CheapTubes.com
NC-7000	1.5µm (Average)	9.5nm (Average)	-	90wt.%	Nanocyl
High Grade	10-30µm	<8nm	2-5nm	>95wt.%	CheapTubes.com

Table 6: Summary of the different grades of multi-walled carbon nanotubes used to make composite specimens

3.2 Powders

Aluminium-2wt. % CNT powders were mixed via 3 routes. The first method used a Fritsch Pulverisette 5 planetary ball miller, a 250ml stainless steel ball milling chamber was used to which 29.4g of pure Aluminium powder and 0.6g of carbon nanotubes were added, giving an overall mass of 30g and an overall nanotube concentration of 2wt.%. 37 stainless steel ball bearings each of diameter 10mm were placed into the chamber to ensure a ball to powder weight ratio of 5:1. Finally 2ml of methanol was added as a process control agent (PCA) to avoid cold welding of particles to chamber wall or to ball bearings. The chamber was then sealed, placed in the planetary ball miller and milled at 250rpm for 1 hour.

The second method was identical with the exception that the milling time was increased from 1 hour to 4 hours.

The final method of powder preparation used a Fritsch turbula mixer. A plastic jar containing 300g of 2wt. % aluminium-carbon nanotube master alloy and 10 stainless steel ball bearings of diameter 10mm was mixed at 49rpm for 8 hours.

Master alloy samples were prepared using all 3 grades of carbon nanotube.

3.3 Powder Compacts

In order to produce green compact specimens, 5.5g of master alloy was placed into a tool steel die and punch system as shown in figures 4 and 5.

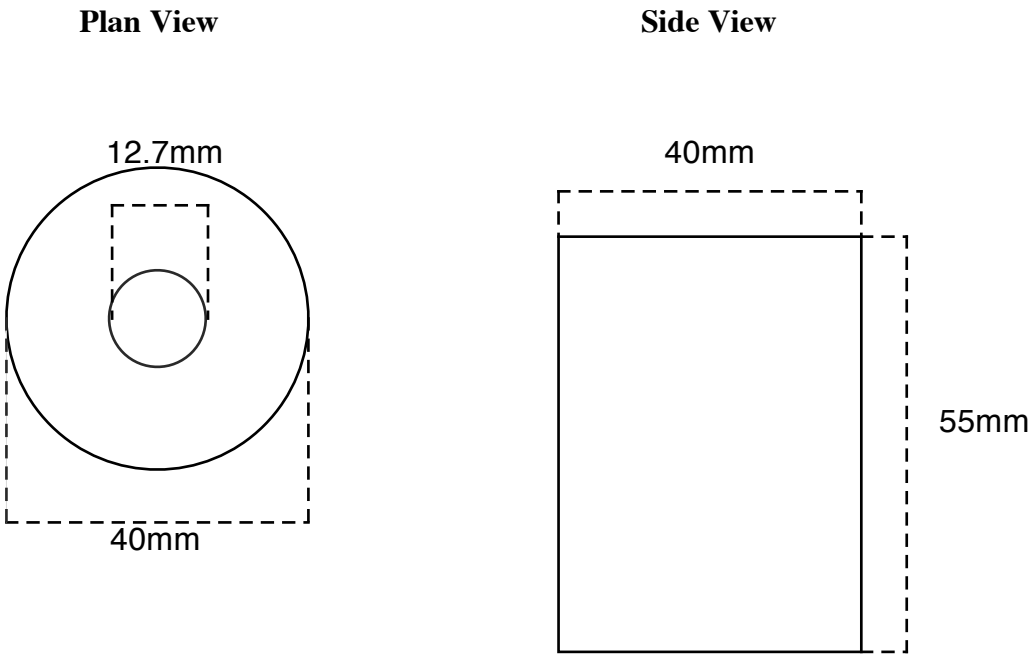

Figure 4: Schematic diagrams of powder compact die showing measurements in the plan and side views

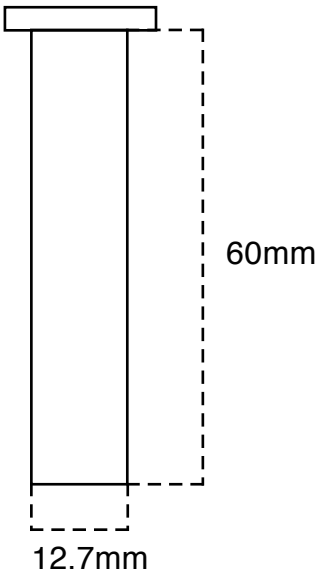

Figure 5: Schematic diagram of the powder compact punch showing measurements and a side view profile

Once the powder had been loaded into a lubricated die (lubricant used was 10% Kenolube and 90% ethanol). It was then pressed using a hydraulic press using a force of 50kN, equivalent to 400MPa. This produced a compact with approximate dimensions of 12.5mm x 15mm.

3.4 Equal Channel Angular Pressing (ECAP)

A second method of compaction (ECAP) was used to investigate the effect of strain during ECAP on porosity and CNT cluster removal.

Green compact specimens were pressed in an ECAP die as shown below**:**

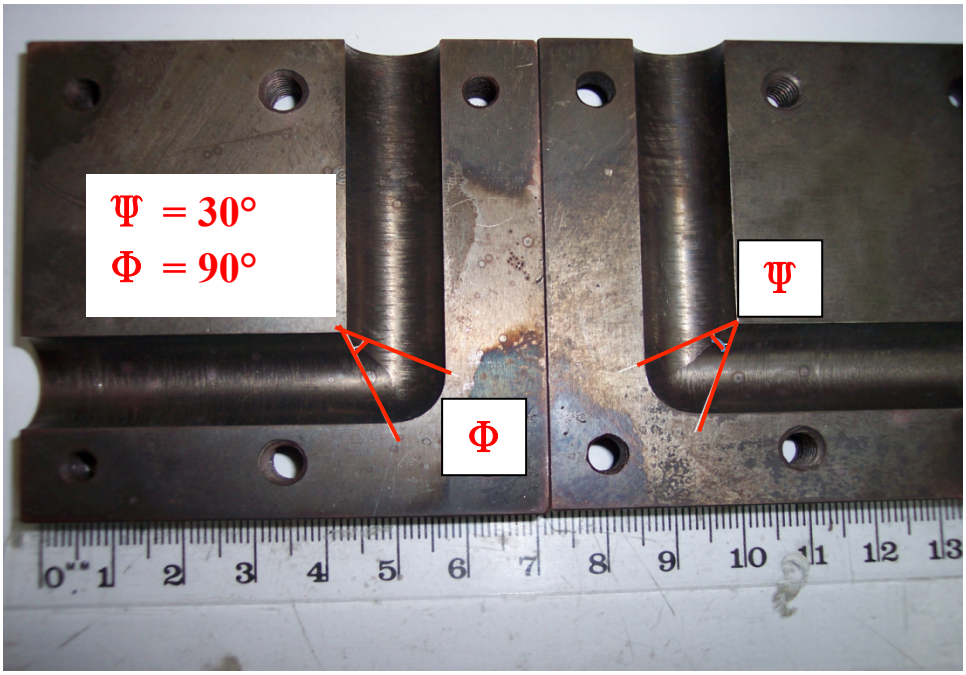

Figure 6: Diagram of the internal geometry of the ECAP die

The press was calibrated to 100kN (800MPa), however, due to lack of backpressure within the die, in practice specimens were pressed through the ECAP die at

approximately 40kN (320MPa). The die was lubricated with a mixture of 10% graphite lubricant and 90% ethanol to ensure no seizures whilst pressing.

3.5 Sintering

Green compact specimens were placed in an Elite tube furnace and heated to 620^{o}C in an inert nitrogen atmosphere at a rate of 10^{o}Cmin^{-1} to prevent further oxidation of aluminium powder. Other inert atmospheres e.g. argon or helium could also be used. Specimens were then held at this temperature for 2 hours before finally being allowed to cool.

3.6 Casting

Cast specimens were prepared by placing 45 grams of super purity aluminium in a conical ALSINT crucible, giving a total casting mass of 50g. The crucible contents were heated to 720^{o}C in a furnace and held until molten, an aluminium-CNT composite ECAP specimen of mass 5 grams was then added to the crucible, giving a total casting mass of 50g. The crucible was then stirred manually using a ceramic rod before being placed back in the furnace for a further 10-15 minutes and finally being removed and allowed to cool in air.

3.7 Sample Preparation

All samples were sectioned, powder compact and sintered specimens were sectioned at the midpoint, ECAP samples were sectioned in the longitudinal and transverse directions and casting were sectioned at the surface, edge and mid-point. Specimens were then either hot mounted in Bakelite or cold mounted in Met Prep vari-set cold mount.

3.7.1 Grinding

Following mounting, samples were ground to achieve a flat surface. The procedure used to grind samples is shown in table 7; all papers used were silicon-carbide (SiC) based.

Paper	Grit	Average Grinding Time (Minutes)	Lubricant
SiC	120	2	Water
SiC	240	2	Water
SiC	400	2	Water
SiC	800	2	Water
SiC	1200	2	Water
SiC	1400	2	Water

Table 7: Summary of grinding procedure used on composite samples

3.7.2 Polishing

In order to prepare samples for SEM examination, samples were polished to achieve a clean flat surface. Samples were polished using a manual polishing wheel using Struers polishing clothes and suspension. The procedure used to polish samples is shown in table 8.

Polishing Media	Size	Average Polishing Time (Minutes)	Diamond Suspension
MD-NAP	3µm	2	Diaduo
MD-CHEM	1µm	1	Diaduo
MD-Chem	0.04µm	0.5	OPS

Table 8: Summary of polishing procedure used on composite specimens

3.7.3 Etching

Samples were etched using Keller's reagent (95ml H_2O, 2.5ml HNO_3, 1.5ml HCl, 1.0ml HF) for approximately 15 seconds.

3.8 Sample Analysis

3.8.1 Microscopy

Jeol 6000 and Jeol 7000 SEM microscopes were used to perform microscopy on all samples.

3.8.2 Grain size measurements

Micrographs were taken using an SEM; the images were loaded into JMicroVision program where the image scale was calibrated. Approximately 100 aluminium/CNT particles were then drawn around using the software and the equivalent circle diameters were calculated using the scale bar calibration. These values were then tabulated and plotted in histogram format.

3.8.3 Density

Compacted, ECAP, sintered and cast samples were weighed and then submersed in a 250ml beaker of water and placed in a desiccator attached to a vacuum pump. The vacuum pump was then used to remove all air from the desiccator and from within the samples. Any air present within sample pores was replaced by water. Once this was complete, samples were removed from the desiccator and weighed again, while submersed, and in air. This was done in order to determine the degree of porosity within the specimens, as a greater the degree of porosity within the sample would result in a greater volume of air to be replaced by water during vacuum pumping and thus a greater the mass of the final sample once removed from the desiccator. A schematic of the equipment used is shown in figure 7. The density of the sample was then calculated using equation 3.2.

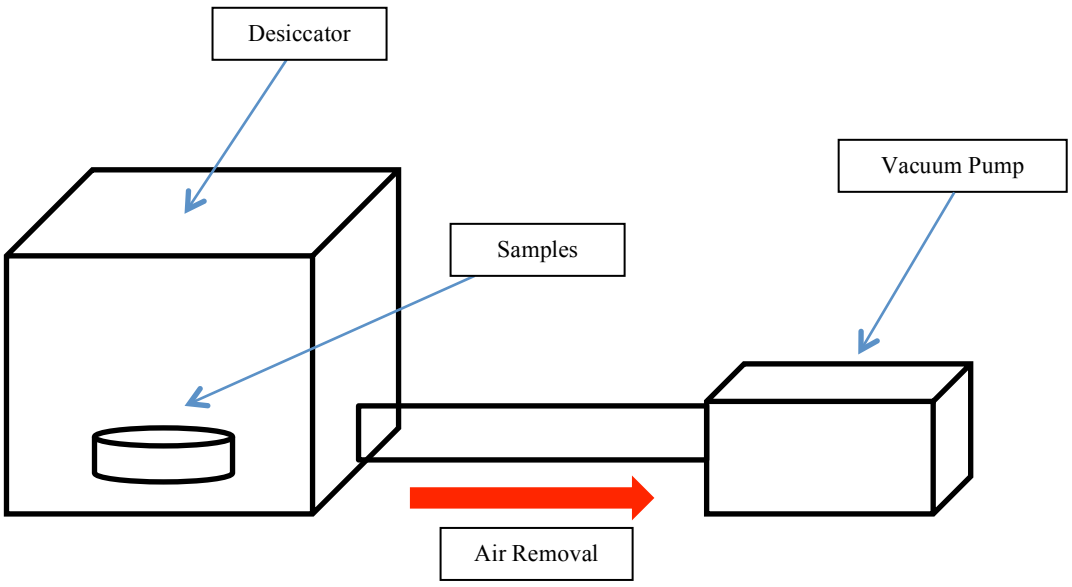

Figure 7: Schematic of desiccator apparatus used density measurement

$$\rho = \left[\frac{\text{Mass}_{\text{Initial}}}{\text{Mass}_{\text{Final wet}} - \text{Mass}_{\text{Final Dry}}}\right] \text{x } \rho_{\text{water}} \qquad \text{Equation 3.2}$$

Where:

ρ = composite density

$\text{Mass}_{\text{Initial}}$ = initial mass of sample

$\text{Mass}_{\text{Final wet}}$ = final mass of composite submerged

$\text{Mass}_{\text{Final Dry}}$ = final mass of composite in air

ρ_{water} = density of water = 0.9987gcm^{-3}

3.8.4 Hardness

Samples were sectioned, ground to a 400 grade finish using silicon carbide papers, cleaned using methanol, and then tested using an Indentec micro hardness tester under a load of 5kg. Hardness measurements were taken across the full diameter of specimens in order to produce a through thickness hardness profile. In the case of ECAP specimens, hardness measurements were taken both in longitudinal and transverse orientations relative to the direction of the ECAP pressing.

Chapter 4

Results

4.1 Carbon Nanotubes

As-received carbon nanotubes were analysed using (SEM). It was observed that industrial grade (90wt. % purity) and NC-7000 (90wt. % purity) were agglomerated to form particles of approximately 40-60μm in diameter (figures 8 & 8.1) however high grade carbon nanotubes (95wt. % purity) showed agglomerate particles ≤10μm in diameter (figure 8.2). The most common method of carbon nanotube production is Catalytic Chemical Vapour Deposition (CCVD). During this process, hydrocarbons are decomposed over a transition metal catalyst (e.g. Fe, Ni, Co) to form CNTs. Catalytic particles facilitate the growth of CNTs and can be located either at the tip or base of the CNT (C.H. See et al., 2006). These catalytic particles cannot be seen by in the micrographs, but are presumed to lie at the centre of entangled CNT network.

Higher magnification images showed individual carbon nanotubes entangled to form agglomerates (Figures 8.3-8.5)

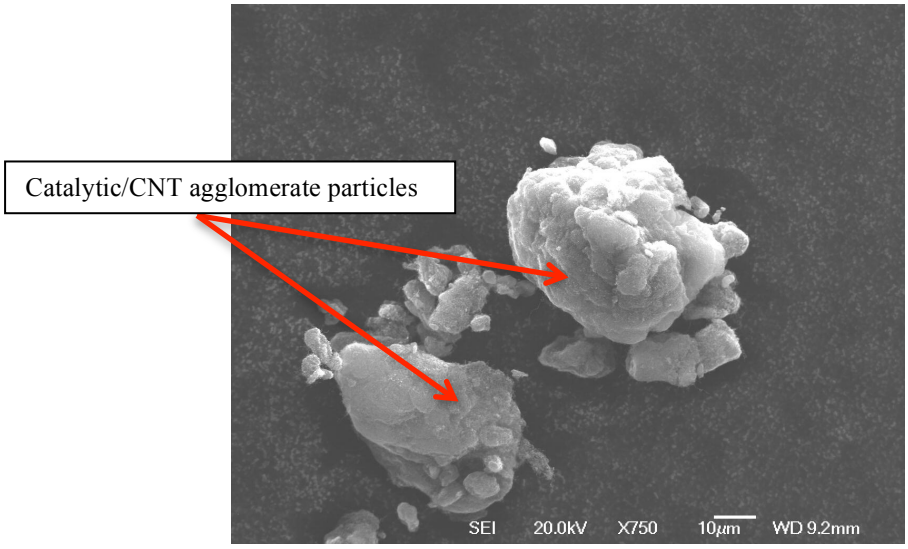

Figure 8: Micrograph showing industrial grade carbon nanotube agglomerate particles

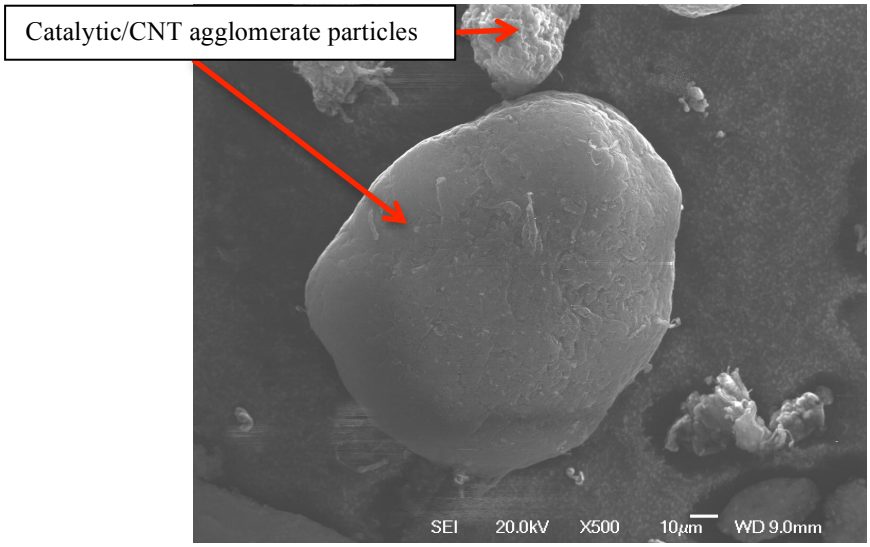

Figure 8.1: Micrograph showing NC-7000 carbon nanotube agglomerate particles

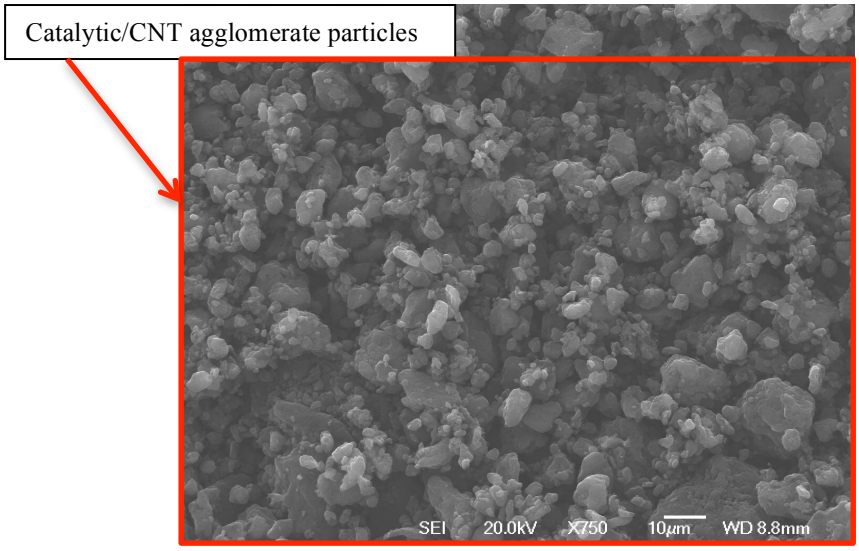

Figure 8.2: Micrograph showing high grade carbon nanotube agglomerate size

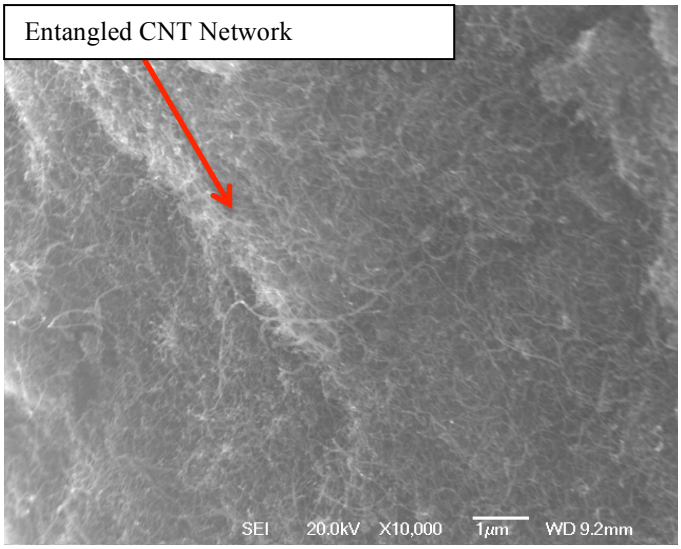

Figure 8.3: High magnification image showing entangled industrial carbon nanotubes

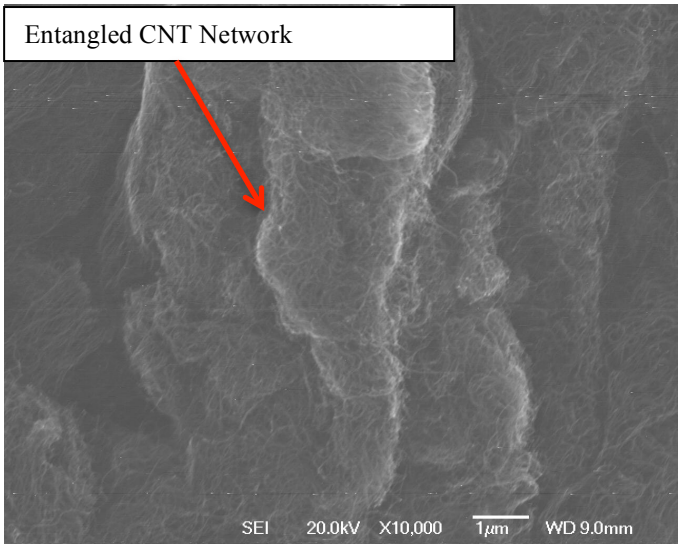

Figure 8.4: High magnification image showing entangled NC-7000 carbon nanotubes

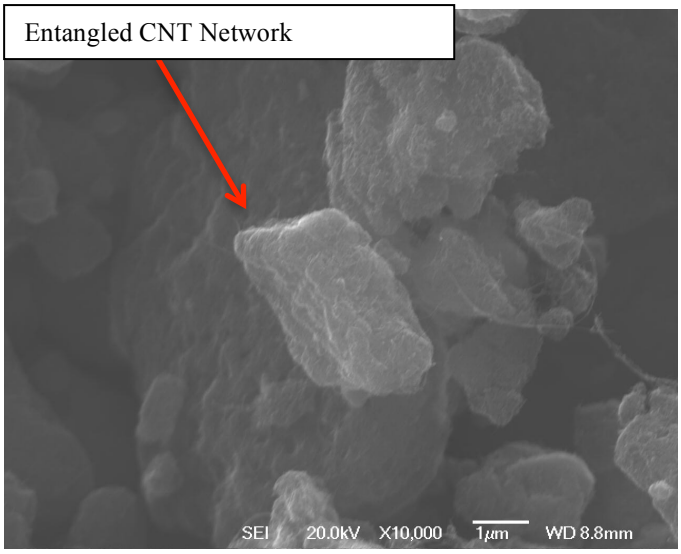

Figure 8.5: High magnification image showing entangled high grade carbon nanotubes

4.2: Composite Preparation (mixing and compaction)

4.2.1 Turbula Mixing for 8 Hours

4.2.1.1 Aluminium-Carbon Nanotube Powders

Powders containing pure aluminium powder and 2wt. % carbon nanotubes that were mixed for 8 hours in the Fritsch turbula mixer (see figure 9) resulted in smooth, uniform aluminium particle morphology with rounded particle edges. Turbula mixed powders were mixed gently at 49rpm and the aluminium particles suffered no damage and were not broken. Particle size analysis was conducted using JMicroVision software and plotted in histogram form (figures 9.1-9.3). Industrial grade carbon nanotube powders placed in a turbula mixer for 8 hours displayed a peak in frequency of particle size at around 7-8μm, a reduction of 2μm from the peak frequency of the starting aluminium powder. This confirmed a loss of material during the mixing process. Similarly, powders mixed for 8 hours in a turbula mixer using NC-7000 carbon nanotubes showed a distribution with a peak at 7-8μm. High grade aluminium-carbon nanotube powders prepared by turbula mixing for 8 hours also showed a particle size distribution with a peak at 7-8 μm. These results showed that turbula mixing had a similar effect on powder preparation, resulting in a reduction in peak particle size.

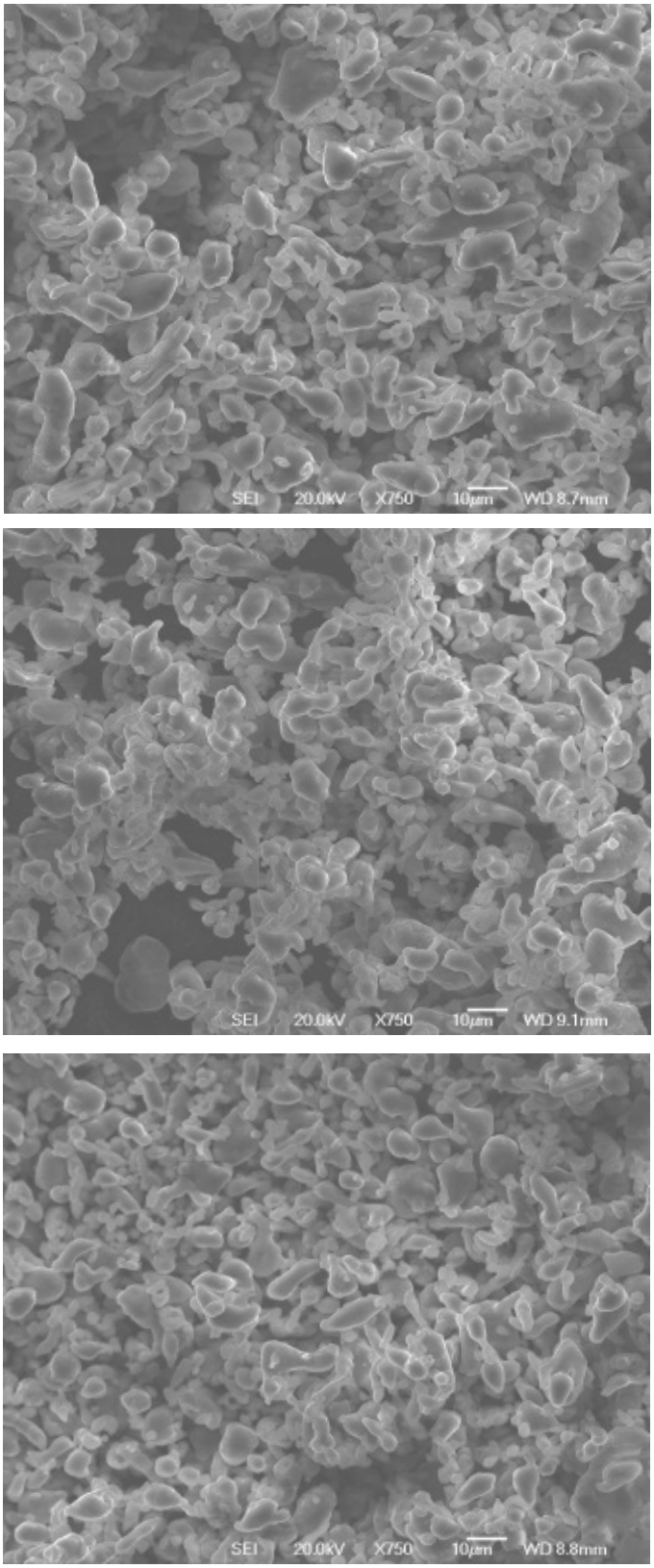

Figure 9: Powder micrographs of Al-2wt. % CNT powders prepared by turbula mixing for 8 hours containing: Industrial grade carbon nanotubes (top), NC-7000 carbon nanotubes (centre) and high-grade carbon nanotubes (bottom)

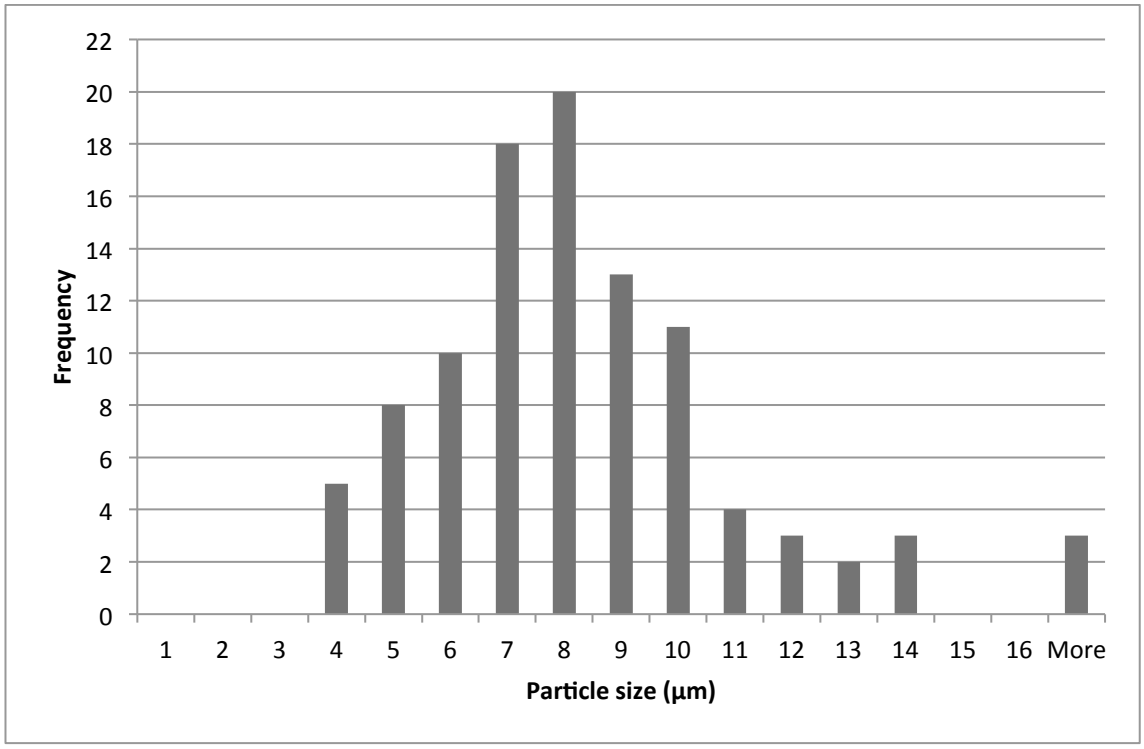

Figure 9.1: Histogram showing particle size distribution in Al-2wt. % CNT powder using industrial grade nanotubes prepared by turbula mixing for 8 hours.

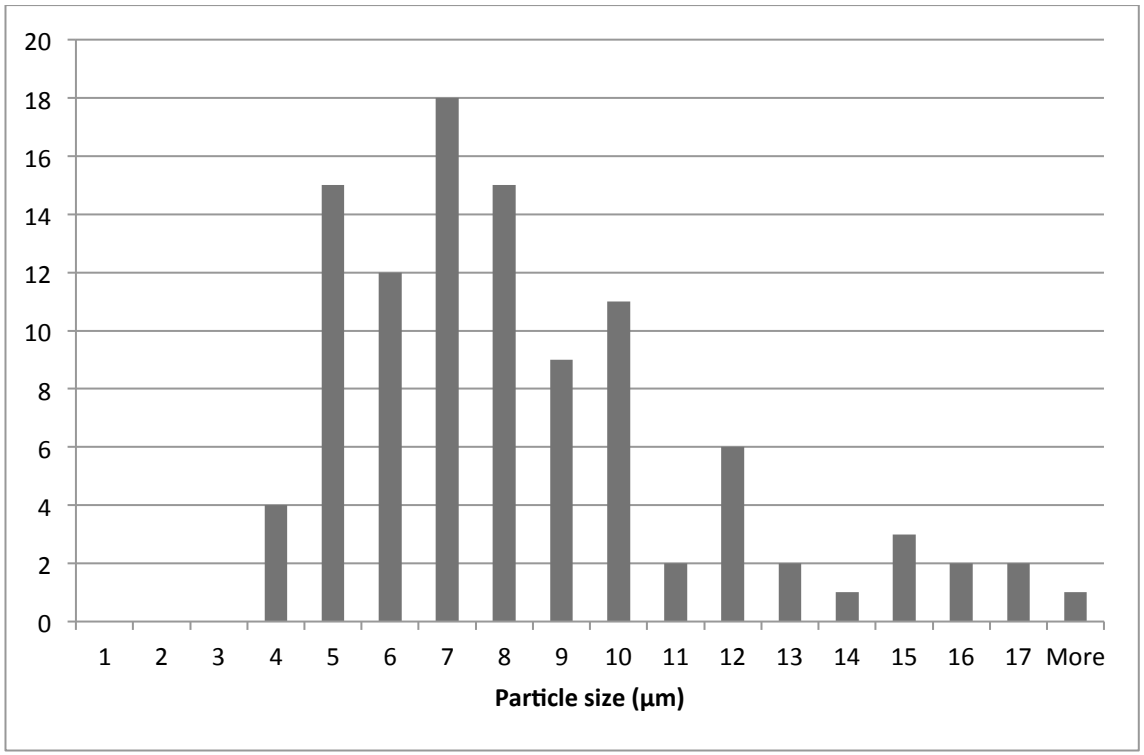

Figure 9.2: Histogram showing particle size distribution in Al-2wt. % CNT powder using NC-7000 nanotubes prepared by turbula mixing for 8 hours.

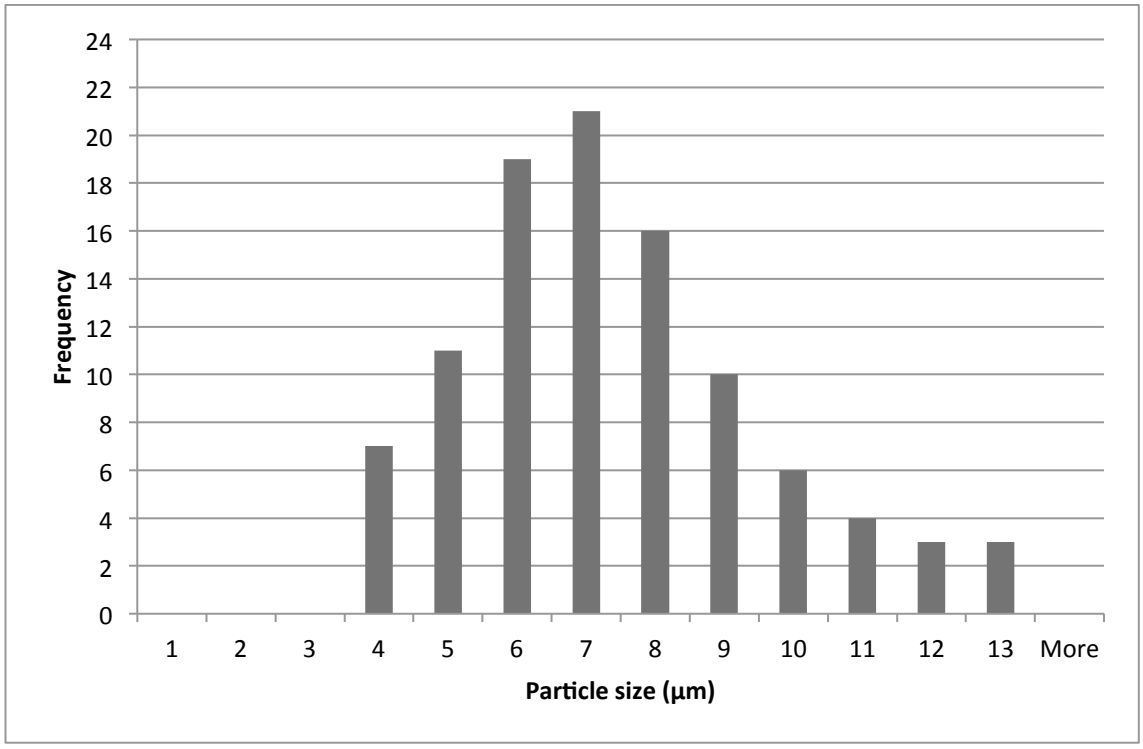

Figure 9.3: Histogram showing particle size distribution in Al-2wt. % CNT powder using high-grade nanotubes prepared by turbula mixing for 8 hours

4.2.1.2 Powder Compaction

Powder compacts containing Al-2wt. % carbon nanotubes were compressed at 200MPa in air and examined by SEM. An example micrograph of is shown in figure 9.4 where porosity can be seen, which was expected given the semi-dense nature of the green compact material. The amount of porosity is quantified in the following section.

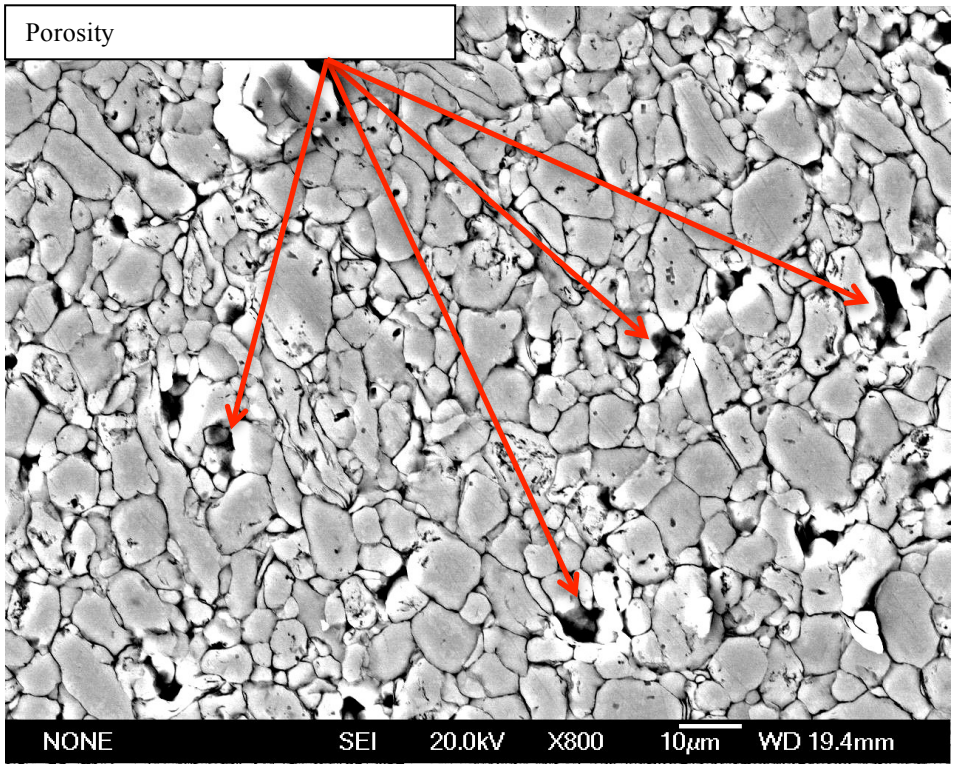

Figure 9.4: Micrograph of Al-2wt. % CNT powder compact specimen produced by turbula mixing for 8 hours

4.2.1.3 Density Evaluation

In order to evaluate the density of the compacts fully and determine the degree of success of compaction, a theoretical maximum density for a fully compacted aluminium-2wt. % CNT compact was calculated using the rule of mixtures principle, as shown below:

$$\rho = V_a \rho_a + V_b \rho_b \qquad \text{Equation 4}$$

Where V_a and V_b are the volume fractions of phase a (aluminium) and phase b (carbon nanotubes) respectively, and ρ_a and ρ_b refer to the densities of phase a and phase b. Each grade of carbon nanotubes supplied had a quoted true density of 2.1gcm^{-3} and the density of the aluminium powder supplied was quoted as 2.70gcm^{-3}at room temperature; the calculated theoretical maximum density of an aluminium composite system containing 2wt.% carbon nanotubes was therefore 2.68gcm^{-3}. Samples from each mixing method, and each grade of carbon nanotube, as well as pure aluminium specimens, were measured using pycnometry. The density of samples prepared by turbula mixing for 8 hours (figure 8.5) showed that a maximum density of 2.45gcm^{-3} was achieved. This was calculated to be 91% of the maximum theoretical density.

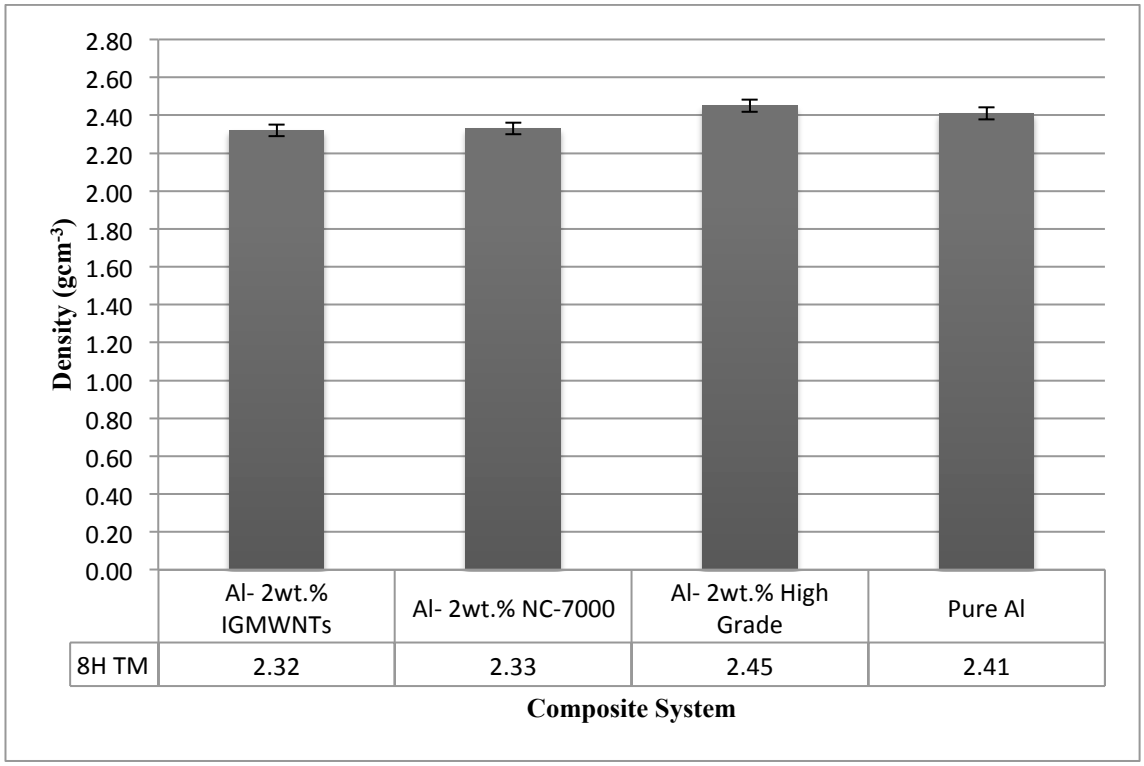

Figure 9.5: Graph showing density values measured from Al-2wt. % CNT samples prepared by turbula mixing for 8 hours

4.2.1.4 Hardness Evaluation

Green compact samples were subjected to Vickers hardness testing under a load of 2.5kg. Hardness data obtained from the green compact specimens prepared by turbula mixing for 8 hours is shown in figure 9.6 and showed a low mean through-thickness Vickers hardness of between 11 and 30. Samples which used both industrial grade and NC-7000 carbon nanotubes showed a large degree of fluctuation in the through thickness hardness, with a peak in hardness seen at the centre of the sample. Samples prepared using high grade carbon nanotubes however produced the highest average through-thickness hardness and also were the most consistent with the least variation in hardness.

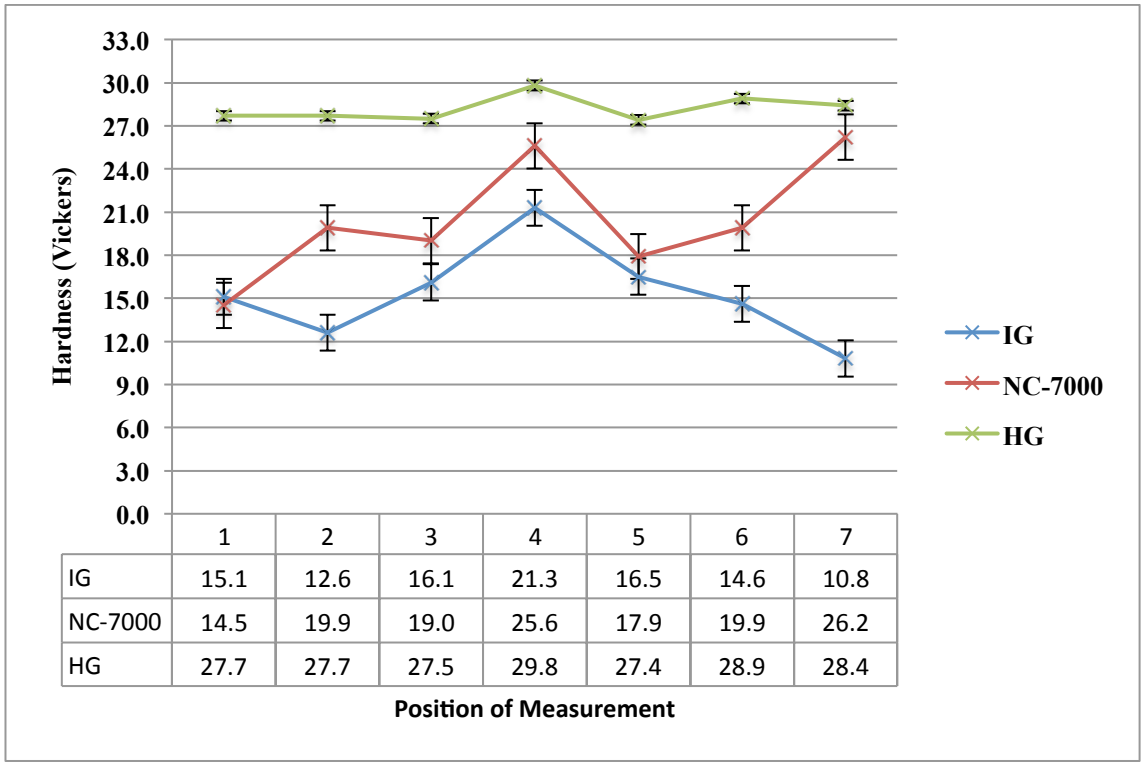

	1	2	3	4	5	6	7
IG	15.1	12.6	16.1	21.3	16.5	14.6	10.8
NC-7000	14.5	19.9	19.0	25.6	17.9	19.9	26.2
HG	27.7	27.7	27.5	29.8	27.4	28.9	28.4

Figure 9.6: Graph showing through thickness Vickers hardness measurements from compacted aluminium-2wt. % CNT samples prepared by turbula mixing for 8 hours with standard error bars.

4.2.2: Ball Milling for 1 Hour

4.2.2.1 Aluminium-Carbon Nanotube Powders

Analysis of 1 hour ball milled powders, shown in figure 10, revealed that powders ball milled at 250 rpm for 1 hour in a Fritsch planetary ball miller showed more angular particle morphology, with sharp particle edges. Planetary ball milling is a more aggressive mixing method than turbula mixing, and consequently powders produced by this method contained uneven broken aluminium particles. Particle size analysis (figures 10.1-10.3) showed that powder samples ball-milled for 1 hour using industrial grade carbon nanotubes produced a reduction in particle size with the most frequent sizes occurring at 4-7μm. Powders using NC-7000 and high grade carbon nanotubes also show modal particle size values of 5-7μm. These results showed that ball milling for 1 hour has a different effect upon all powder compositions to that of turbula mixing for 8 hours. Ball milling for 1 hour produced a smaller final particle size (4-7μm) than that of turbula mixing for 8 hours (7-8μm).

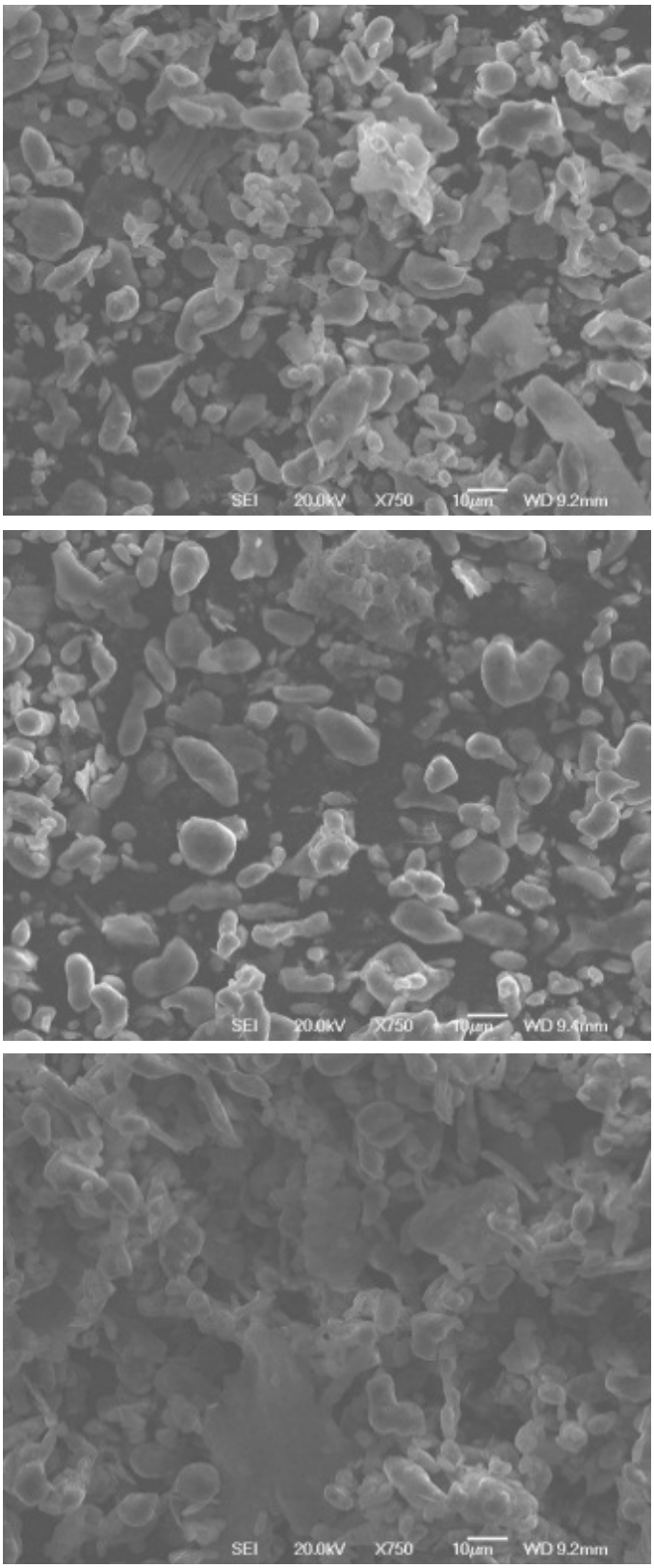

Figure 10: Powder micrographs of Al-2wt.% CNT powders prepared by ball milling for 1 hour containing: Industrial grade carbon nanotubes (top), NC-7000 carbon nanotubes (centre) and high-grade carbon nanotubes (bottom)

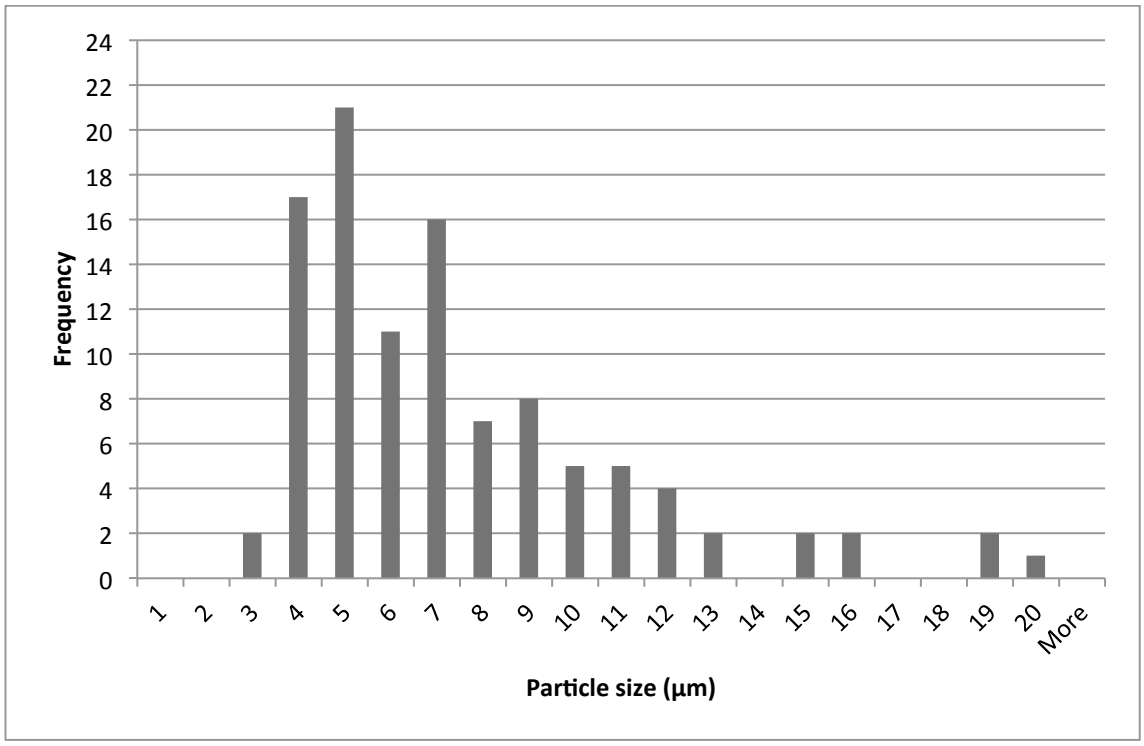

Figure 10.1: Histogram showing particle size frequencies in Al-2wt.% CNT powder using industrial grade carbon nanotubes prepared by ball milling for 1 hour

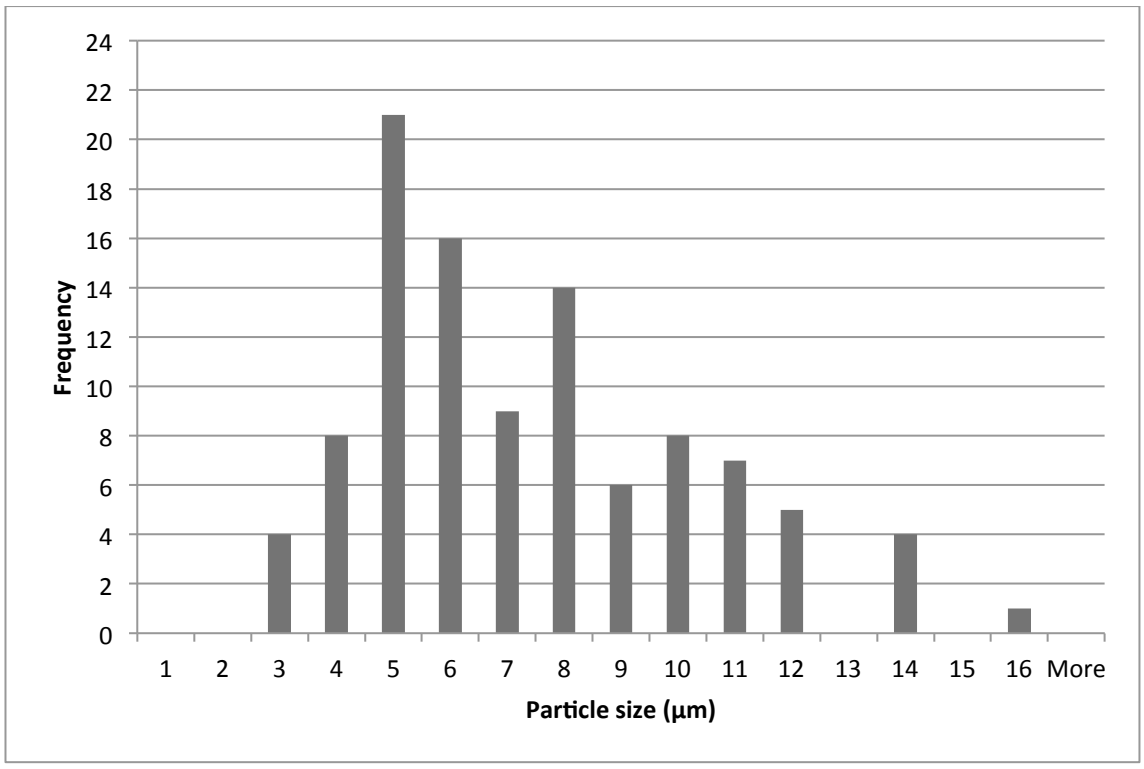

Figure 10.2: Histogram showing particle size frequencies in Al-2wt.% CNT powder using NC-7000 carbon nanotubes prepared by ball milling for 1 hour

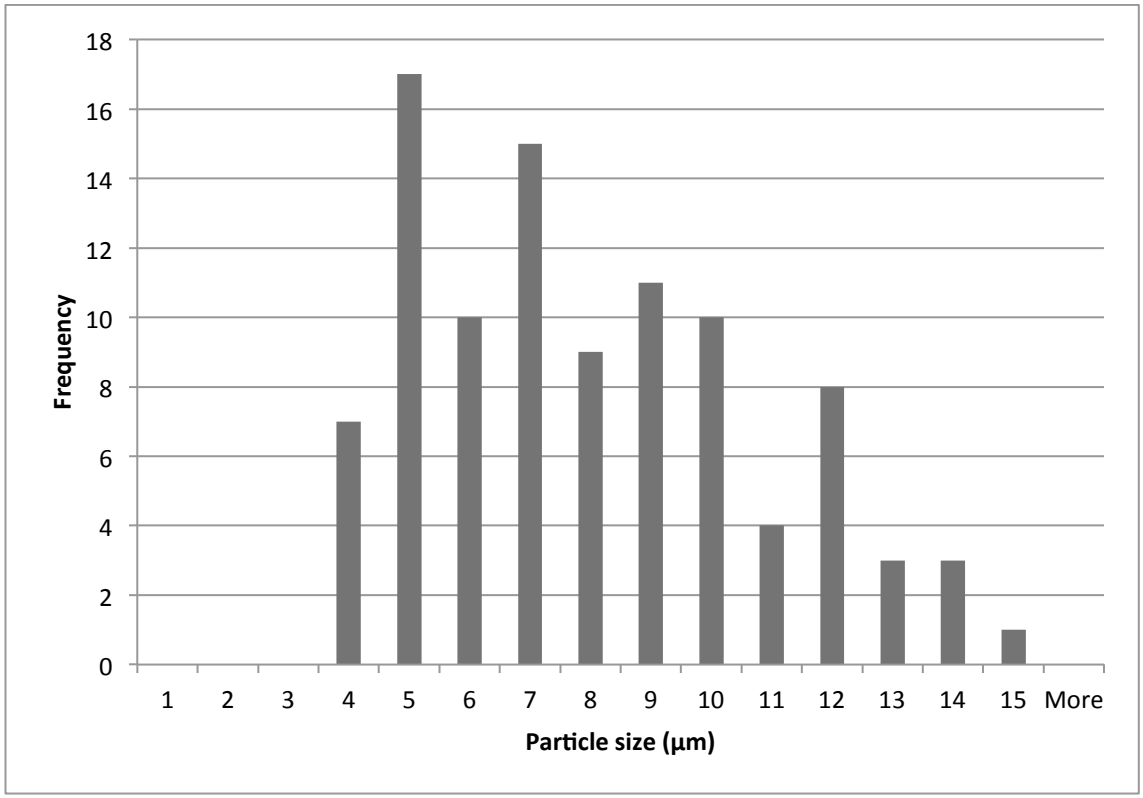

Figure 10.3: Histogram showing particle size frequencies in Al-2wt. % CNT powder using high-grade carbon nanotubes prepared by ball milling for 1 hour

4.2.2.2 Powder Compaction

A typical microstructure of a powder compact produced from Al-2wt. % CNT powders prepared by ball milling for 1 hour is shown in figure 10.4. All powder compositions (industrial grade, NC-7000 and high grade) showed similar microstructures including the presence of porosity.

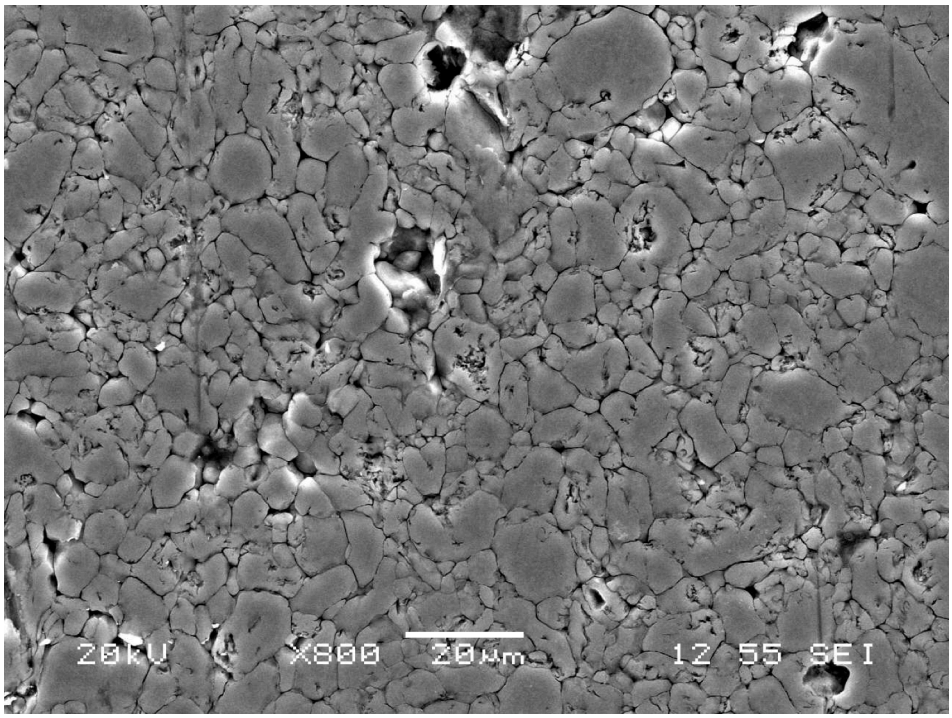

Figure 10.4: Example micrograph from compacted Al-2wt.% CNT powder prepared by ball milling for 1 hour

4.2.2.3 Density Evaluation

Density values from specimens prepared by ball milling for 1 hour followed by compaction are shown in figure 10.5 and revealed a correlation in mean density to that of equivalent turbula mixed powder compact specimens. Preparation using high grade carbon nanotubes yielded samples with the highest average density value of 2.39gcm^{-3} taken from a population of 3 samples. When compared to the maximum theoretical density value of 2.68gcm^{-3} it was calculated that specimens prepared by ball milling for 1 hour achieved a maximum of 89% of the maximum theoretical density.

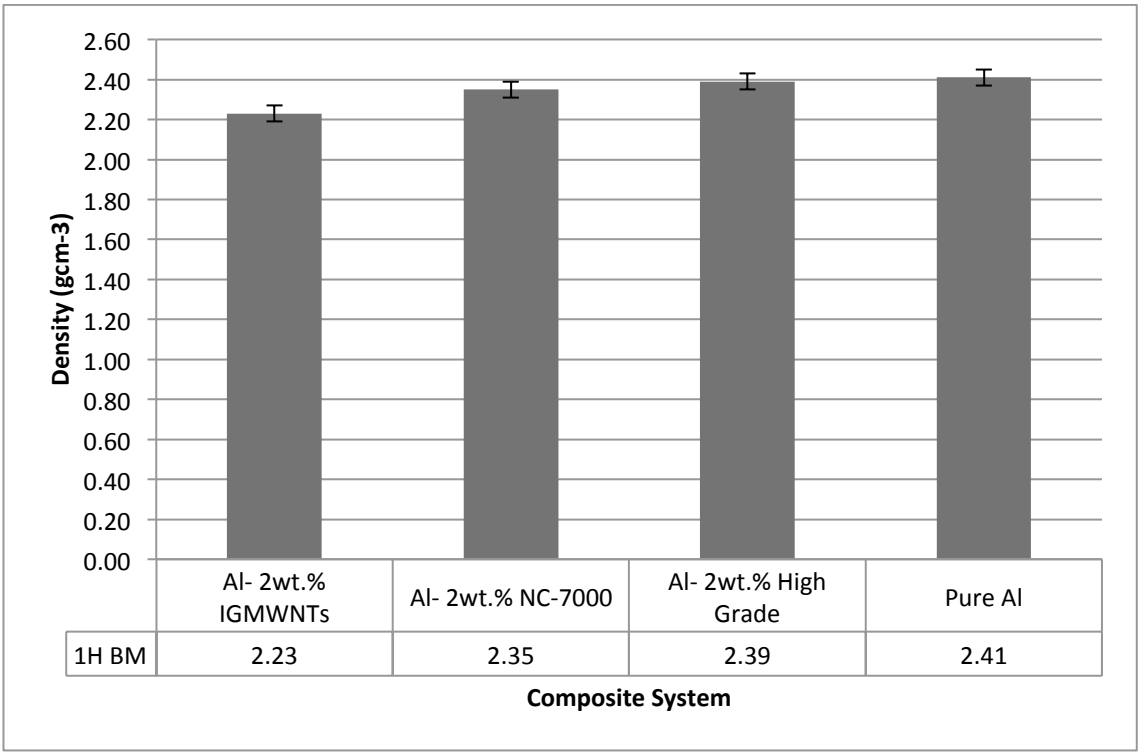

Figure 10.5: Graph showing comparison of density values measured from Al-2wt. % CNT powders prepared by ball milling for 1 hour.

4.2.2.4 Hardness Evaluation

Micro hardness test data from specimens prepared by ball milling for 1 hour and compacted (figure 10.6) showed an improvement in hardness compared to specimens turbula mixed powder compact for 8 hours. The average hardness achieved by turbula mixed specimens was 21.3Hv whereas the average hardness produced by specimens prepared by ball milling for 1 hour was 33.4Hv, an increase of 64%. High grade carbon nanotubes were again shown give the highest hardness values. The degree of variation in through thickness hardness was seen to be reduced by preparing the powder by ball milling for 1 hour, compared to turbula mixing for 8 hours.

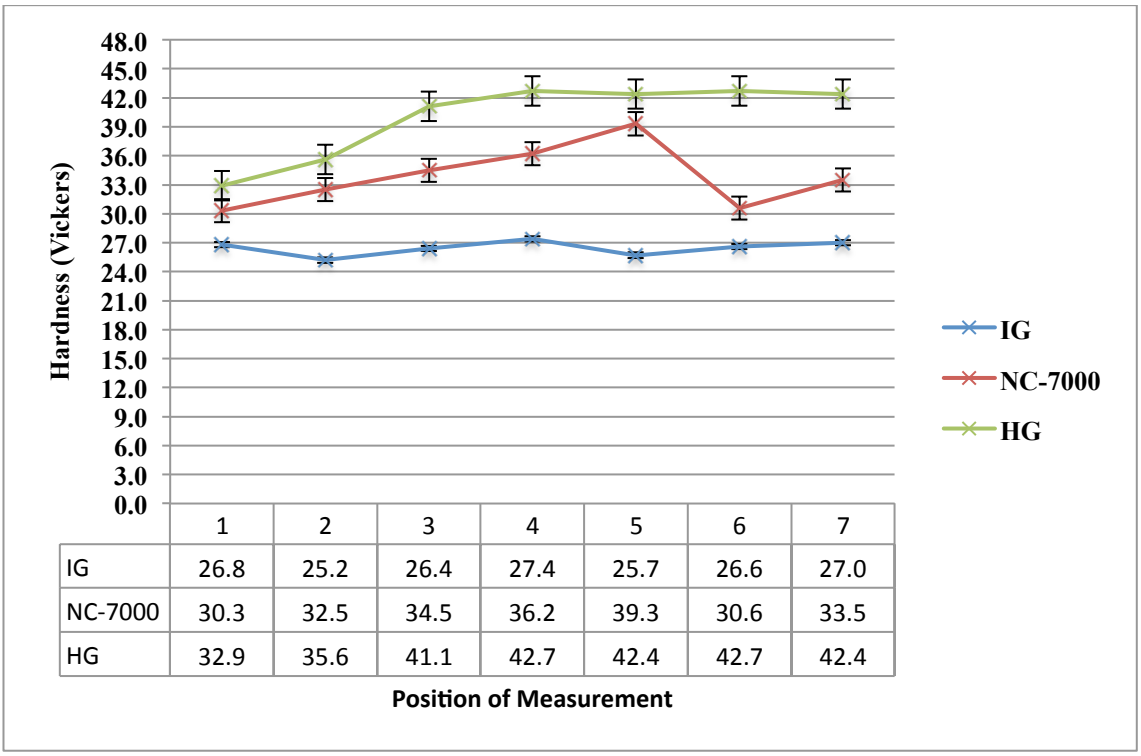

	1	2	3	4	5	6	7
IG	26.8	25.2	26.4	27.4	25.7	26.6	27.0
NC-7000	30.3	32.5	34.5	36.2	39.3	30.6	33.5
HG	32.9	35.6	41.1	42.7	42.4	42.7	42.4

Figure 10.6: Graph showing through-thickness hardness of Al-2wt. % CNT composite specimens prepared by ball milling for 1 hour

4.2.3: Ball Milling for 4 Hours

4.2.3.1 Aluminium-Carbon nanotube powders

Powders produced by ball milling for 4 hours (figure 11) showed the sharpest and most varied particle morphologies of all mixing methods. Analysis of particle sizes (figures 11.1-11.3) showed that an increase in milling time further reduced particle size. Samples ball milled for 4 hours showing the highest frequency of particles in the 3-6μm size range.

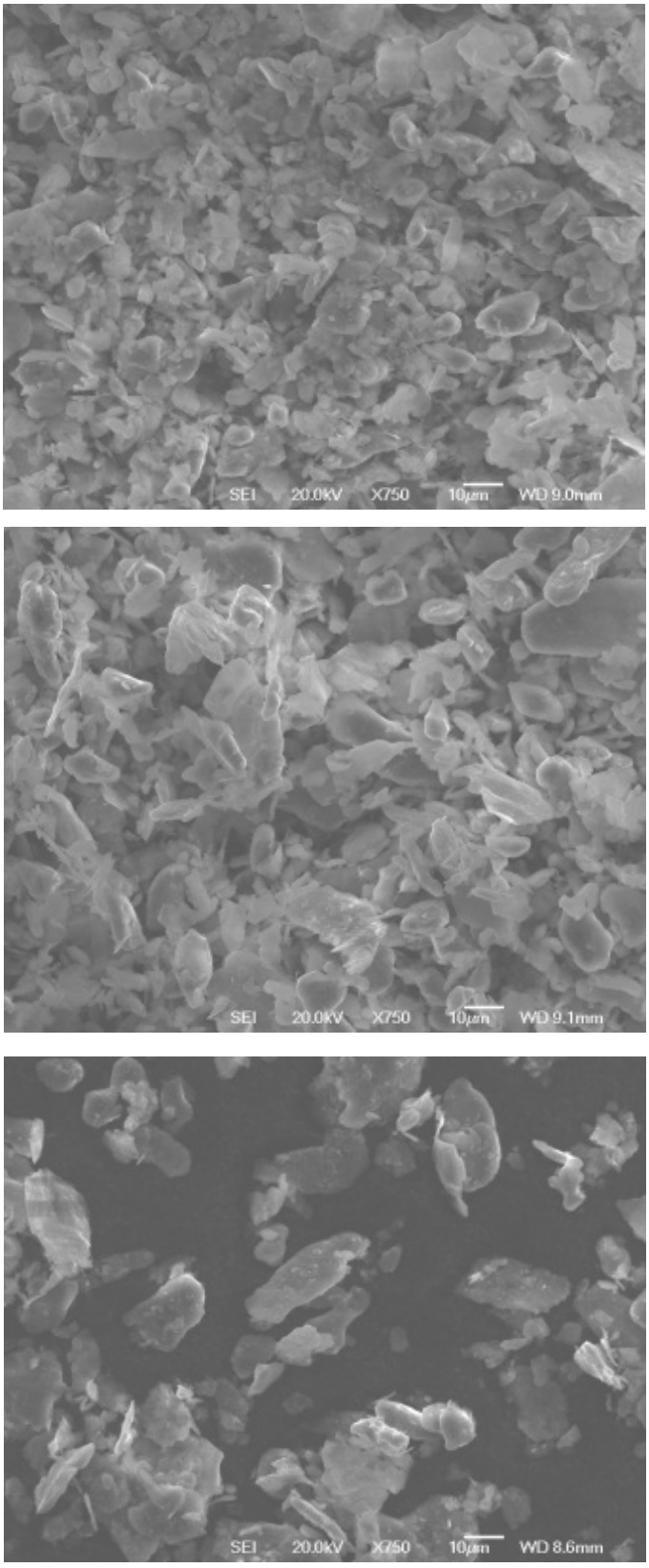

Figure 11: Micrographs showing Al-2wt.% CNT powders produced by ball milling for 4 hours using industrial grade carbon nanotubes (top), NC-7000 carbon nanotubes (centre) and high grade carbon nanotubes (bottom).

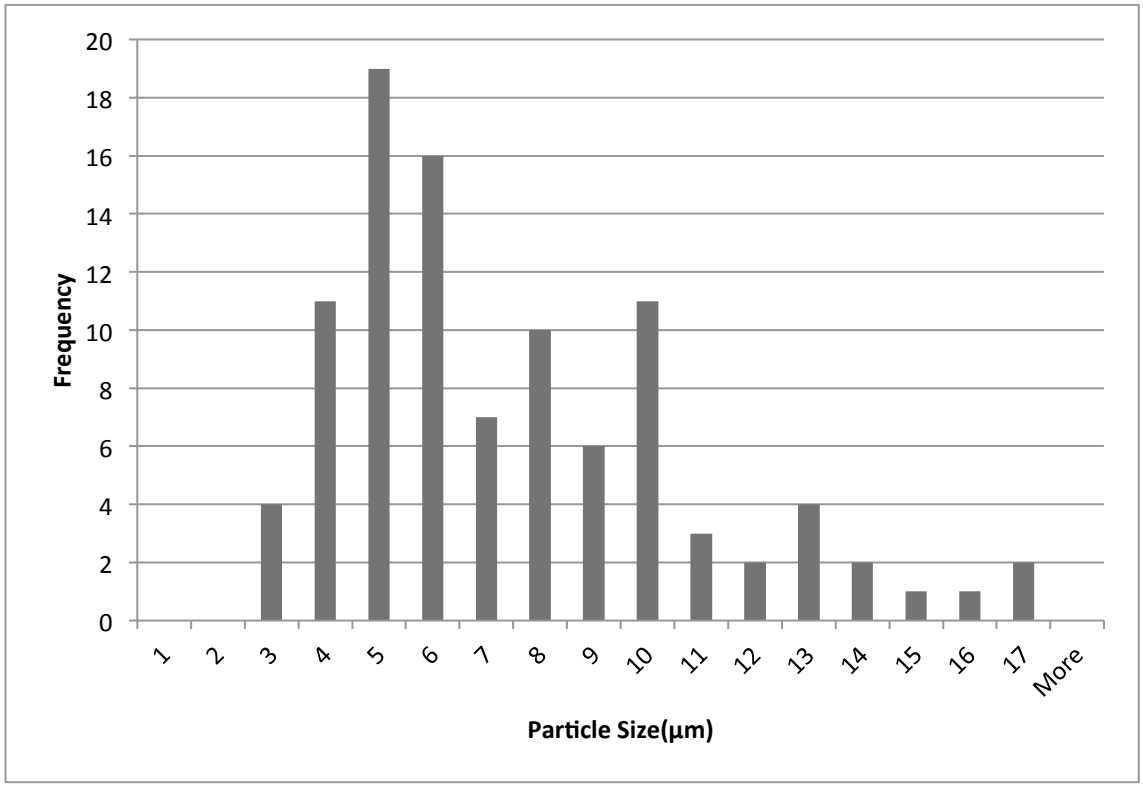

Figure 11.1: Histogram showing particle size frequencies in Al-2wt.% CNT powders prepared by ball milling for 4 hours and using industrial grade carbon nanotubes

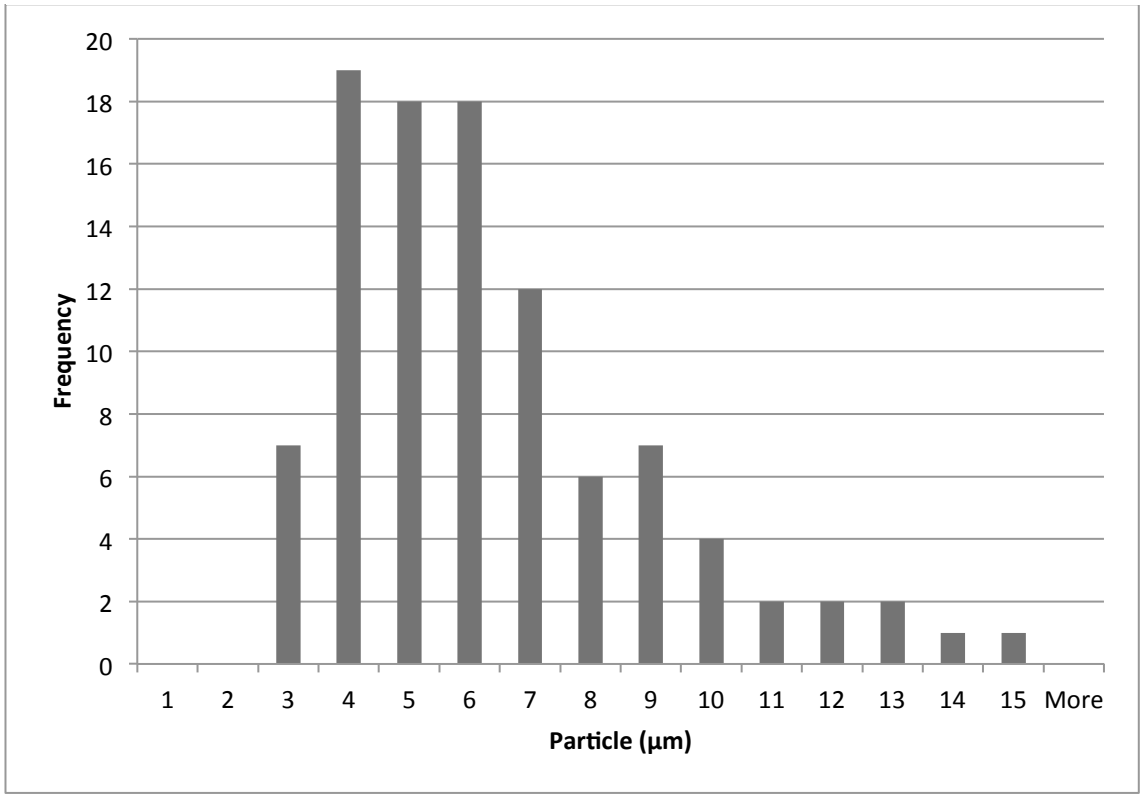

Figure 11.2: Histogram showing particle size frequencies in Al-2wt. % CNT powders prepared by ball milling for 4 hours and using NC-7000 carbon nanotubes

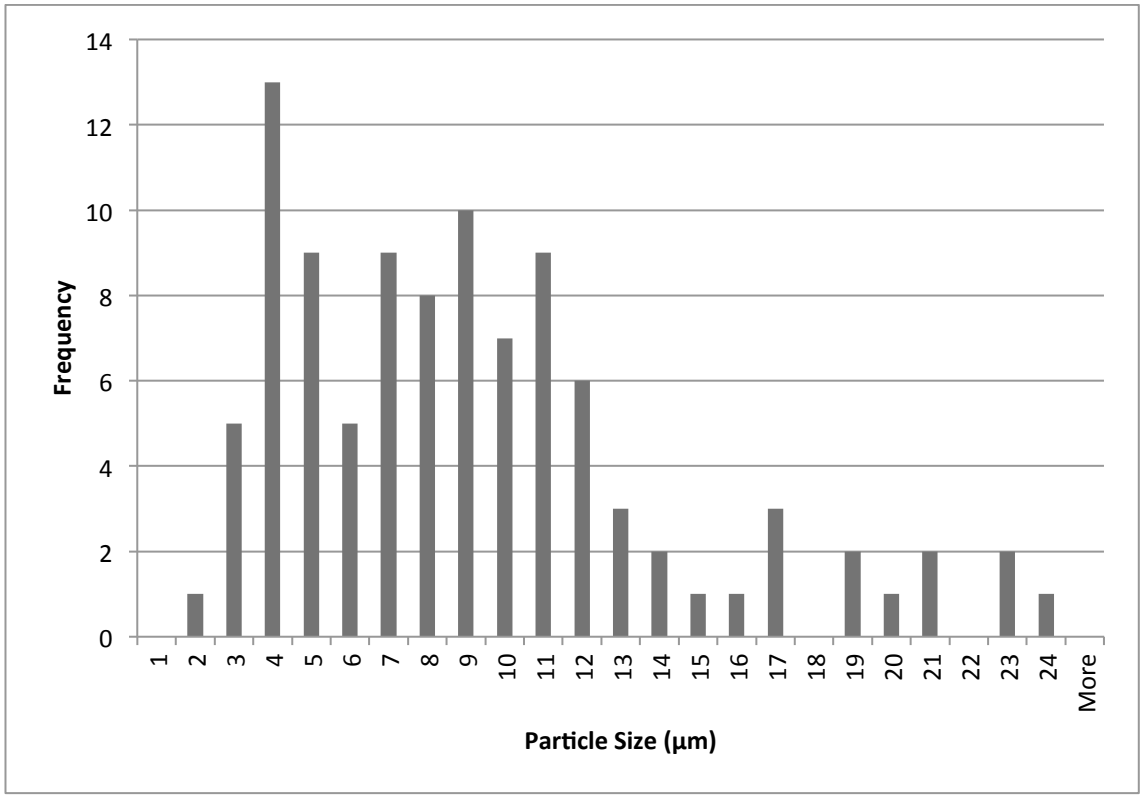

Figure 11.3: Histogram showing particle sizes in Al-2wt. % CNT powder prepared by ball milling for 4 hours and using high grade carbon nanotubes

4.2.3.2 Powder Compaction

A micrograph of an Al-2wt. % CNT compacted specimen prepared by ball milling for 4 hours is shown in figure 11.4. Samples using each grade of carbon nanotube showed comparable microstructures, with each showing porosity.

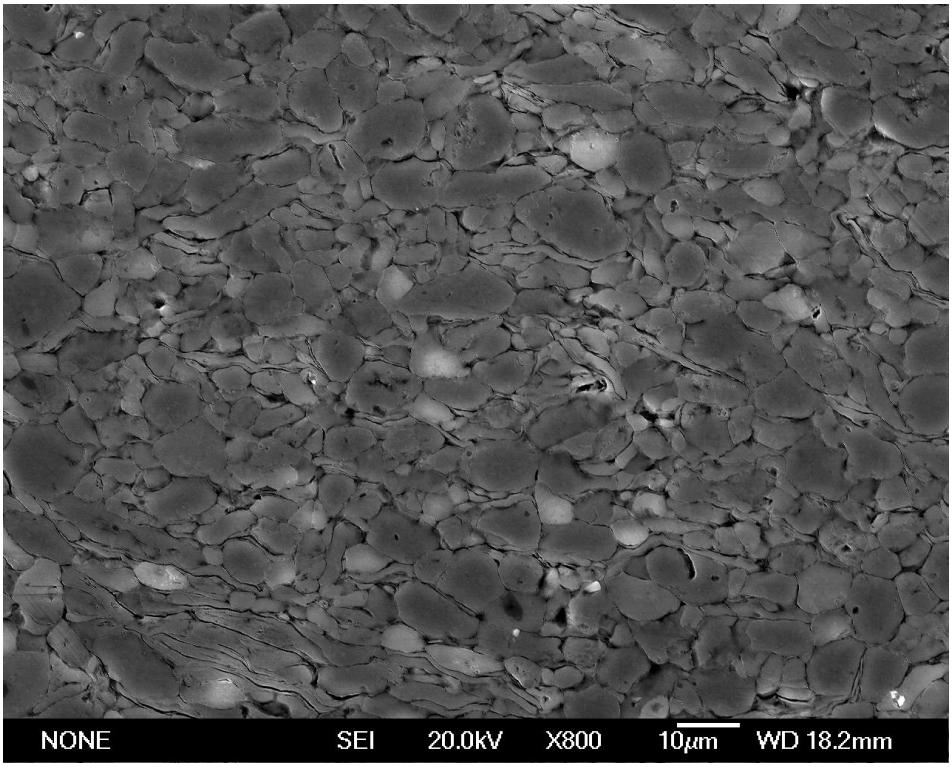

Figure 11.4: Example micrograph of cold compacted Al-2wt. % CNT composite prepared by ball milling for 4 hours

4.2.3.3 Density Evaluation

Results from green compacts prepared by ball milling for 4 hours (figure 11.5) showed a maximum density of 2.41gcm^{-3}, which was achieved by aluminium-2wt.% carbon nanotube specimens using industrial grade nanotubes. When compared to the maximum theoretical density of 2.68 gcm^{-3} calculated by the rule of mixtures, specimens prepared by ball milling for 4 hours achieved a maximum of 90% of the theoretical maximum density.

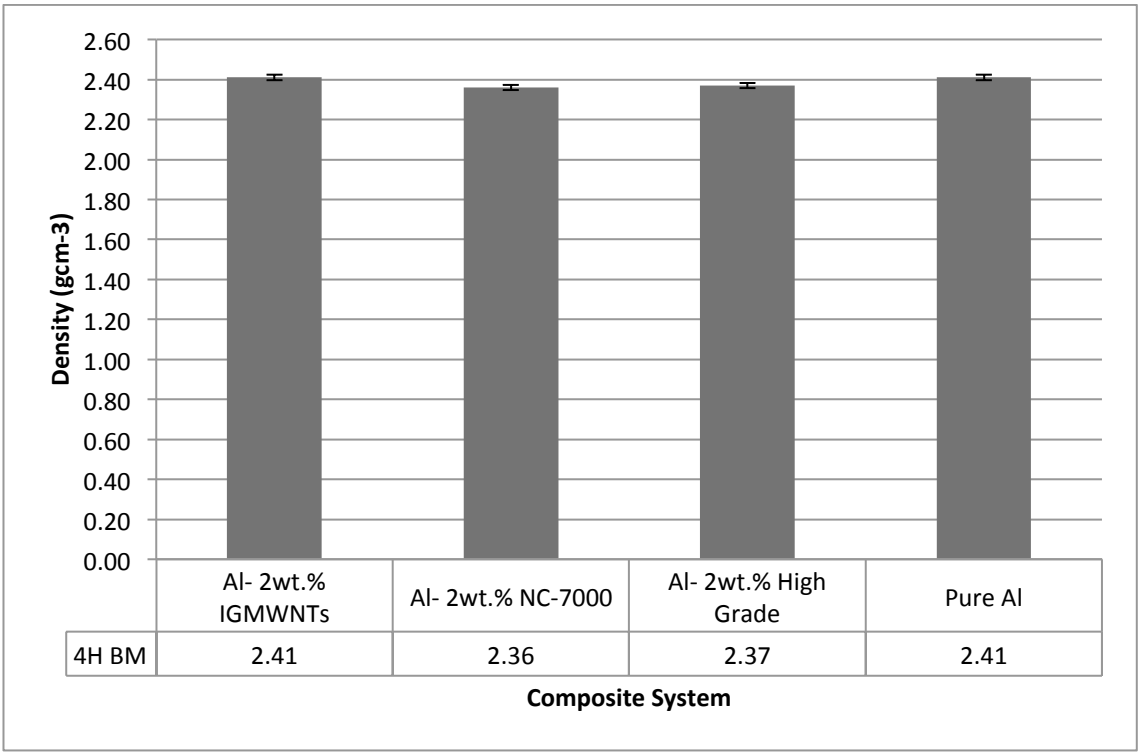

Figure 11.5: Graph showing density measurements taken from Al-2wt. % CNT cold compacted specimens produced by ball milling for 4 hours

4.2.3.4 Hardness Evaluation

Hardness results (figure 11.6) showed consistent through thickness hardness for all samples. Variation in hardness was seen to be slightly reduced compared to equivalent powder compact samples prepared by turbula mixing for 8 hours and ball milling for 1 hour respectively. The variation between maximum and minimum hardness in samples prepared by turbula mixing for 8 hours was 19 Hv, in samples prepared by ball milling for 1 hour it was 17.5 Hv and in samples prepared by ball milling for 4 hours it was 16.8 Hv.

As with hardness data measured in other powder compact specimens, samples using high grade carbon nanotubes produced the highest hardness values.

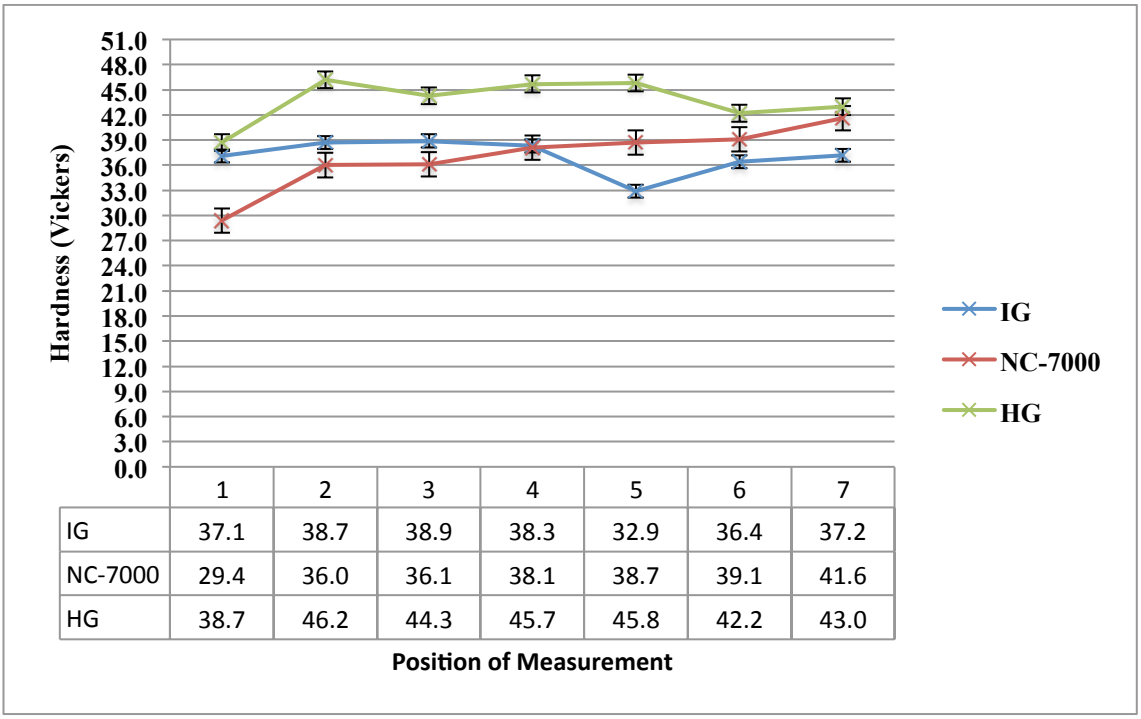

	1	2	3	4	5	6	7
IG	37.1	38.7	38.9	38.3	32.9	36.4	37.2
NC-7000	29.4	36.0	36.1	38.1	38.7	39.1	41.6
HG	38.7	46.2	44.3	45.7	45.8	42.2	43.0

Figure 11.6: Graph showing through thickness hardness measurements from Al-2wt. % CNT powder compact specimens prepared by ball milling for 4 hours

4.3: Sintering

4.3.1 Sintered Microstructures

SEM micrographs of sintered Al-2wt. % carbon nanotube specimens are shown below in figures 12-12.2. When compared to green compact microstructures, sintered specimens showed an improvement in densification with visible necking between powder particles. Individual particle boundaries were still visible in parts of the samples, indicating incomplete sintering (figure 12.3). Figure 12.3 also shows a comparison of cold compacted and sintered composite specimens, where particle boundaries in the sintered specimen showed necking.

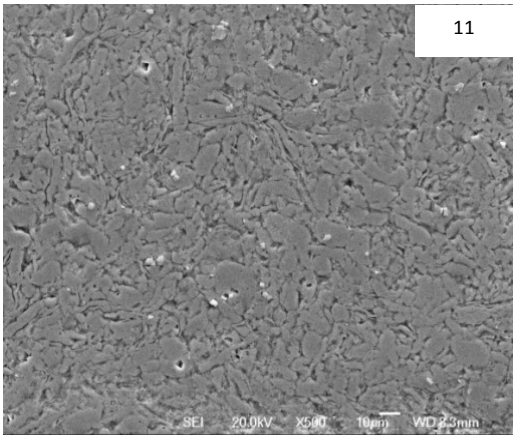

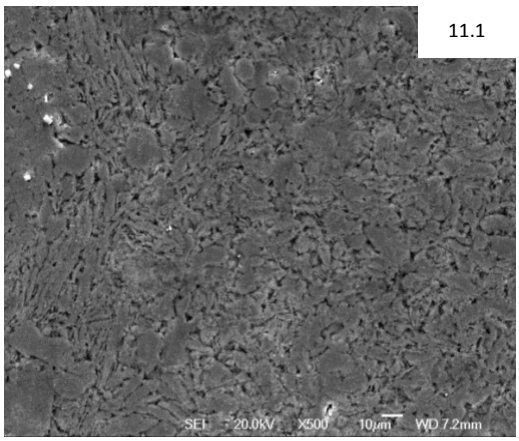

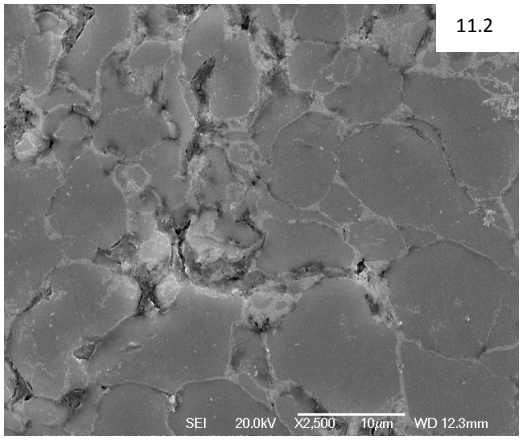

Figures 12-12.2: Example micrographs from sintered Al-2wt.% CNT composite specimens

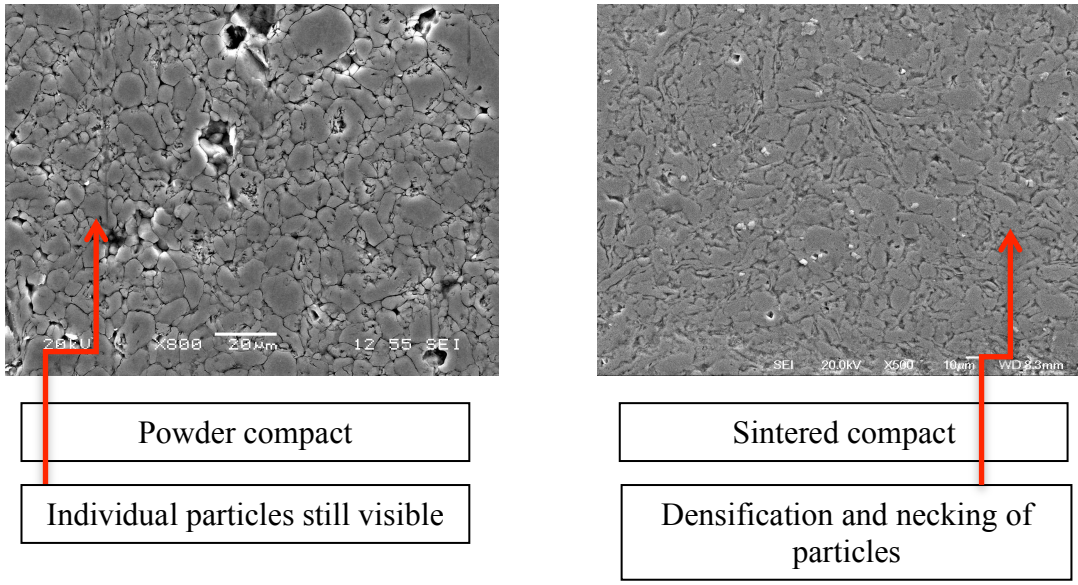

Figure 12.3: Comparison of powder compact and sintered compact microstructures and highlighting necking in sintered microstructures

4.3.2 Density evaluation of sintered composites prepared by turbula mixing for 8 hours

Pycnometry data shown in figure 12.4 revealed an improvement in density between the sintered compacts and green compact specimens. As with the green compact specimens, the density values closest to the theoretical maximum calculated by the rule of mixtures were shown by specimens using the highest grade nanotubes, which was 2.46gcm^{-1}. Samples turbula mixed for 8 hours showed an average density value of 2.43gcm^{-3}. The improvement in density from green compact specimens to sintered specimens was calculated and it was found that sintering composite samples produced by turbula mixing for 8 hours produced, on average, an improvement in density of 2.7%.

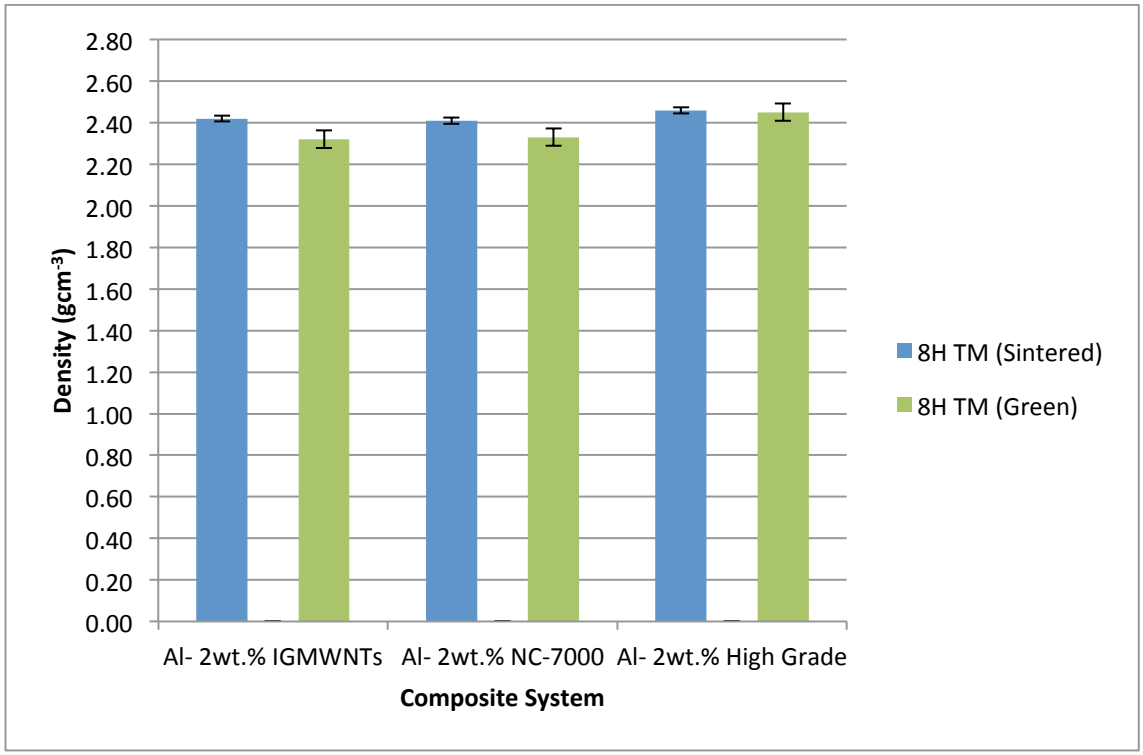

Figure 12.4: Graph showing density comparison of sintered and green Al-2wt.% CNT specimens prepared by turbula mixing for 8 hours

4.3.3 Hardness evaluation of sintered Al-2wt.% composite specimens prepared by turbula mixing for 8 hours

Hardness results obtained from sintered Aluminium-carbon nanotube composite specimens prepared by turbula mixing for 8 hours have been shown in figure 12.5. Specimens prepared by turbula mixing for 8 hours followed by sintering produced low mean hardness values and samples also showed fluctuations in through thickness hardness. Specimens with NC-7000 carbon nanotubes produced the highest through thickness hardness values with industrial grade and high grade nanotubes producing lower and similar values.

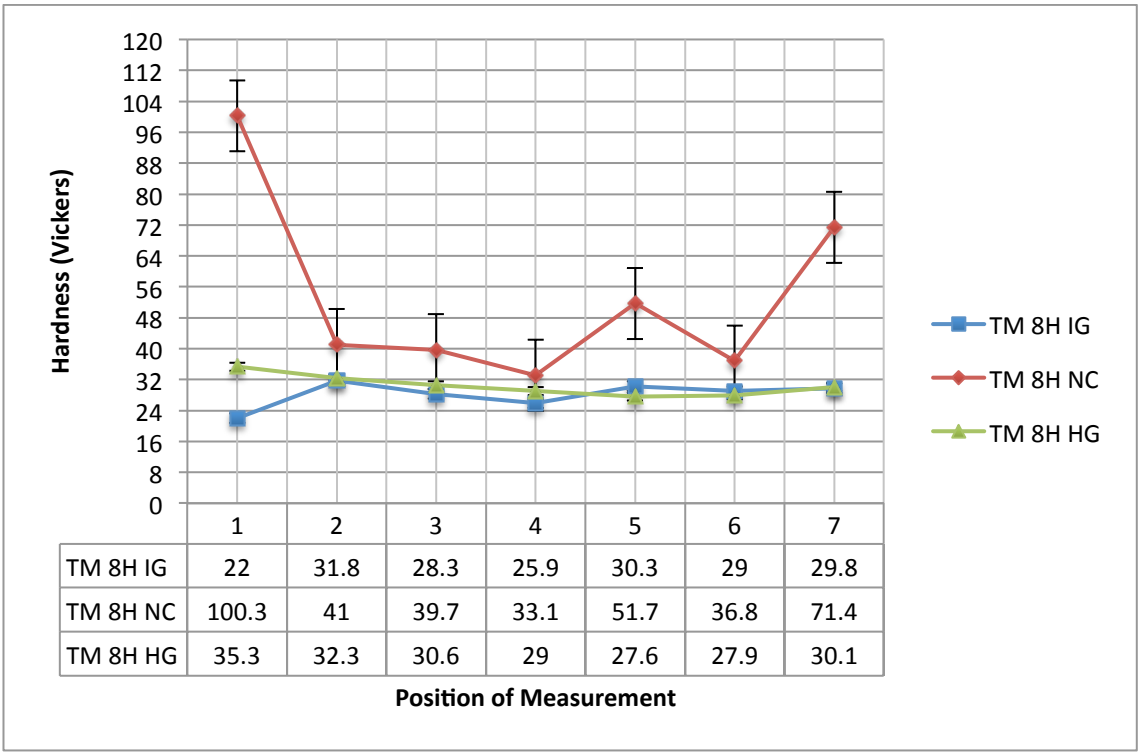

Figure 12.5: Graph showing through thickness hardness measurements of sintered Al-2wt.% CNT specimens prepared by turbula mixing for 8 hours

4.3.4 Density evaluation of sintered Al-2wt.% CNT composite specimens prepared by ball milling for 1 hour

Density comparisons of both the powder compact and sintered Al-2wt.% CNT specimens (prepared by ball milling for 1 hour) are shown in figure 12.6. As with the turbula mixed sintered samples, sintered specimens prepared by ball milling for 1 hour showed an improvement in density compared to equivalent powder compact samples. The mean density of sintered specimens prepared by ball milling for 1 hour was calculated to be 2.42gcm^{-3}, slightly lower than that of the turbula mixed sintered specimens (2.43gcm^{-3}).

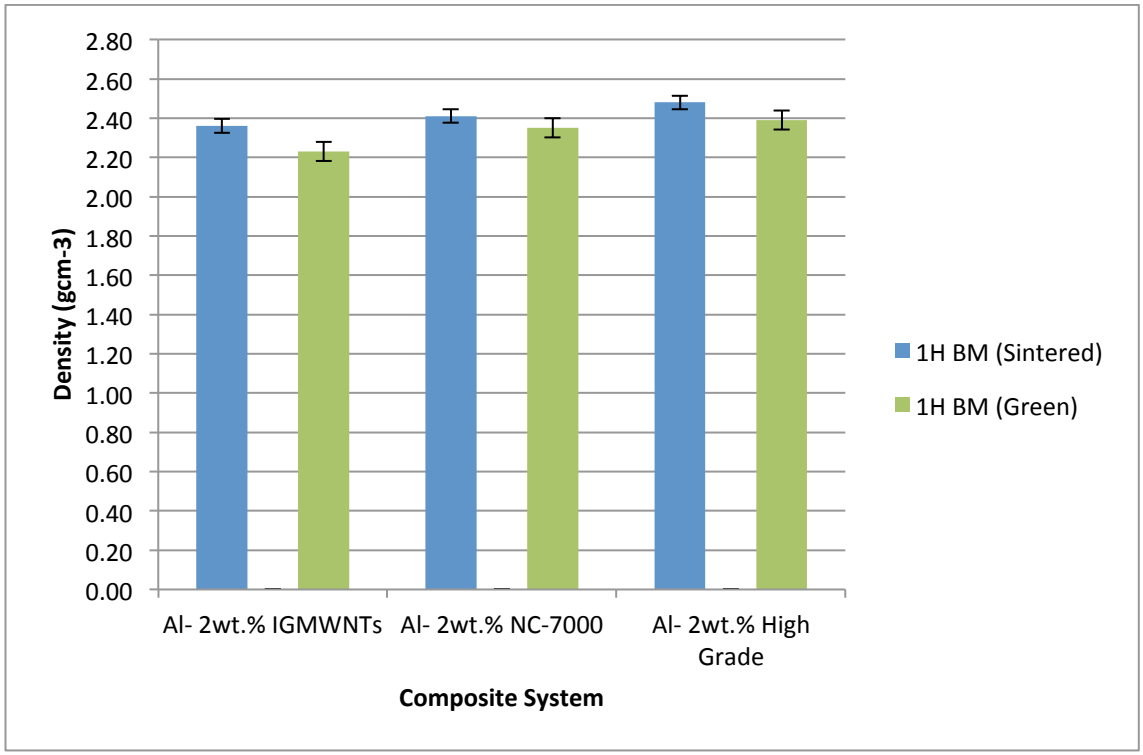

Figure 12.6: Graph showing density comparison between sintered and green compact composite specimens of Al-2wt.% CNT prepared by ball milling for 1 hour

4.3.5 Hardness evaluation of sintered Al-2wt.% CNT composite specimens prepared by ball milling for 1 hour

Hardness data obtained from the sintered compacts prepared by ball milling for 1 hour (figure 12.7) showed an improvement in hardness compared to equivalent green compact samples. Hardness was also seen to improve relative to the sintered compacts prepared by turbula mixing for 8 hours. On average, samples prepared using high grade carbon nanotubes produced the highest hardness of 36.1Hv. The variation in the through thickness hardness was seen to be comparable relative to equivalent sintered specimens prepared by turbula mixing for 8 hours. The difference between highest and lowest hardness values for sintered specimens prepared by turbula mixing for 8 hours was 9.8Hv (Figure 12.5) for industrial grade nanotube systems, 67.2Hv (Figure 12.9) for

NC-7000 nanotube systems and 7.7Hv for high grade nanotube systems. The greater difference for NC-7000 samples was attributed to CNT agglomerates causing a hard 'region' within the compact. For sintered specimens prepared by ball milling for 1 hour the differences between the minimum and maximum hardness were: 19Hv, 13.5Hv and 8.5Hv for industrial grade, NC-7000 grade and high grade CNTs, respectively.

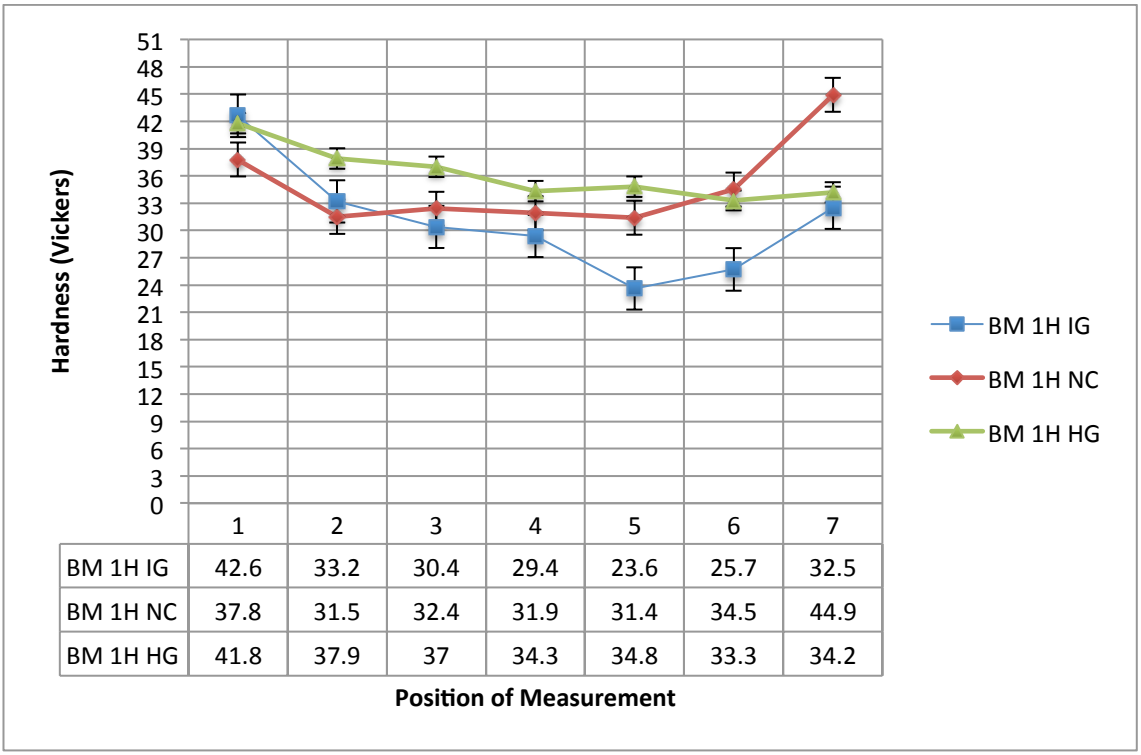

Figure 12.7: Graph showing through thickness hardness measurements from sintered Al-2wt.% CNT specimens prepared by ball milling for 1 hour

4.3.6 Density evaluation of sintered Al-2wt.% CNT composite specimens prepared by ball milling for 4 hours

As shown in figure 12.8, measured density values from the sintered aluminium-2wt. % CNT specimens prepared by ball milling for 4 hours showed an improvement in

densification relative to non-sintered compacts. The average density of green compact specimens prepared by ball milling for 4 hours was 2.38gcm^{-3}, while after sintering the average density was calculated to be 2.51gcm^{-3}.

As with other mixing methods, the samples prepared using high grade carbon nanotubes produced the highest density values, in this case 2.65gcm^{-3}.

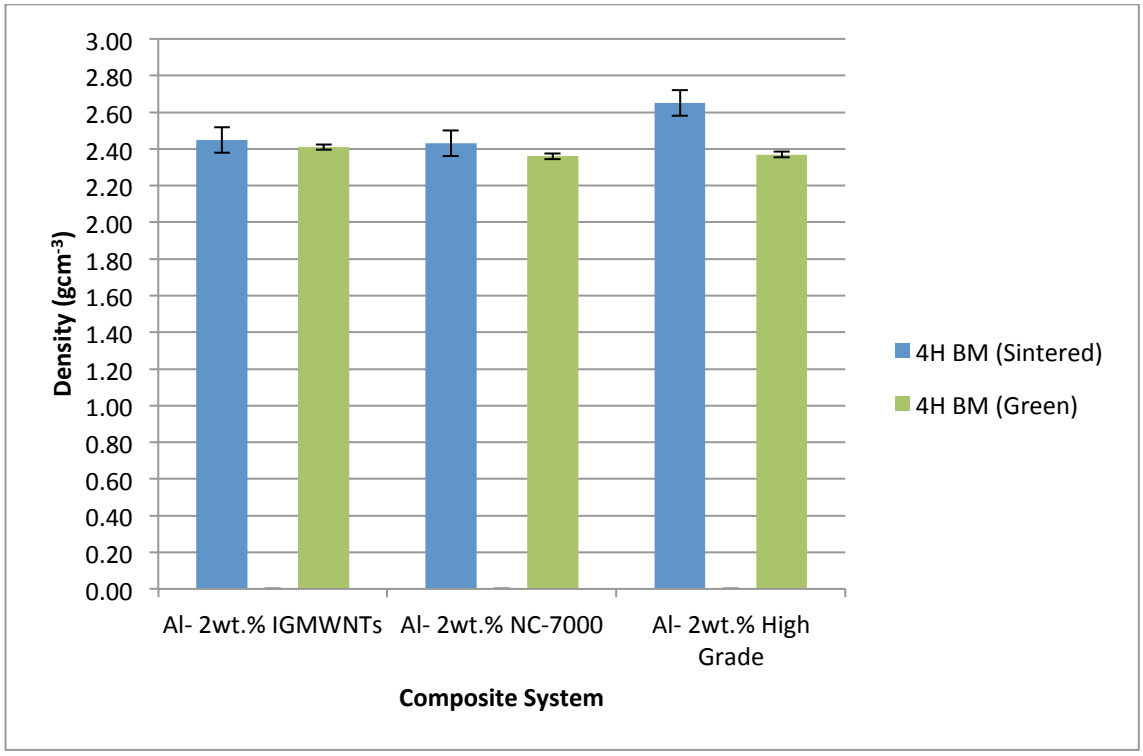

Figure 12.8: Graph showing comparison of density measurements from green and sintered Al-2wt.% CNT composite specimens prepared by ball milling for 4 hours

4.3.7 Hardness evaluation of sintered Al-2wt.% CNT composite specimens prepared by ball milling for 4 hours

Hardness results from sintered aluminium-carbon nanotube samples prepared by ball milling for 4 hours (figure 12.9) showed an increase in hardness compared to un-sintered compact specimens. High grade carbon nanotubes were shown to produce the highest average hardness in both the green condition (43.7Hv) and sintered condition (57.9Hv). Variation in through thickness hardness was also noted to be less than that seen in samples prepared by other mixing methods.

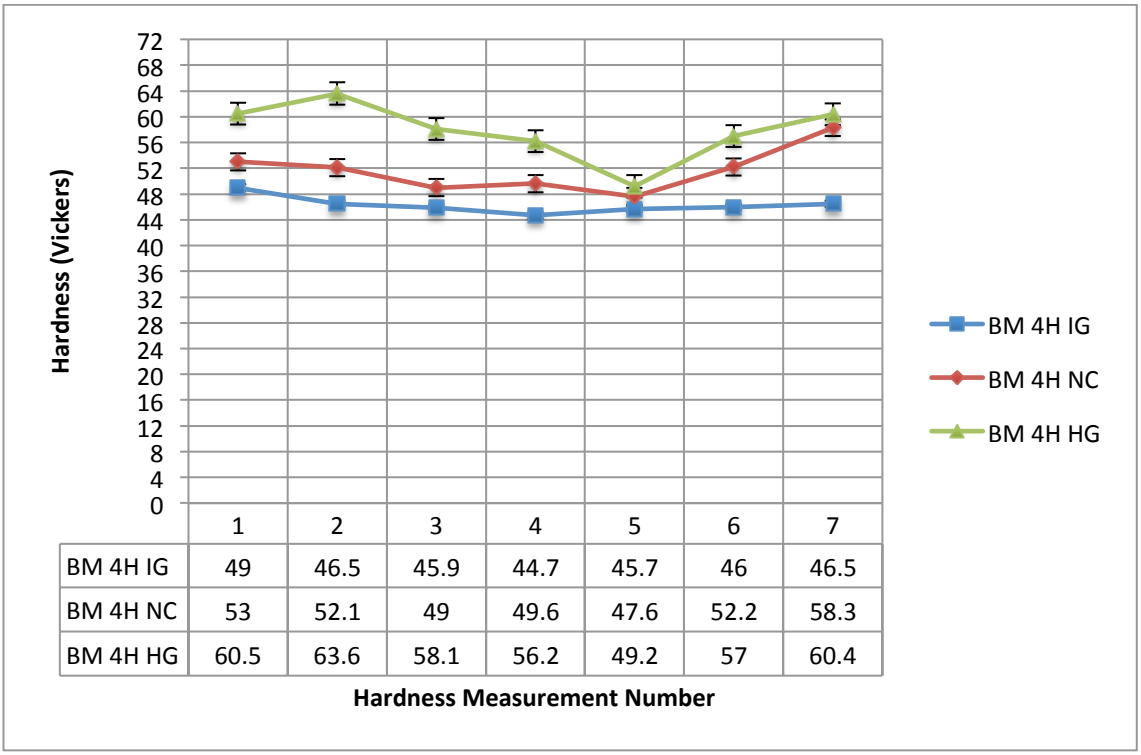

	1	2	3	4	5	6	7
BM 4H IG	49	46.5	45.9	44.7	45.7	46	46.5
BM 4H NC	53	52.1	49	49.6	47.6	52.2	58.3
BM 4H HG	60.5	63.6	58.1	56.2	49.2	57	60.4

Figure 12.9: Graph showing through thickness hardness comparison of sintered Al-2wt.% CNT specimens prepared by ball milling for 4 hours

4.4 Equal Channel Angular Pressing (ECAP) specimens

4.4.1 ECAP Microstructures

Powder compacts were pressed through an ECAP die at approximately 250MPa (25kN). The force at which each sample was pressed was estimated by the value of the oil pressure displayed by the press, but was not identical for each press due to a lack of back pressure within the die. The resultant ECAP samples have been shown in figures 13-13.1 and showed a distinct orientation of microstructure. Aluminium/CNT particles were seen to be elongated parallel to the ECAP direction, micrographs taken perpendicular to the ECAP direction showed ends of elongated particles, these were seen to be equiaxed in shape. Samples also appeared to show an improvement in density compared to green compact microstructures. Densities of ECAP specimens are quantified in sections 5.4.2, 5.4.4 and 5.4.6

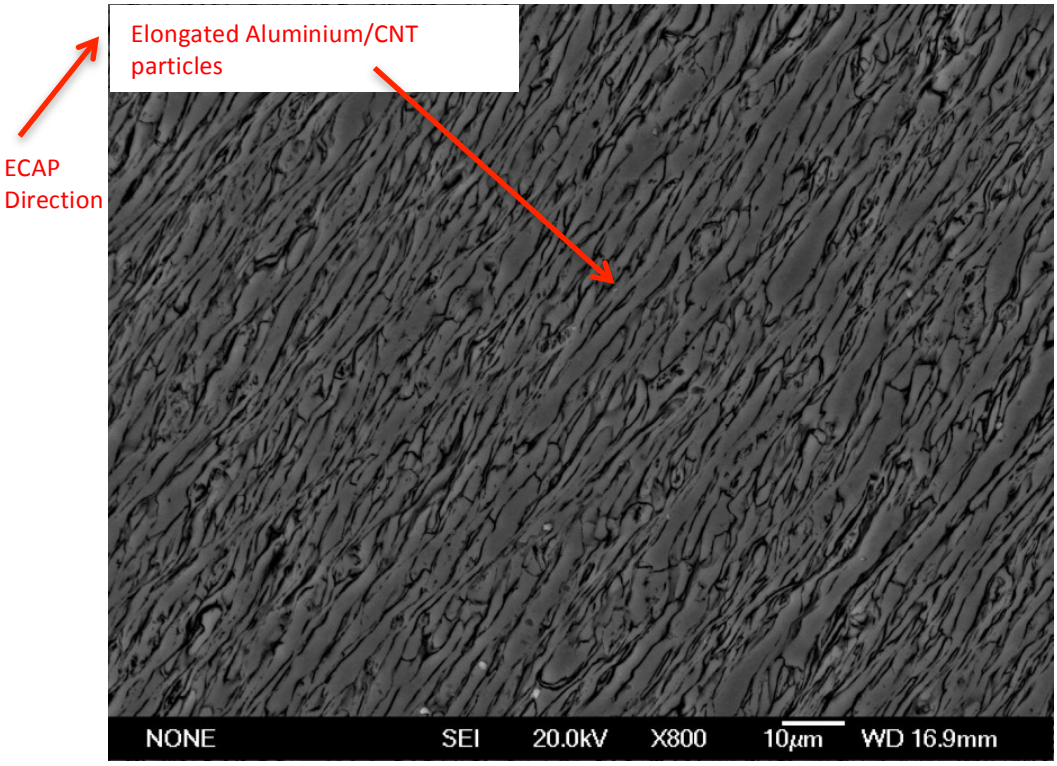

Figure 13: Micrograph of ECAP microstructure parallel to ECAPed direction

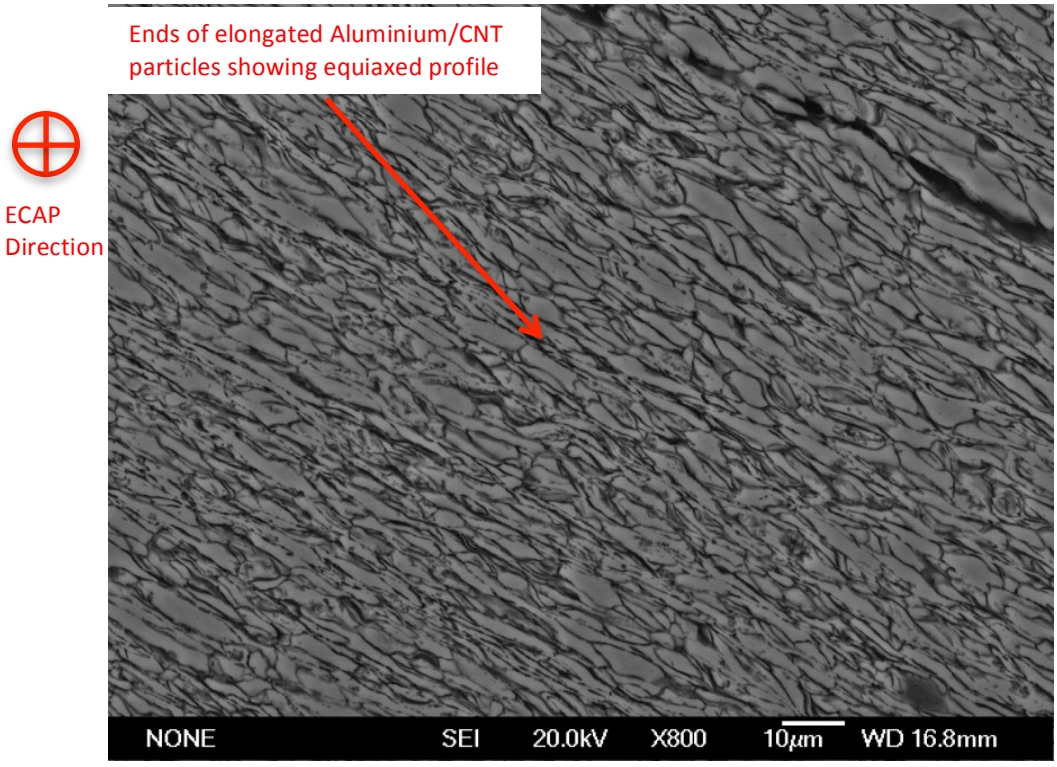

Figure 13.1: Micrograph of ECAP microstructure perpendicular to ECAPed direction

4.4.2 Density evaluation of ECAP Al-2wt.% CNT composite specimens prepared by turbula mixing for 8 hours

Pycnometry of ECAP specimens produced by turbula mixing for 8 hours (figure 13.2) showed that the highest density value achieved was 2.53gcm^{-3}, lower than the theoretical maximum of 2.68gcm^{-3} calculated from the rule of mixtures equation. High grade carbon nanotube ECAP samples produced the highest density values. A comparison of density measurements from powder compact and ECAP specimens is shown in figure 13.3 and revealed a consistent improvement in density with the ECAP process. The theoretical maximum density calculated for an Al-2wt.% CNT composite specimen was 2.68gcm^{-3}. Powder compact specimens prepared by turbula mixing for 8 hours achieved 91% of this theoretical maximum, while ECAP specimens prepared by turbula mixing for 8 hours produced a maximum density of 2.59gcm^{-3}, this was 96% of the calculated theoretical maximum density.

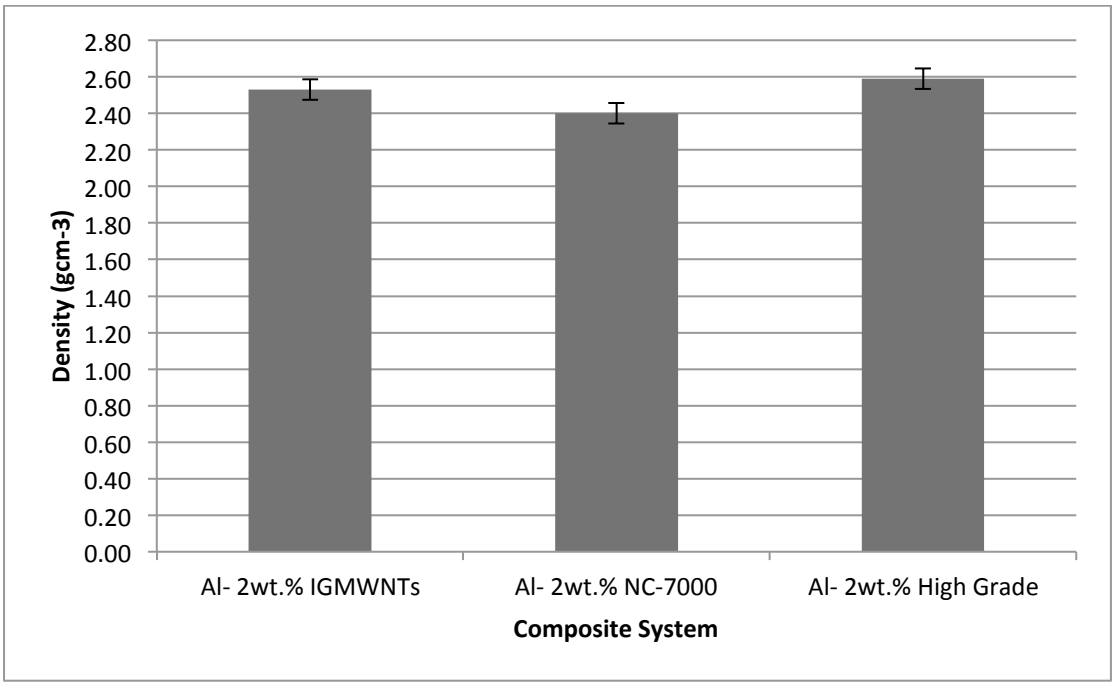

Figure 13.2: Graph showing density measurements taken from Al-2wt. % CNT ECAP specimens prepared by turbula mixing for 8 hours

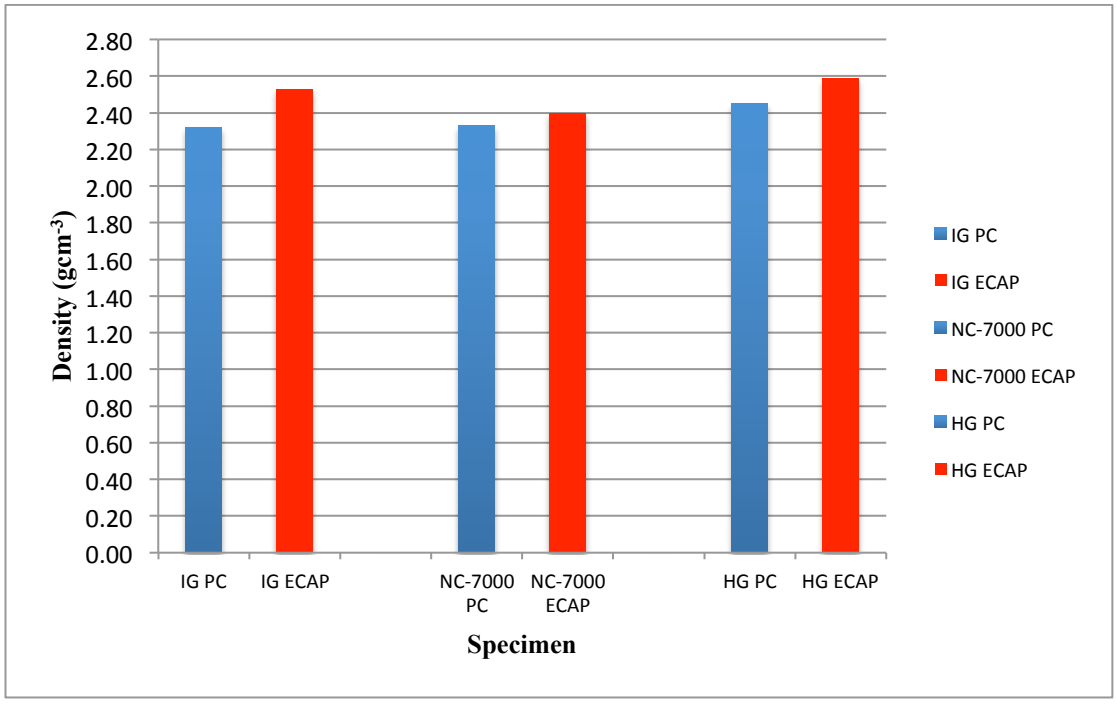

Figure 13.3: Graph showing comparison of density measurements from both powder compact and ECAP specimens prepared by turbula mixing for 8 hours

4.4.3 Hardness evaluation of ECAP Al-2wt.% CNT composite specimens prepared by turbula mixing for 8 hours

Results showed an improvement in hardness in comparison to green compact hardness data. The hardness results from ECAP specimens prepared by turbula mixing for 8 hours are shown below in figures 13.4 and 13.5. Fluctuations in hardness were seen in both the longitudinal direction of the specimens parallel to the ECAP press and in the transverse regions perpendicular to the ECAP direction. Table 8 shows the average hardness values for all green and ECAPed specimens prepared by turbula mixing for 8 hours. Unlike hardness data obtained from the powder compact specimens, ECAP specimens prepared by turbula mixing for 8 hours did not indicate an optimum grade of carbon nanotube. Samples turbula mixed for 8 hours showed low average hardness values in both longitudinal and transverse regions. These specimens had a larger particle size following mixing (7-8μm) compared to ball milled specimens, therefore a lower hardness was expected.

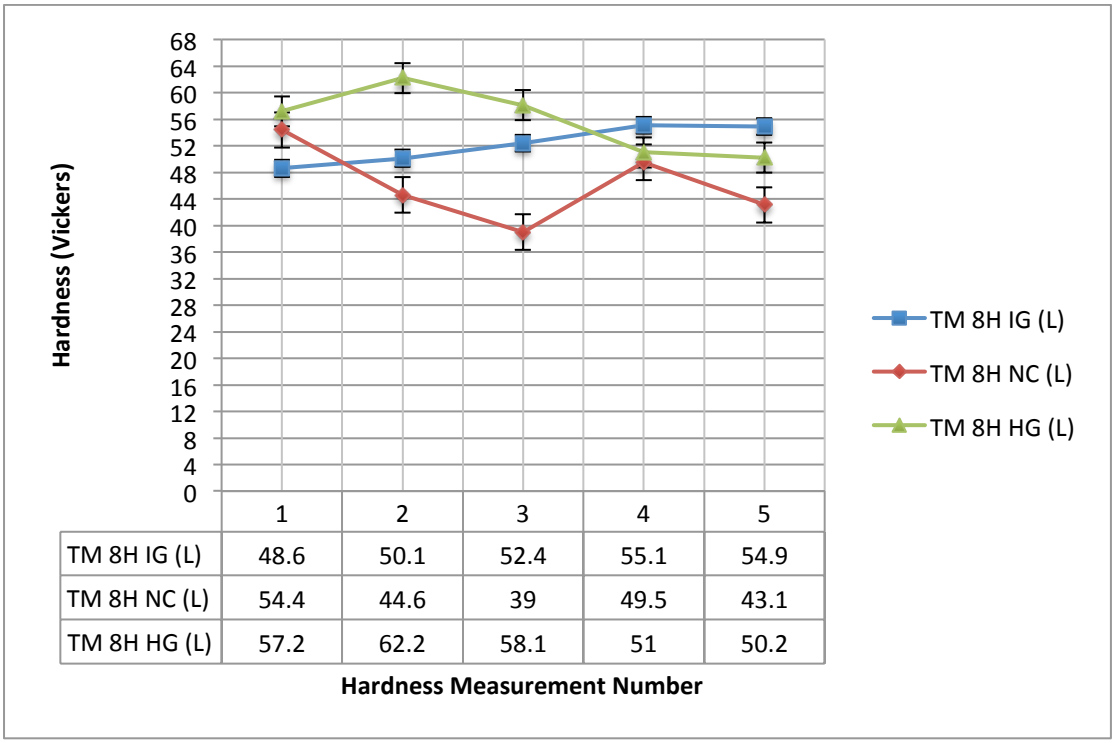

	1	2	3	4	5
TM 8H IG (L)	48.6	50.1	52.4	55.1	54.9
TM 8H NC (L)	54.4	44.6	39	49.5	43.1
TM 8H HG (L)	57.2	62.2	58.1	51	50.2

Figure 13.4: Graph showing Vickers hardness comparison of longitudinal ECAP specimens prepared by turbula mixing for 8 hours

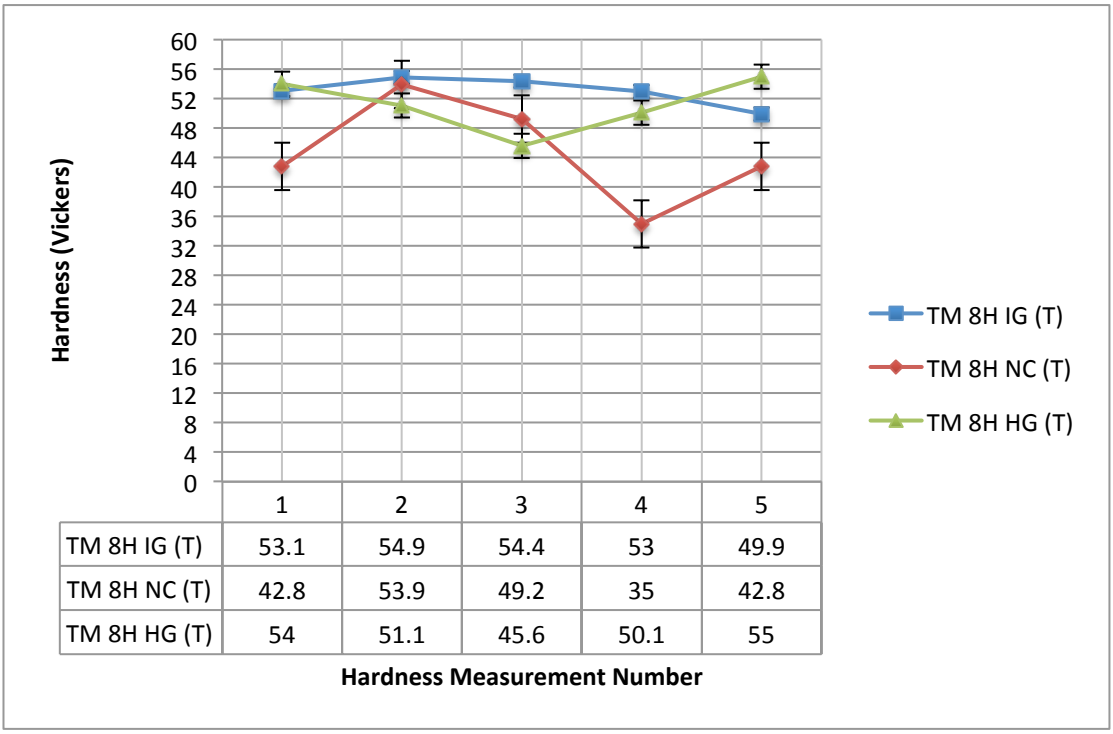

	1	2	3	4	5
TM 8H IG (T)	53.1	54.9	54.4	53	49.9
TM 8H NC (T)	42.8	53.9	49.2	35	42.8
TM 8H HG (T)	54	51.1	45.6	50.1	55

Figure 13.5: Graph showing Vickers hardness comparison of transverse ECAP specimens prepared by turbula mixing for 8 hours

	Average Hardness (Green)	Average Hardness (ECAP Longitudinal)	Average Hardness (ECAP Transverse)
TM 8H IG	15.3	52.2	53.0
TM 8H NC-7000	20.4	46.1	44.7
TM 8H HG	28.2	55.7	51.2

Table 9: Average Vickers hardness measurements taken from powder compact and ECAP specimens prepared by turbula mixing for 8 hours

4.4.4 Density evaluation of ECAP Al-2wt. % CNT composite specimens prepared by ball milling for 1 hour

Results obtained from ECAP specimens prepared by ball milling for 1 hour (figures 13.6-13.7) showed an improvement in density compared to equivalent powder compact specimens. It was calculated that green compact specimens prepared by ball milling for 1 hour achieved 89% of the maximum theoretical density (figure 10.5), ($2.68 gcm^{-3}$), ECAP specimens prepared by ball milling for 1 hour produced a maximum density of $2.47 gcm^{-3}$, which was 92% of the maximum theoretical density. Unlike results from the powder compact specimens however, only small differences in the densities of samples were observed between the 3 types of carbon nanotube.

As with the results from the turbula mixed ECAP specimen densities, the largest improvements in density were produced by samples using industrial grade and high grade carbon nanotubes.

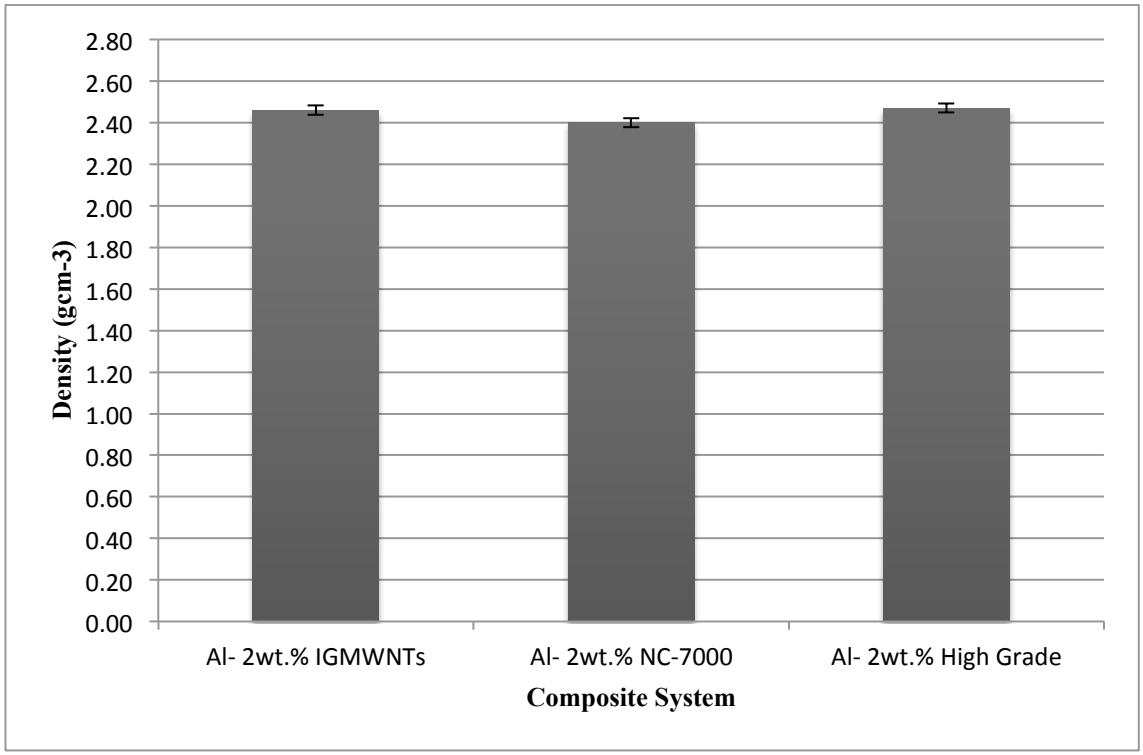

Figure 13.6: Graph showing average density measurements of ECAP Al-2wt. % CNT specimens prepared by ball milling for 1 hour

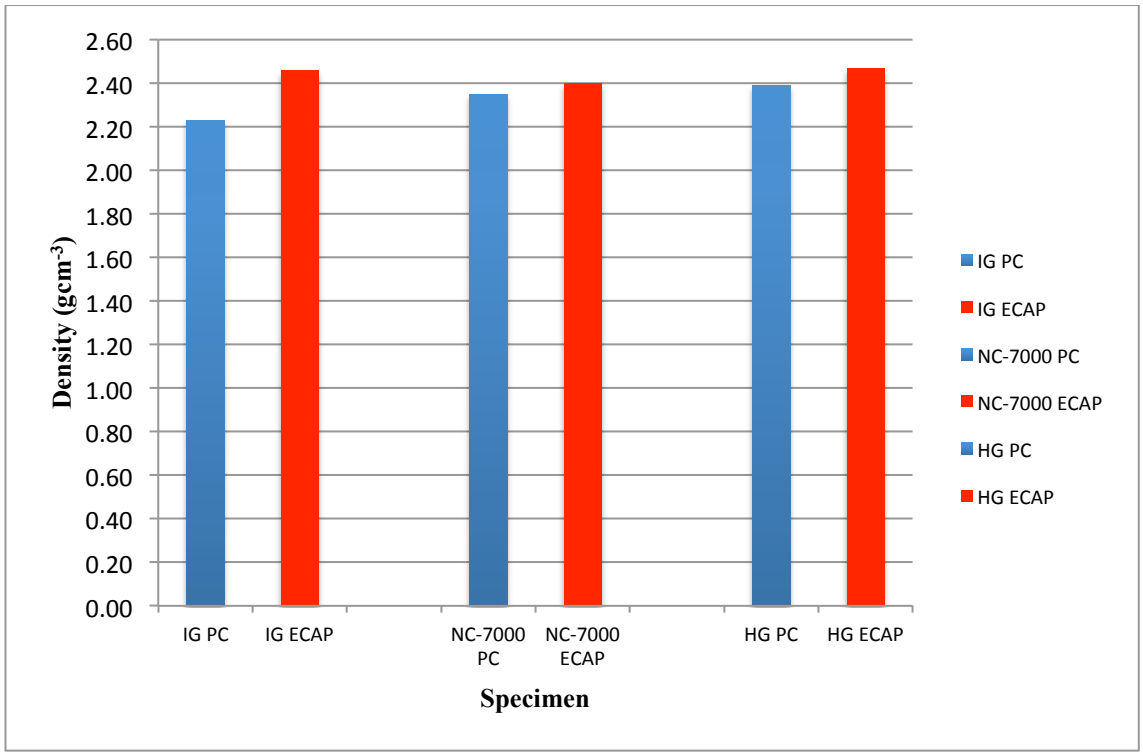

Figure 13.7: Graph showing comparison of average density measurements from green compact and ECAP Al-2wt. % CNT specimens prepared by ball milling for 1 hour.

4.4.5 Hardness evaluation of ECAP Al-2wt. % CNT composite specimens prepared by ball milling for 1 hour

Figures 13.8 and 13.9 show hardness results from ECAP specimens prepared by ball milling for 1 hour. An improvement in hardness was noted relative to equivalent powder compact samples. Table 9 shows the average hardness values from powder compact and ECAP specimens prepared by ball milling for 1 hour. Hardness results were comparable to those seen from ECAP samples prepared by turbula mixing. In both longitudinal and transverse directions, it was observed that samples using industrial grade carbon nanotubes had the highest hardness values; this showed a correlation with results observed from turbula mixed ECAP samples. Through thickness hardness was also seen to vary as with the turbula mixed ECAP samples.

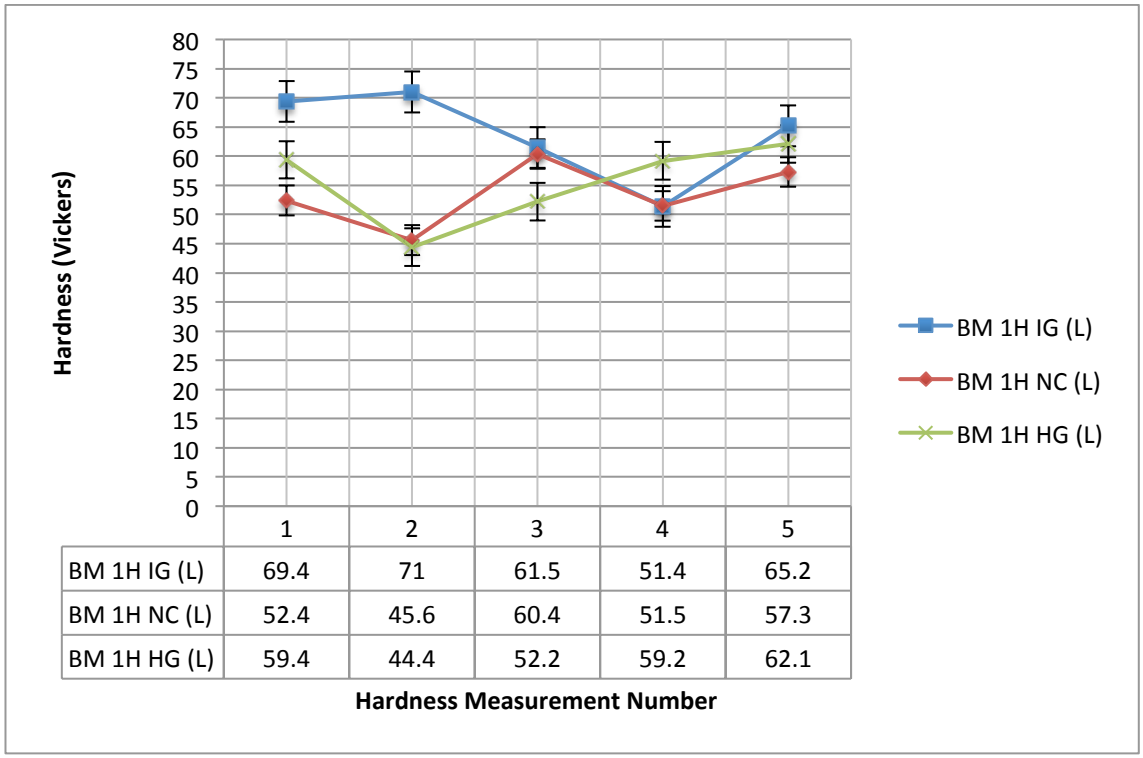

	1	2	3	4	5
BM 1H IG (L)	69.4	71	61.5	51.4	65.2
BM 1H NC (L)	52.4	45.6	60.4	51.5	57.3
BM 1H HG (L)	59.4	44.4	52.2	59.2	62.1

Figure 13.8: Graph showing longitudinal hardness comparison of ECAP Al-2wt. % CNT composite specimens prepared by ball milling for 1 hour

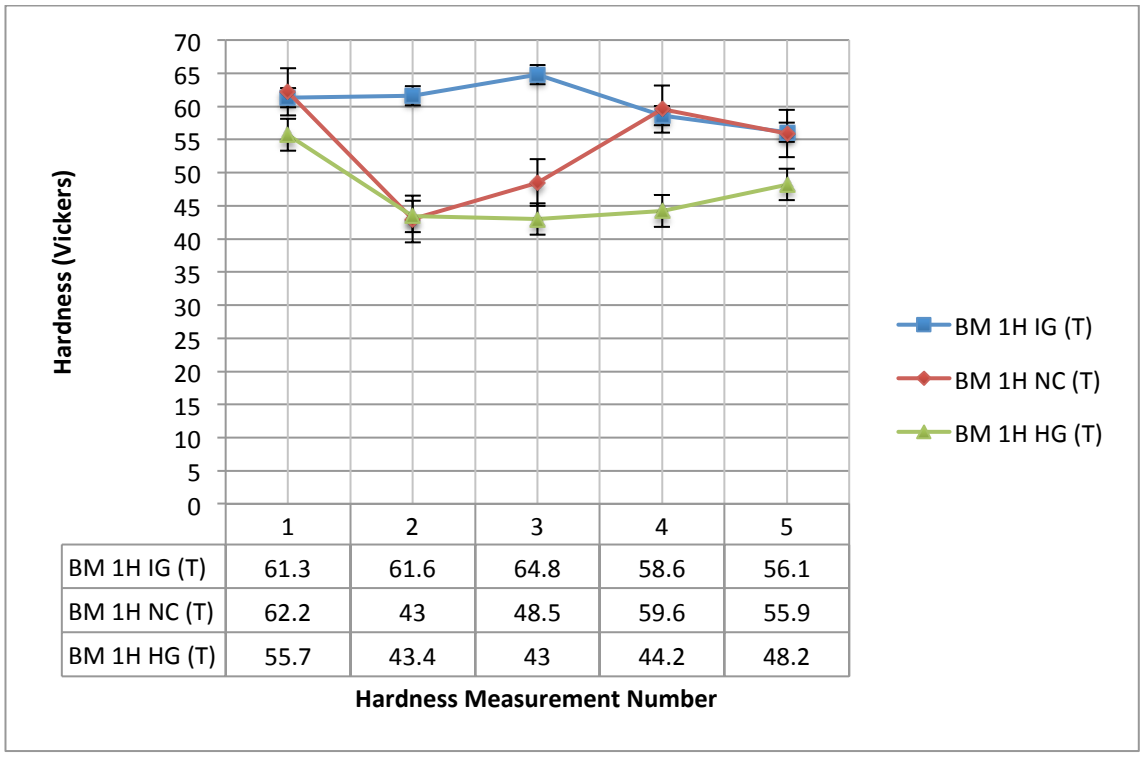

	1	2	3	4	5
BM 1H IG (T)	61.3	61.6	64.8	58.6	56.1
BM 1H NC (T)	62.2	43	48.5	59.6	55.9
BM 1H HG (T)	55.7	43.4	43	44.2	48.2

Figure 13.9: Graph showing transverse hardness comparison of ECAP Al-2wt. % CNT composite specimens prepared by ball milling for 1 hour

	Average Hardness (Green)	Average Hardness (ECAP Longitudinal)	Average Hardness (ECAP Transverse)
BM 1H IG	26.4Hv	63.7Hv	60.5Hv
BM 1H NC-7000	33.9Hv	53.4Hv	53.8Hv
BM 1H HG	40.0Hv	55.5Hv	46.9Hv

Table 10: Average Vickers hardness measurements taken from powder compact and ECAP specimens prepared by ball milling for 1 hour

4.4.6 Density evaluation of ECAP Al-2wt. % CNT composite specimens prepared by ball milling for 4 hours

Figures 13.10 and 13.11 show ECAP density measurements from specimens prepared by ball milling for 4 hours. A slight improvement in density relative to equivalent ball milled powder compact specimens using NC-7000 and high grade carbon nanotubes was observed. Powder compacts prepared by ball milling for 4 hours achieved a maximum of 90% of the theoretical maximum density ($2.68gcm^{-3}$) whereas ECAP specimens prepared by ball milling for 4 hours achieved a maximum of 93% of the maximum theoretical density. Aluminium-2wt. % CNT specimens that used industrial grade carbon nanotubes showed a slight reduction in density. Powder compact specimens using industrial grade carbon nanotubes prepared by ball milling for 4 hours produced an average density value of $2.41gcm^{-3}$, however ECAP specimens prepared using industrial grade carbon nanotubes produced an average density of $2.36gcm^{-3}$ Specimens prepared using high grade carbon nanotubes produced the highest density values.

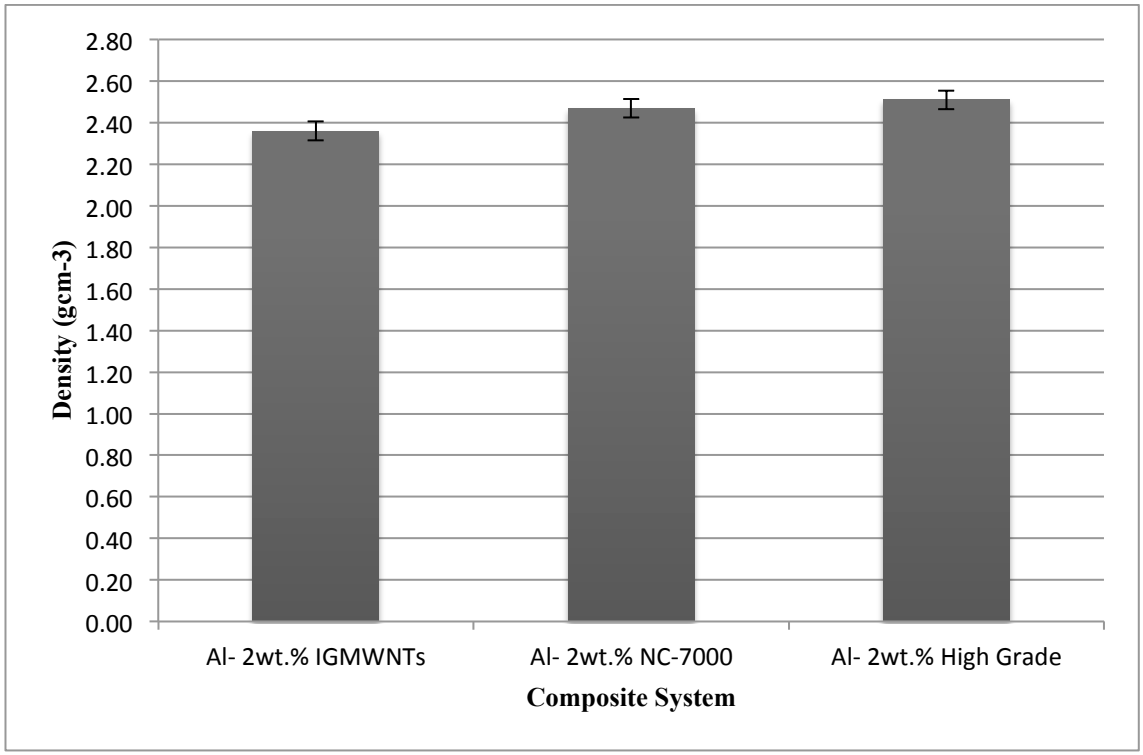

Figure 13.10: Graph showing average density measurements of ECAP Al-2wt. % CNT specimens prepared by ball milling for 4 hours

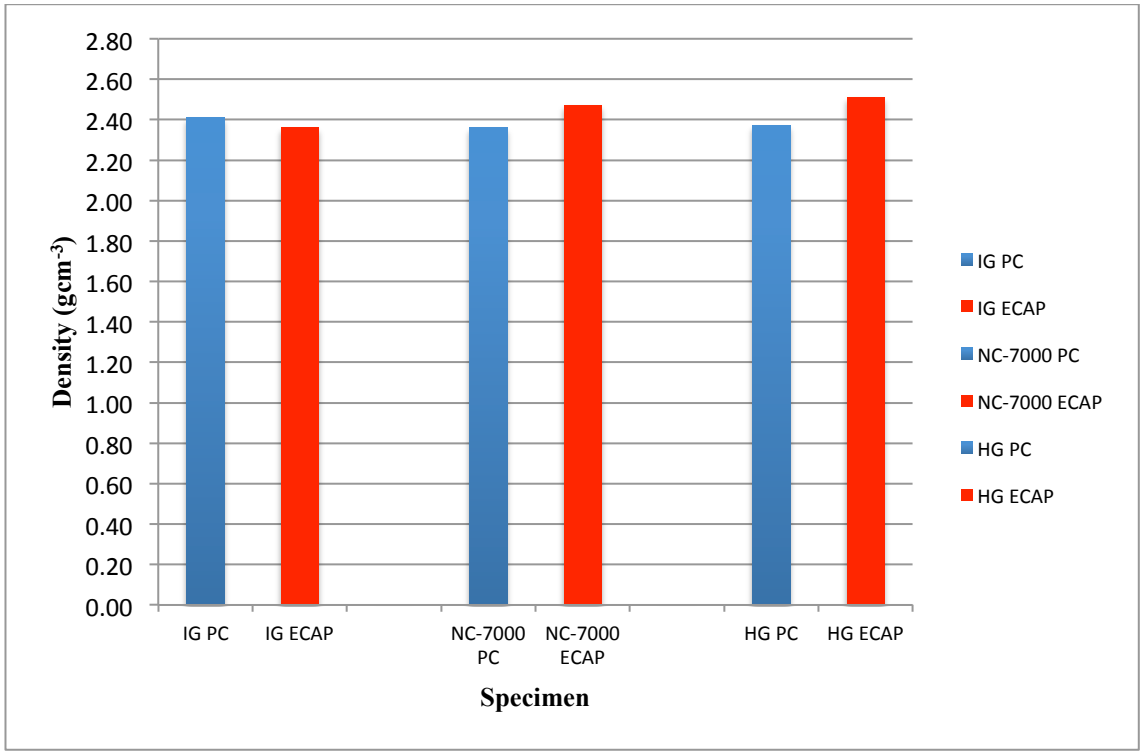

Figure 13.11: Graph showing average density measurement comparison of green compact and ECAP Al-2wt. % CNT specimens prepared by ball milling for 4 hours

4.4.7 Hardness evaluation of ECAP Al-2wt. % CNT composite specimens prepared by ball milling for 4 hours

Hardness measurements are shown in figures 13.12 and 13.13. Table 4 shows average hardness measurements from green and ECAP specimens prepared by ball milling for 4 hours, which showed an improvement relative to powder compact specimens as with other mixing methods. The 3 types of carbon nanotube used all produced similar hardness values. The variations between maximum and minimum hardness values for ECAP samples using all mixing methods are shown in table 11. A notable observation was that the degree of variation in hardness in both longitudinal and transverse regions was reduced compared to equivalent ECAP specimens using other mixing methods.

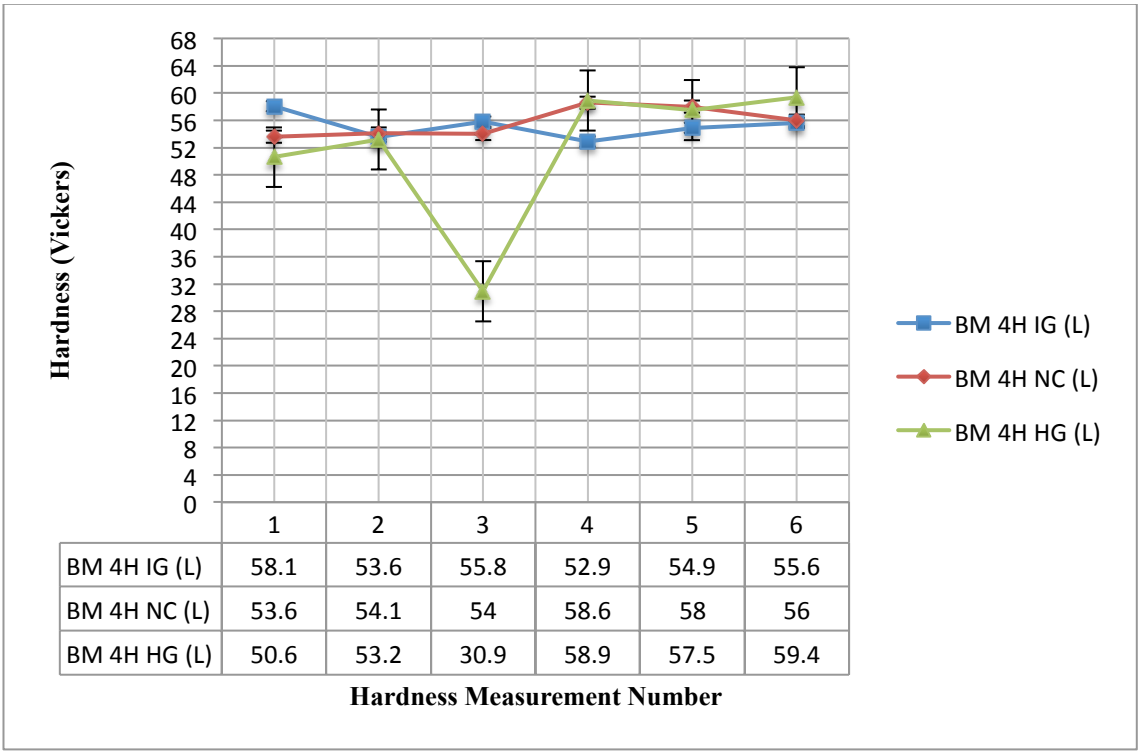

	1	2	3	4	5	6
BM 4H IG (L)	58.1	53.6	55.8	52.9	54.9	55.6
BM 4H NC (L)	53.6	54.1	54	58.6	58	56
BM 4H HG (L)	50.6	53.2	30.9	58.9	57.5	59.4

Figure 13.12: Graph showing longitudinal Vickers hardness comparison of ECAP Al-2wt. % CNT composite specimens prepared by ball milling for 4 hours

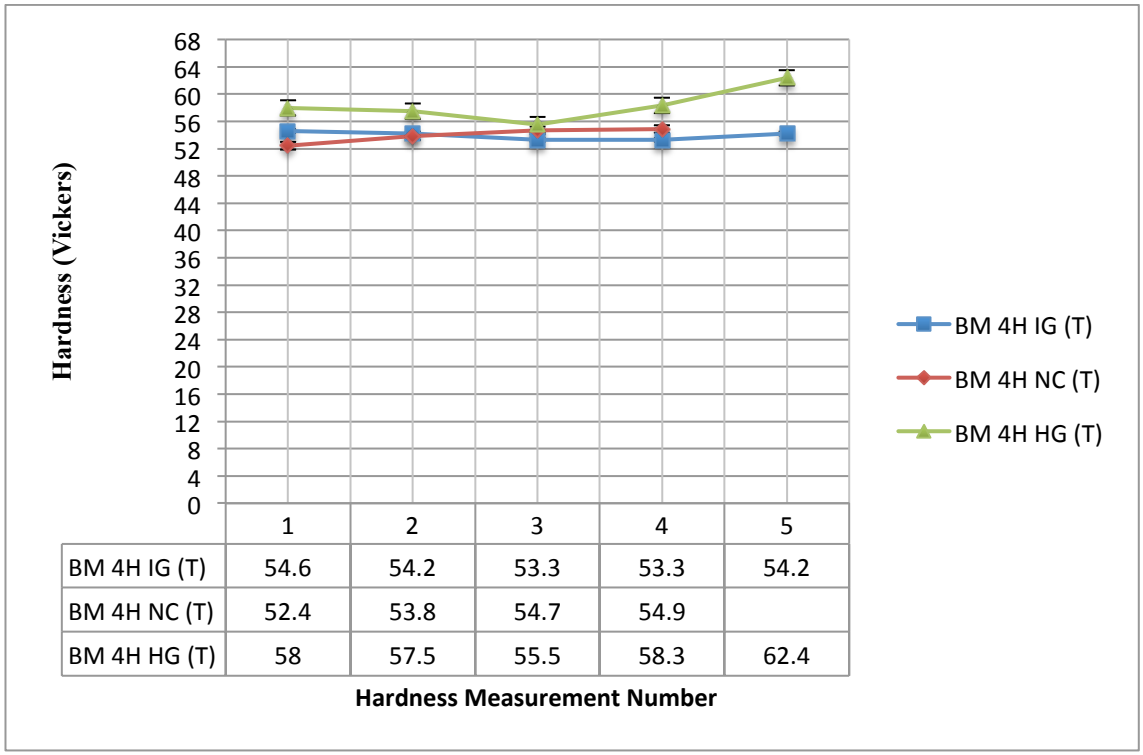

Figure 13.13: Graph showing transverse Vickers hardness comparison of ECAP Al-2wt. % CNT composite specimens prepared by ball milling for 4 hours

	Average Hardness (Green)	Average Hardness (ECAP Longitudinal)	Average Hardness (ECAP Transverse)
BM 4H IG	37.0Hv	55.1Hv	53.9Hv
BM 4H NC-7000	37.0Hv	55.7Hv	53.9Hv
BM 4H HG	43.7Hv	51.7Hv	58.3Hv

Table 11: Average Vickers hardness measurements taken from powder compact and ECAP specimens prepared by ball milling for 4 hours

	Difference Between Min and Max Hardness Value Measured (Longitudinal)	Difference Between Min and Max Hardness Value Measured (Transverse)
BM 4H IG	5.2Hv	1.3Hv
BM 4H NC-7000	5.0Hv	2.5Hv
BM 4H HG	28.5Hv	6.9Hv
BM 1H IG	19.6Hv	8.7Hv
BM 1H NC-7000	14.8Hv	19.2Hv
BM 1H HG	17.7Hv	12.7Hv
TM 8H IG	6.5Hv	5.0Hv
TM 8H NC-7000	15.4Hv	18.9Hv
TM 8H HG	12.0Hv	9.4Hv

Table 12: Table showing differences between maximum and minimum Vickers hardness values measured for all ECAP specimens

4.5 Casting

4.5.1 Cast Microstructures

Cast specimens were prepared by adding 2wt.% aluminium-carbon nanotube ECAP specimens of mass ~5.5grams to a crucible of molten super purity pure aluminium at 720^{o}C, of mass ~45grams, giving an approximate final carbon nanotube concentration of 0.2wt%.

Castings were made using both industrial grade and high grade nanotubes in order to establish if changing carbon nanotube purity affected the quality of the resultant casting. Micrographs of the castings shown in figures 14-14.1 revealed that a number of problems occurred regarding casting of aluminium-carbon nanotube composites. Cast microstructures revealed an incomplete melting and distribution of the aluminium-carbon nanotube ECAP specimens within the super purity aluminium matrix material. Regions of microstructure showed grain morphology consistent with that of a cast structure however regions also showed the grain structure of the ECAP specimens,

showing incomplete melting and dispersion of the ECAP specimens within the melt. In addition it was seen that along the interface between the aluminium matrix material and ECAP composite material (figures 14-14.1), porosity was generated and full wetting was not achieved.

Lack of complete melting could be explained by the casting taking place at a lower temperature than was needed, however, in practice it may not be feasible to increase casting temperature due to potential problems with damage to CNTs or reaction of CNTs with the surrounding matrix.

Another possible reason for incomplete melting is that the melt temporarily chilled off during addition of the ECAP table specimens. Equation 5 shows a thermal transfer equation for the aluminium melt. Equation 6 shows the temperature difference upon addition of the ECAP tablet to the pure aluminium melt. Values from these equations show that it is possible the melt temporarily chilled off when the ECAP tablets were added to the pure aluminium melt. Dissolution is also time dependent, The ECAP preform was allowed to remain in the furnace for 15 minutes after addition to the molten super purity aluminium and mechanical stirring. The lack of melting could be an indication that dissolution time was not sufficiently long.

$$Q = mC_p\Delta T$$ Equation 5

$$Q = 0.045 \text{ x } 1000 \text{ x } 70$$

$$Q = 3150J$$

Where:

Q = Energy

m = Mass of melt (kg)

C_p = Specific Heat Capacity of Aluminium

ΔT = Temperature (Kelvin)

$$\Delta T = \frac{Q}{mC_p}$$ Equation 6

$$\Delta T = \frac{3150}{0.005 \text{ x } 1000}$$

$$\Delta T = 630K \sim 60C$$

Where:

ΔT = Temperature change

Q = Energy

m = Mass of ECAP tablet addition

Cp= Specific heat capacity of aluminium

Lack of dispersion could be attributed to the lack of agitation of the melt during holding of the liquid metal. During the casting procedure, the melt was stirred manually and micrographs of the final cast microstructure showed that this was insufficient (figures 14-14.1). This could be improved by implementing a constant mixing of the melt using

a thixocaster, whereby the material is constantly subjected to shear, or by induction stirring.

In addition to the lack of melt agitation, another explanation for the lack of wetting and dispersion of ECAP specimens within the melt could be that the wettability of pure aluminium is too poor to allow carbon nanotube composite material to be melted by the matrix material. This could be improved by use of an alloy composition with a lower surface tension, in order to ensure wetting of all phases by the liquid metal. Material could also be cast at a lower temperature in a semi-solid state to improve dispersion. Use of thixocasting equipment would facilitate this, and would also provide the shearing mechanism to disperse and break up the wetted composite sample throughout the matrix material. The thermal stability of CNTs is another factor to be considered during melt processing. This was not explored in detail within this thesis but is described in section 2.6.4.

As discussed in section 2.6.4, wetting of the carbon nanotube surface will only take place during casting if the contact angel is less than 90^{o}. Using equation 3, surface tension for aluminium at 760^{o}C of 860mN/m (Dujardin et al., 1994)), surface tension of a CNT of 45.3mN/m (Nuriel et al., 2005) it can be calculated that a contact angle of greater than 90^{o} would result and therefore no wetting would occur. If the surface tension of the molten metal were to be reduced, ratio of the difference in substrate tension to liquid surface tension would increase and therefore the contact angel would tend to $<90^{o}$, thus wetting would occur.

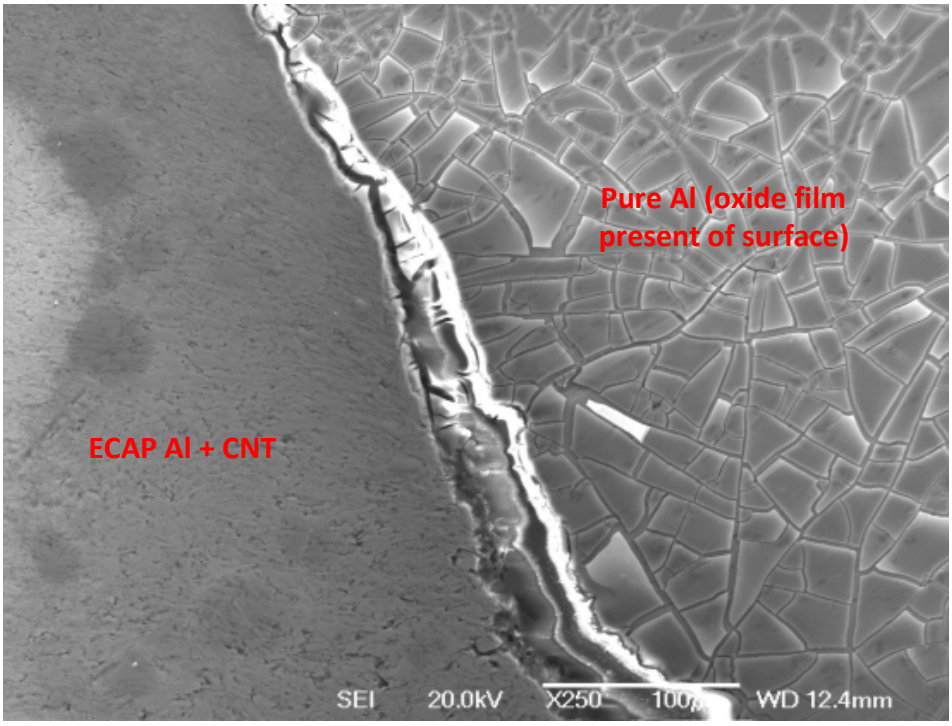

Figure 14: Example micrograph from Al-CNT cast specimen showing incomplete melting and distribution

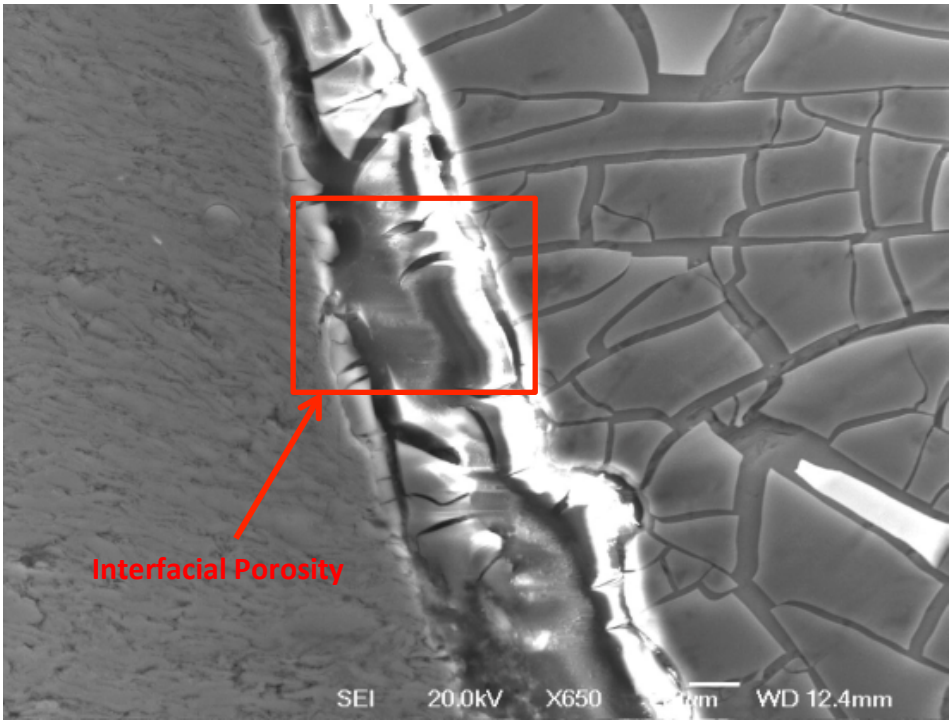

Figure 14.1: Example micrograph from Al-CNT cast specimen showing incomplete melting and distribution

4.5.2 Density evaluation of cast Al-0.2wt. % CNT composite specimens prepared by turbula mixing for 8 hours

The final concentration of CNTs within cast specimens was 0.2wt. %. This was a 10% reduction compared to other specimens, due to the increased mass of pure aluminium matrix material. For this reason the initial theoretical density calculation was no longer valid and a new maximum density for the castings of 2.698gcm^{-3} was calculated using the rule of mixtures.

Table 12 shows that density values obtained from all cast specimens produced similar density values. Castings containing ECAP specimens prepared by turbula mixing for 8 hours produced lower average densities than the equivalent sintered and ECAP samples. High grade carbon nanotubes produced the highest density values amongst turbula mixed castings.

Casting	Density (gcm^{-3})
Al-0.2wt.% IGMWNTs (TM 8H)	2.51
Al-0.2wt.% High Grade (TM 8H)	2.59

Table 13: Density measurements taken from Al-0.2wt. % CNT castings prepared using samples turbula mixed for 8 hours

4.5.3 Hardness evaluation of cast Al-0.2wt. % CNT composite specimens prepared by turbula mixing for 8 hours

Hardness results obtained from turbula mixed cast specimens (figures 14.2-14.3) showed that, as expected from super purity aluminium, the matrix material showed low hardness values, of the order 14-25Hv. However, it was also observed that regions of material within the casting showed high hardness, consistent with the SEM analysis which showed parts of the ECAP aluminium-carbon nanotube specimens which had not been dispersed within the casting. Hardness results also showed that regions of hard ECAP material were only present within the top layer of the castings, suggesting flotation of ECAP specimens had taken place within the molten matrix material despite stirring during the casting process. This was a likely result due to the low density of the samples.

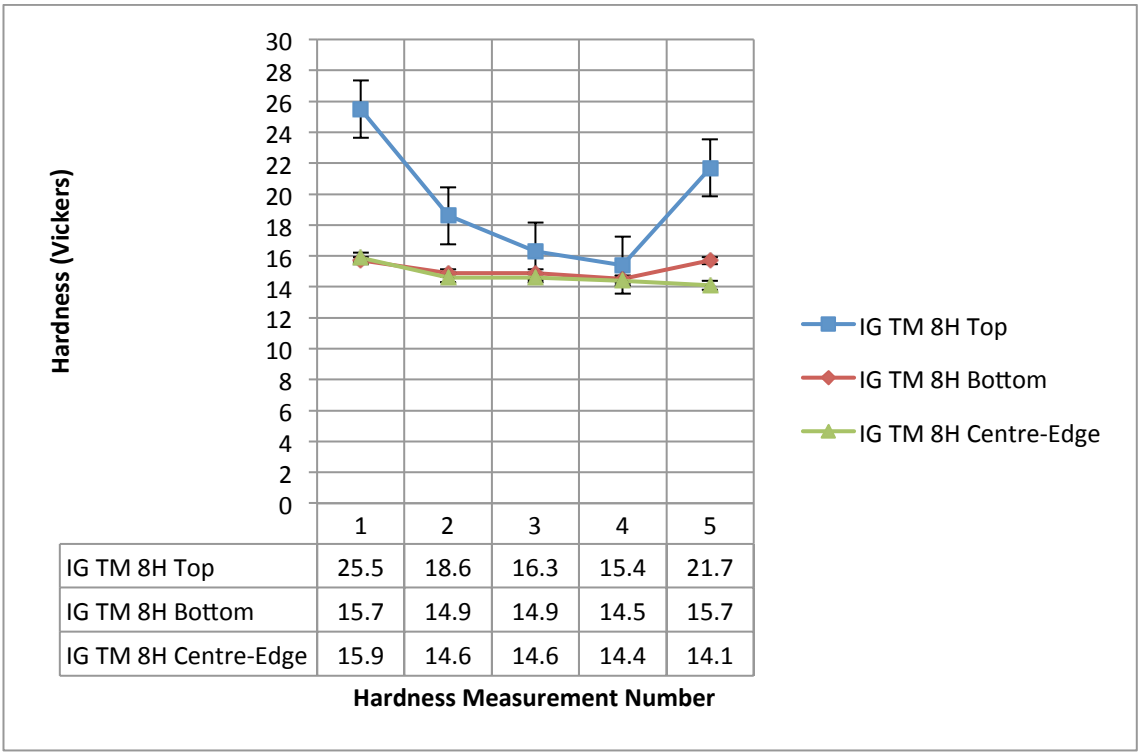

	1	2	3	4	5
IG TM 8H Top	25.5	18.6	16.3	15.4	21.7
IG TM 8H Bottom	15.7	14.9	14.9	14.5	15.7
IG TM 8H Centre-Edge	15.9	14.6	14.6	14.4	14.1

Figure 14.2: Graph showing hardness measurements obtained from Al-0.2wt. % CNT composite castings prepared by using specimens turbula mixed for 8 hours and using industrial grade carbon nanotubes

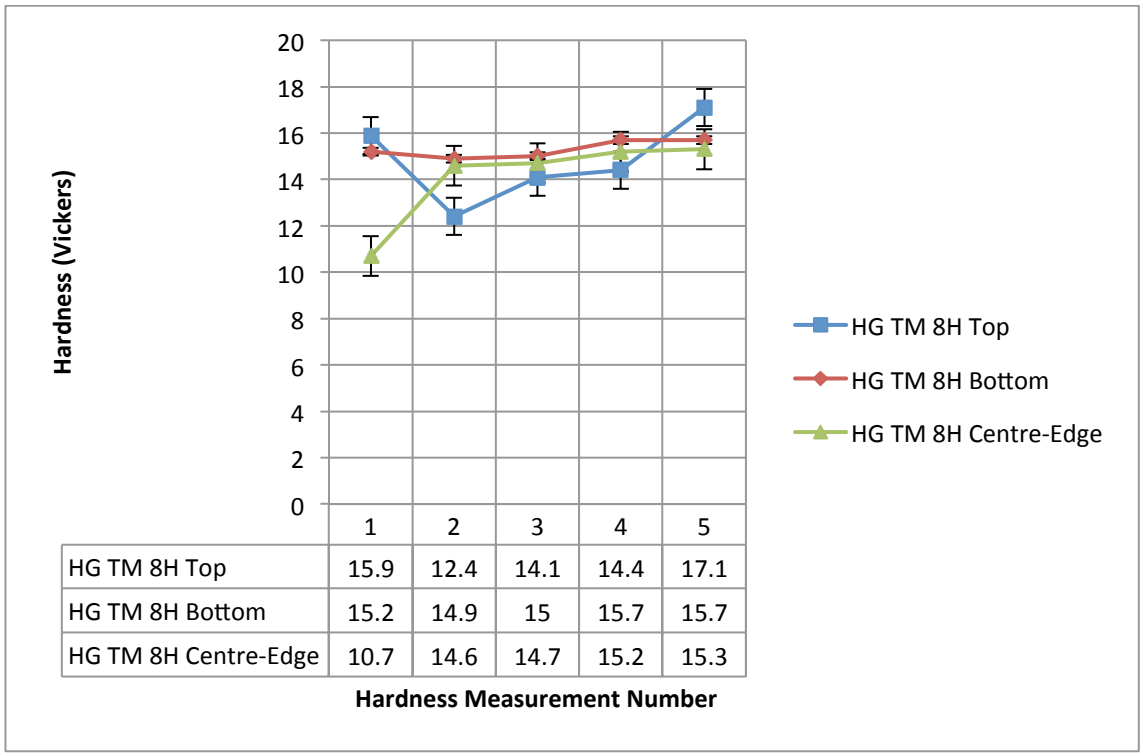

	1	2	3	4	5
HG TM 8H Top	15.9	12.4	14.1	14.4	17.1
HG TM 8H Bottom	15.2	14.9	15	15.7	15.7
HG TM 8H Centre-Edge	10.7	14.6	14.7	15.2	15.3

Figure 14.3: Graph showing hardness measurements obtained from Al-0.2wt. % CNT composite castings prepared by using specimens turbula mixed for 8 hours and using high grade carbon nanotubes

4.5.4 Density evaluation of cast Al-0.2wt. % CNT composite specimens prepared by ball milling for 1 hour

Results from cast specimens using samples prepared by ball milling for 1 hour are shown in table 13. Lower average densities were seen in castings containing samples ball milled for 1 hour compared to castings containing samples prepared by turbula mixing for 8 hours. There was seen to be a negligible difference in the density values produced by samples using industrial grade and high grade carbon nanotubes.

Casting	Density (gcm^{-3})
Al-0.2wt.% IGMWNTs (BM 1H)	2.44
Al-0.2wt.% High Grade (BM 1H)	2.43

Table 14: Density measurements taken from Al-0.2wt. % CNT castings prepared using samples ball milled for 1 hour

4.5.5 Hardness evaluation of cast Al-0.2wt. % CNT composite specimens prepared by ball milling for 1 hour

Hardness results are shown in figures 14.4 and 14.5. Results were similar to those seen in castings using turbula mixed specimens, with hard regions of material noted in the top surface of castings indicating poor and uneven dispersion of the reinforcement phase.

Base and centre regions of the castings showed no signs of hard material regions. The hardness in these regions are consistent with super purity aluminium matrix hardness values measured in castings using turbula mixed specimens, as shown in section 5.5.3.

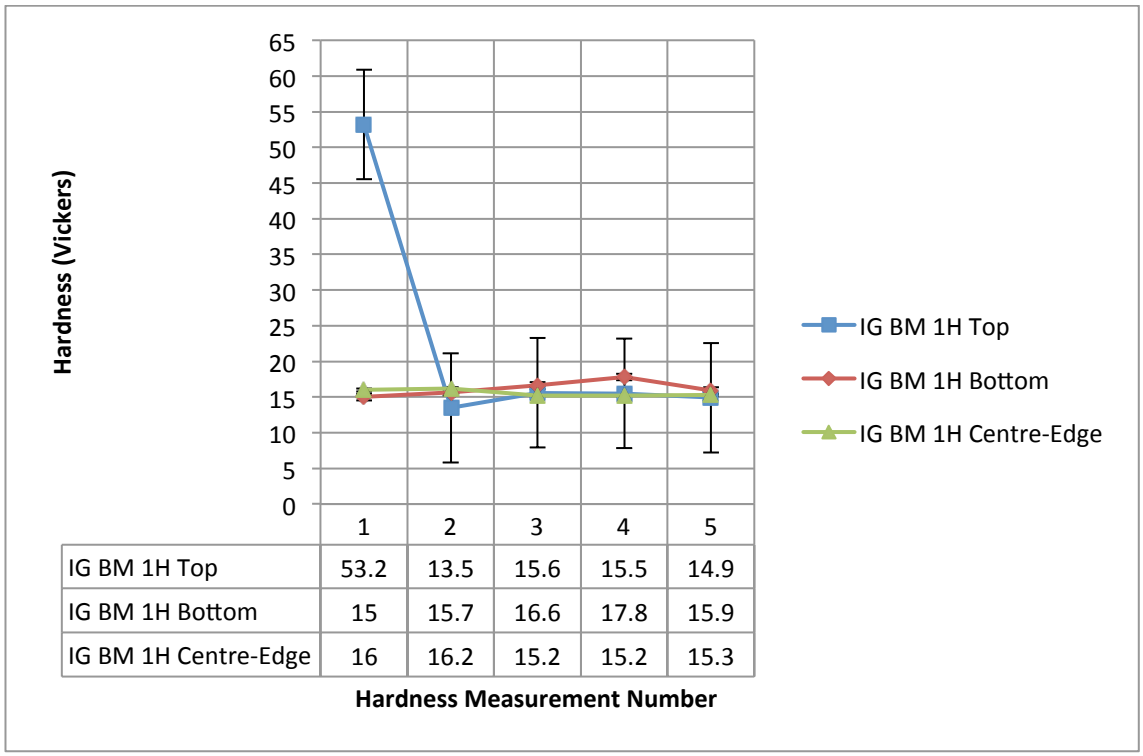

IG BM 1H Top	53.2	13.5	15.6	15.5	14.9
IG BM 1H Bottom	15	15.7	16.6	17.8	15.9
IG BM 1H Centre-Edge	16	16.2	15.2	15.2	15.3

Figure 14.4: Graph showing hardness measurements obtained from Al-0.2wt. % CNT castings prepared using specimens ball milled for 1 hour and using industrial grade carbon nanotubes

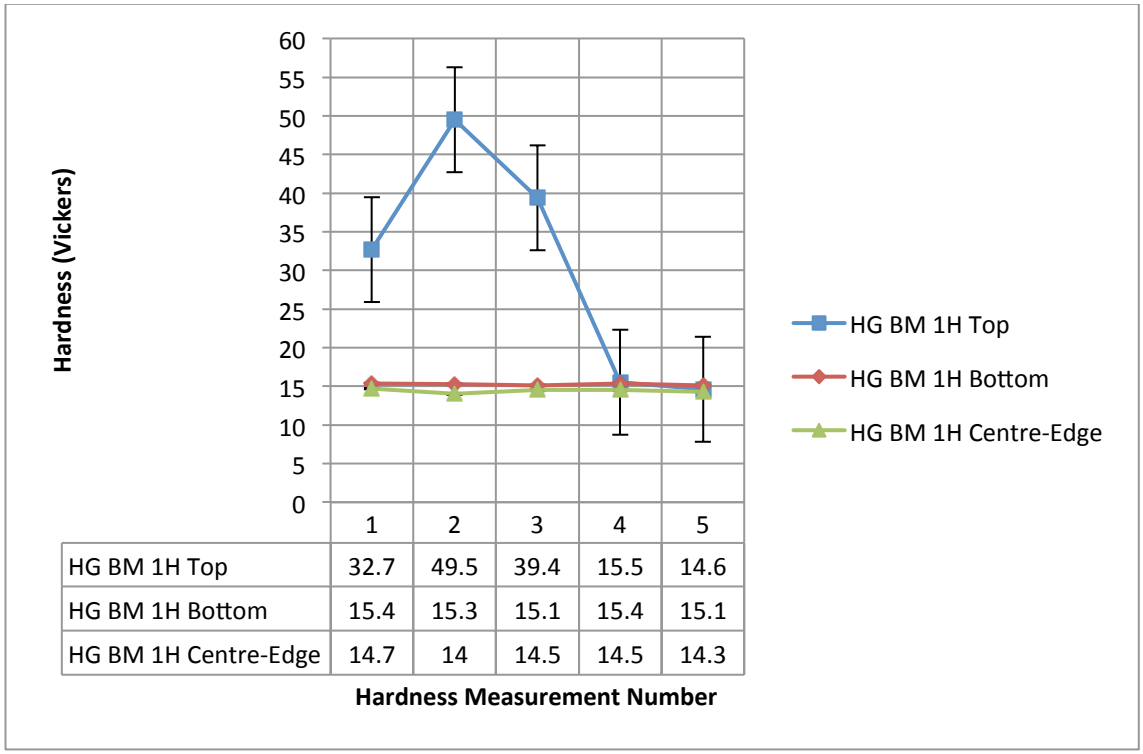

HG BM 1H Top	32.7	49.5	39.4	15.5	14.6
HG BM 1H Bottom	15.4	15.3	15.1	15.4	15.1
HG BM 1H Centre-Edge	14.7	14	14.5	14.5	14.3

Figure 14.5: Graph showing hardness measurements obtained from Al-0.2wt. % CNT castings prepared using specimens ball milled for 1 hour and using high grade carbon nanotubes

4.5.6 Density evaluation of cast Al-0.2wt. % CNT composite specimens prepared by ball milling for 4 hours

Density values for castings prepared from samples using ball milling for 4 hours as a mixing method showed that all specimens produced comparable density values. Density measurements are shown in table 14. Density values produced by castings using specimens prepared by ball milling for 4 hours were seen to be the lowest of all castings measured.

Casting	Density (gcm^{-3})
Al-0.2wt.% IGMWNTs (BM 4H)	2.46
Al-0.2wt.% High Grade (BM 4H)	2.40

Table 15: Density measurements taken from Al-0.2wt. % CNT castings prepared using samples ball milled for 4 hours

4.5.7 Hardness evaluation of cast Al-0.2wt. % CNT composite specimens prepared by ball milling for 4 hours

Hardness data obtained from cast specimens prepared using specimens mixed by ball milling for 4 hours (figures 14.6 and 14.7) showed hard regions of material in the upper regions of the castings, again indicating full dispersion had not taken place.

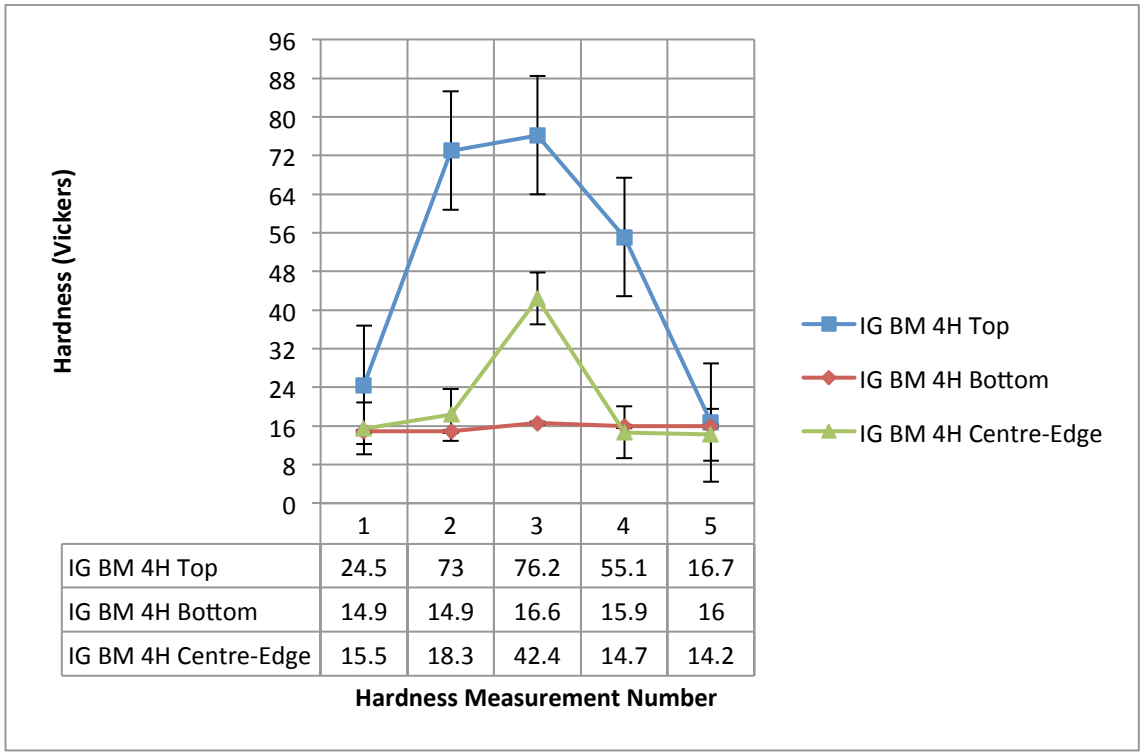

IG BM 4H Top	24.5	73	76.2	55.1	16.7
IG BM 4H Bottom	14.9	14.9	16.6	15.9	16
IG BM 4H Centre-Edge	15.5	18.3	42.4	14.7	14.2

Figure 14.6: Graph showing hardness measurements obtained from Al-0.2wt. % CNT castings prepared by using specimens ball milled for 4 hours and using industrial grade carbon nanotubes

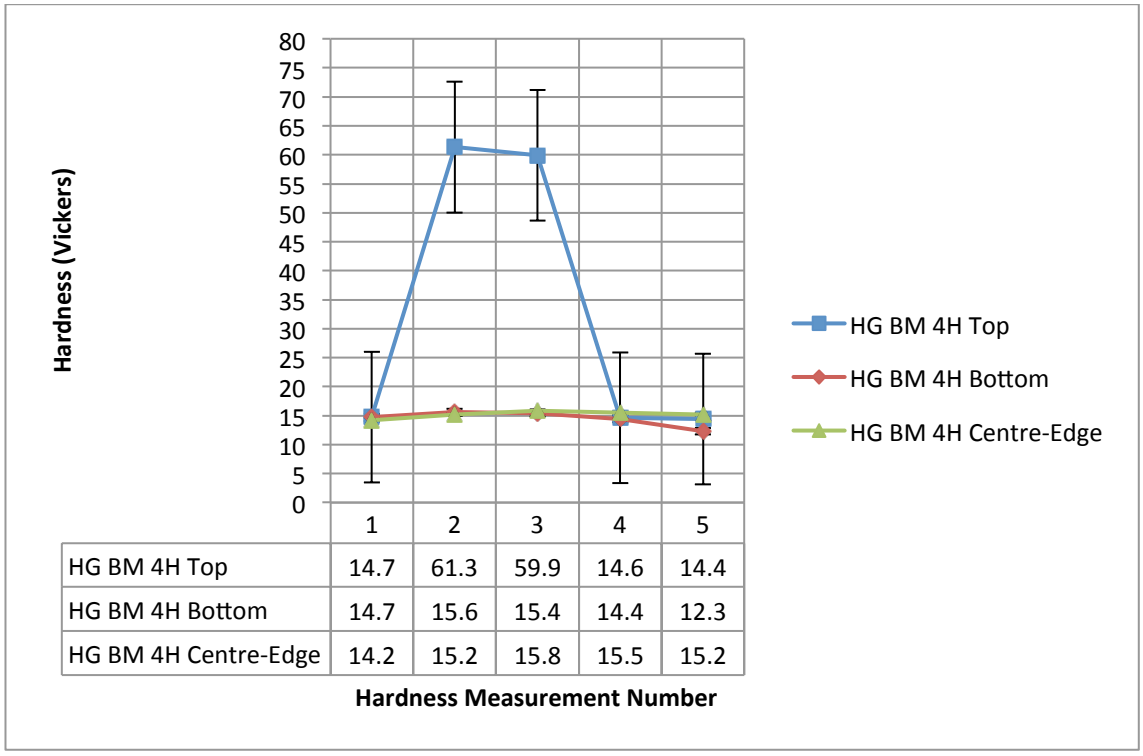

HG BM 4H Top	14.7	61.3	59.9	14.6	14.4
HG BM 4H Bottom	14.7	15.6	15.4	14.4	12.3
HG BM 4H Centre-Edge	14.2	15.2	15.8	15.5	15.2

Figure 14.7: Graph showing hardness measurements obtained from Al-0.2wt. % CNT castings prepared by using specimens ball milled for 4 hours and using high grade carbon nanotubes

4.6 Results Summary

In summary, results showed that in the majority of cases high grade nanotubes were the preferred grade of nanotube to use for aluminium-carbon nanotube reinforced composite specimens. This was attributed to the smaller as-received carbon nanotube agglomerate size, as seen in the CNT micrographs.

Comparisons of mixing methods revealed that ball milling for 4 hours was the optimum mixing method to effectively distribute carbon nanotubes. Results showed that samples prepared by ball milling for 4 hours consistently produced composite samples at all processing stages, with density values closest to the theoretical maximum, as well as highest and least variable though-thickness hardness values. This indicated an effective distribution of the CNT reinforcement.

The ECAP process was investigated to ascertain if it was an effective means of further distributing the CNT reinforcement. The process was shown to have a reproducible effect upon composite samples and improvement in both density and hardness properties relative to green compact specimens.

Sintered specimens were seen to have further improved density and hardness. From the results obtained, sintered and ECAP specimens produced, on average, the best combination of density and hardness from all samples measured.

Finally, cast specimens highlighted numerous issues with liquid metal processing of carbon nanotube composite specimens. Cast samples were shown to contain partially melted ECAP tablet specimens within the pure aluminium structure. Porosity was seen at the interface between the two structures indicating poor wetting during holding in the liquid metal. In addition it was noted that hard regions of material were only seen in the upper regions of the castings.

These results suggested an ineffective distribution and melting of ECAP tablet specimens and therefore ineffective distribution of the carbon nanotube reinforcement. This could be improved by firstly ensuring constant melt agitation to encourage break-up and distribution of ECAP tablets and prevent flotation of tablets to upper regions of castings. In addition, an alloy composition with lower surface tension could also be used in order to facilitate wetting during casting and eliminate segregation of structures.

Chapter 5

Discussion

From the results obtained it was found that high-grade carbon nanotubes were more often than not the optimum choice for preparation of aluminium-carbon nanotube reinforced composite specimens. In almost all cases specimens prepared using high grade carbon nanotubes produced the best density and hardness values when compared to specimens prepared using industrial grade or NC-7000 carbon nanotubes.

This was attributed to the greater ease of distribution of the smaller as-received carbon nanotube/catalytic particle agglomerate size, as seen in the high grade carbon nanotube micrographs. Figures 8 and 8.1 show industrial grade and NC-7000 carbon nanotube agglomerates of approximately 30-50μm in size. Figure 8.2 shows high grade carbon nanotube agglomerates with an approximate size of 10 μm. Individual entangled CNTs are shown in figures 8.3-8.5. The catalytic particle centres are not visible from the micrographs taken but are presumed to be at the centres of the entangled CNTs.
Due to the higher purity of high-grade nanotubes, catalytic particle agglomerates resulting from the production process are smaller in size, as can be seen from figures 8-8.2.

Therefore smaller agglomerate particle size resulted in easier distribution of CNTs within the aluminium matrix and ultimately better density and hardness properties of the resultant composite specimens. (Morcom et al., 2010) investigated the effect of different

CNT properties on the degree of dispersion. Results from this study showed that larger diameter CNTs produced large tightly packed entangled agglomerates; this made ingress of matrix material into the CNT clusters more difficult.

5.1 Preparation Techniques

Analysis of the morphologies of the aluminium-2wt. % carbon nanotube master alloy powders showed differences with different preparation and mixing methods. Turbula mixed powders were shown to produce smooth particle morphologies with rounded edges and no visible damage or fracturing of the aluminium particles (figure 9). This was attributed to the gentle nature of the turbula mixing process, given that it was only conducted at 49 rpm. Particle size analysis of these powders produced peak particle sizes around a modal value of 7-8μm. A reduction of 2μm from the diameter of the initial aluminium powder was noted. This small reduction in size was further evidence of the gentle mixing process with minimal material loss from the powder particles. The reduction was attributed to the small material loss caused by the smoothing of powder particle edges.

Master alloy powders prepared by ball milling showed notable differences compared to turbula mixed powders. Firstly, ball milled powder particles were seen to have more angular morphologies, which was more pronounced in samples ball-milled for longer times (4 hours), as shown in figures 10 and 11. The more aggressive nature of the ball milling mixing process led to more severe fracturing of particles compared to turbula mixing. In addition it was found that powders prepared by a ball milling mixing process

produced modal particle sizes of 5-7μm (at 1 hour) and 3-6μm (at 4 hours) which were smaller than those observed in powders prepared by turbula mixing. The higher speed of the ball milling process and the greater number of ball bearings were the reason for this, causing more severe fracture of particles and loss of material. Greater ball bearing numbers produced a higher ball to powder weight ratio (5:1) for ball milling than for turbula mixing. This caused a greater number of ball bearing-powder particle impacts per unit time, with greater kinetic energy, due to the increased rotation speed of the ball miller chambers.

After comparison of the investigated powder preparation methods, it was concluded that ball milling for 4 hours was the most effective mixing method for distributing carbon nanotubes. The more aggressive nature of the ball milling process and the longer milling time was concluded to have provided sufficient means to break up CNT agglomerates and distribute CNTs within the matrix. These samples consistently produced harder samples when compared to other mixing methods. Powder compact specimens produced by ball milling for 4 hours showed negligible difference in density to those produced by turbula mixed and 1 hour ball milled specimens. Specimens ball milled for 4 hours showed improvements in hardness of 18Hv (87%) and 6Hv (17%) compared to turbula mixed and 1 hour ball milled samples respectively. Sintered specimens prepared by ball milling for 4 hours showed similar densities to sintered specimens prepared by turbula mixing for 8 hours and ball milling for 1 hour respectively (figures 12.4, 12.6 and 12.8). Hardness however was seen to improve by 15Hv (39%) and 18Hv (53%) relative to turbula mixing and ball milling for 1 hour respectively. Results from ECAPed and cast specimens ball milled for 4 hours were

more variable; ECAPed specimens produced by ball milling for 4 hours showed negligible differences in density compared to the values produced by turbula mixing and ball milling for 1 hour, this is shown in figures 13.3, 13.7 and 13.11. In terms of hardness, ECAPed, 4 hour ball milled specimens produced a small improvement of 4Hv (8%) relative to specimens prepared by turbula mixing for 8 hours. Hardness results compared to 1 hour ball milled ECAP samples were similar. Castings prepared from specimens ball milled for 4 hours produced slightly lower densities than turbula mixed castings with a reduction of $0.1gcm^{-3}$ (5%). 1 hour ball milled castings produced the same hardness as 4 hour ball milled castings. The hardness of 4 hour ball milled castings was superior to other specimens, showing improvements of 9Hv (58%) over turbula mixed castings and 6Hv (29%) compared to 1 hour ball milled castings.

Densification was seen as an indication that a more homogenous distribution of carbon nanotubes had been achieved, which minimised the amount of porosity formed around carbon-nanotube/catalytic particle agglomerates. CNT agglomerates have high stiffness due to the high modulus of the CNTs themselves, (approximately 1TPa (Agarwal et al., 2011)), and the high hardness of the catalytic constituents such as iron or nickel. Larger agglomerates can therefore cause the formation of porosity during sample pressing, no deformation of these agglomerates will occur during pressing and as a result aluminium powder deforms around larger particles rather than infiltrating into catalytic/CNT clusters, causing voids in the final microstructure. Higher purity carbon nanotubes with smaller catalytic particle agglomerates will be easier to infiltrate and distribute within the microstructure, and result in smaller voids and a more dense final structure. Of the preparation techniques investigated, ball milling powders for 4 hours appeared to be, on

average, the most effective mixing method for breaking up agglomerates. This was concluded due to the generally improved density and hardness properties of specimens prepared by ball milling for 4 hours compared to other mixing methods. A future investigation into ball milling times longer than 4 hours would be useful to determine the optimum density of composite specimens that can be achieved. Higher hardness of composite specimens prepared by ball milling for 4 hours was attributed to both the increased amount of work hardening of the aluminium powder imparted during processing compared to turbula mixing, and to a more homogeneous distribution of carbon nanotube reinforcement within the composite structure. A homogenous microstructure means an even distribution of carbon nanotubes. An inhomogeneous microstructure would be manifested in variable through thickness hardness, i.e. regions of hard material (where there were many CNT agglomerates) surrounded by softer material (the pure aluminium matrix), due to the large difference between the hardness of the CNT agglomerates and the aluminium matrix. A homogeneous microstructure would produce a consistent through thickness hardness and thus indicate an even distribution of the CNT reinforcement phase. The higher impact frequency and greater kinetic energy of impacts between ball bearings and aluminium powder particles caused the aluminium powder particles to work harden to a greater extent than in other preparation methods, and caused a higher base hardness of the composite specimens. Further investigation into the consequences of this work hardening and the extent of the damage caused to carbon nanotubes during processing is needed. Results obtained agree with other studies such as (Esawi et al., 2007) and (Morsi et al., 2007), both of which reported that longer milling times produced samples with superior density and mechanical properties.

5.2 Equal Channel Angular Pressing (ECAP)

The Equal Channel Angular Pressing (ECAP) process, at room temperature, showed promising results for consolidation of aluminium-carbon nanotube specimens. The strain introduced into the composite specimens during processing (around 2%) was found to be sufficient to improve both density and hardness properties when compared to cold compacted composite specimens of the same composition. This is shown in figures 13.3-13.9 and table 9. The average increase in hardness for specimens using industrial grade CNTs was 35Hv, for specimens using NC-7000 CNTs the average increase was 39Hv, and the average improvement was 11Hv for high grade CNT composite specimens. This indicated that the distribution of CNTs was superior within original powder compact specimens using high grade CNTS prior to ECAPing. Results also suggested that ECAP was effective in removing CNT agglomerates, with greatest improvement in hardness seen within specimens using low purity CNTs. The ECAP process was concluded to have a more significant effect on lower purity CNT samples due to the greater agglomeration in low-purity CNT cold compacted specimens.

Results in sections 4.4.2-4.4.7 and specifically tables 11 & 12 showed that the process had a reproducible effect upon all composite samples and was seemingly unaffected by changes in nanotube type or master alloy mixing method i.e., ball milling or turbula mixing. The results collected from analysis of ECAP specimens concur with studies by Derakhshandeh et al., (2011), Kollo et al., (2012) and Quang et al., (2007), all of whom found the ECAP process produced an improvement in density and hardness of varying types of aluminium composite specimens at both elevated temperatures: 200^{o}C for

Derakhshandeh et al., (2011) and room temperature Quang et al., (2007). ECAP results obtained in this report were from room temperature pressing, agreeing with the results of Quang et al., (2007) that the ECAP process can improve the properties of composite specimens without the need for elevated temperature.

The work of Quang et al., (2007) also suggested that the properties of ECAP specimens could be improved with multiple passes through an ECAP die. Results collected in this report only focused on samples pressed with one pass due to limitations on die sample sizes, multiple passes could be investigated in future work.

5.3 Sintering

After sintering, the hardness and density properties of composite specimens were seen to further improve relative to ECAP and cold compacted specimens. Sintered specimens produced, on average, the best combination of density and hardness from all samples measured in this report. Densification of composite specimens during the sintering process was identified as the cause of this improvement and 'necking' between aluminium particles was visible upon microscopic analysis (figures 12-12.3).

Despite the fact that sintering was conducted under an inert argon atmosphere, it was unclear if any carbide formation occurred during sintering, and if so what amount was formed. This could be investigated in future work using X-Ray Diffraction (XRD) to tailor sintering parameters in order to achieve optimum properties.

5.4 Casting

A number of issues with liquid metal processing of carbon nanotube composite specimens were identified within the cast composite specimens. Partially melted ECAP tablet specimens were visible within the pure aluminium matrix upon microscopic examination of the castings. This suggested that the melt may have temporarily chilled off upon addition of the ECAP tablets. Energy transfer calculations in section 4.5.1 showed that this could have occurred. Results also suggested that insufficient melt agitation was applied to effectively disperse the tablets.

Porosity was also identified at the interface between partially melted ECAP specimens and aluminium matrix materials (figures 14 & 14.1), an indication of poor wetting during casting as a result of either the presence of oxide film or temporary melt chilling. During insertion of the ECAP tablets into the aluminium melt, an oxide film may have been incorporated onto the surface of the ECAP tablets, with non-wetting characteristics and therefore delayed or prevented ECAP tablets from being wetted and incorporated into the melt (Campbell., 1991). Upon hardness testing, it was noted that hard regions of material were present only within the upper regions of the casting, indicating that ECAP tablets had floated within the melt. Given that ECAP tablets achieved lower densities than pure aluminium, this was a possible outcome. Ineffective and inhomogeneous distribution of ECAP tablets had occurred within the bulk casting and resulted in inhomogeneous properties of the final casting.

Results obtained in this report were in agreement with work done by (Dujardin et al., 1994), which predicted that aluminium in its pure state would not wet and adhere to the surface of carbon nanotubes. The results also agreed with the work of (Uozumi et al., 2007) who calculated, using the sessile drop method, that molten aluminium would not wet the surface of a graphite substrate.

It was indicated that insufficient work was imparted into the castings in order to distribute carbon nanotubes effectively. These findings agreed with the work of (Uozumi et al., 2008) which calculated that work must be done during casting in order to induce wetting of carbon nanotubes by aluminium. The study devised a formula to calculate the threshold pressure required in order to induce infiltration using the fibre volume fraction, fibre diameter, surface tension of the matrix alloy and the contact angle. These studies however did not investigate the effect of oxide entrainment on the wetting characteristics of CNTs.

The results obtained from castings in this report could potentially be improved by implementing a number of changes to the casting process, as follows.

Removal of the oxide film layer could help to induce wetting and dissolution of the ECAP tablets into the melt. One way in which this could be done is by adding the ECAP specimen tablets into the molten aluminium through a liquid salt flux on the surface of the melt. Casting at a higher temperature, or holding for a longer time could also aid with melting of the ECAP tablets and dispersing the CNTs within the bulk metal, however it is unknown what effect this may have on the carbon nanotube

reinforcement in terms of chemical reactions and thermal degradation and this would need to be investigated further. Alloying additions to lower the surface tension such as caesium, rubidium or selenium, could also be used to improve the wetting characteristics between the aluminium matrix and the CNT reinforcement phase.

A more practical solution may be to ensure continuous melt shearing/agitation to facilitate distribution of the ECAP tablets within the matrix using, for instance, equipment such as the melt conditioner developed by (Fan et al., 2009) and (Fan et al., 2010).

Alternatively, the surface of the carbon nanotubes could be modified to improve wetting characteristics by, for example, applying a coating to the surface of the carbon nanotubes by a deposition process, in order to produce a more compatible surface for interaction. This approach was taken by (Abbasipour et al., 2010) who applied a Ni-P coating to CNT surfaces via electroless plating before casting in A356. This was shown to induce wetting between the carbon nanotubes and the matrix material. Composite samples produced using this method achieved hardness values of up to 70 Brinell hardness (HB). However results also showed a reduction in density between monolithic A356 samples and A365-CNT specimens. This was attributed to both the presence of the lower density CNTs and the possibly higher porosity the of composite specimens.

5.5 Summary

The results from this investigation showed that ball milling for 4 hours produced samples with the best combination of density and hardness compared with other preparation methods. The ECAP process was conducted at room temperature and showed promising results. It consistently improved the properties of cold compacted composite specimens in both the longitudinal and transverse directions. Further work to investigate the capabilities of the ECAP process for producing MMCs is needed. Sintering produced the best combination of properties compared with other processing routes. Casting was attempted and presented numerous challenges, principally due to oxide film entrainment and poor wettability.

5.6 Further Work

Further work is needed to investigated the following:

1. The effect of longer milling times on powder morphology, particle size and compaction properties.
2. Multiple ECAP passes to determine effect of repeat pressing on CNT agglomerate removal, density and hardness properties.
3. The effect of sintering on stability of CNTs, XRD could potentially used to quantify degree of reaction between CNTs and matrix material.
4. The effect of casting parameters on preform dissolution and final composite properties. Higher casting temperature, longer dissolution times could be investigated to determine optimum parameter whilst preserving CNT integrity.
5. Melt agitation techniques could be investigated further to attempt to achieve full dissolution and uniform dispersion of CNTs within the matrix material.
6. Functionalisation of CNT surfaces could be investigated as a means to improve wettability during melt processing. For example nickel plating could be used to further induce wetting of CNTs by matrix material.

Chapter 6

Conclusions

1. High grade carbon nanotubes produced the most dense and hard samples when compared to industrial grade and NC-7000 carbon nanotubes.
2. When powder preparation methods were compared it was concluded that preparation using ball milling for 4 hours was the preferred method in order to effectively distribute carbon nanotubes. Specimens prepared by ball milling for 4 hours consistently produced density values closest to the theoretical maximum density, in addition to the highest and most consistent hardness values.
3. Equal Channel Angular Pressing (ECAP) was concluded to have consistently improved both density and hardness of aluminium-carbon nanotube composite specimens when compared to equivalent cold compacted specimens.
4. Sintered specimens produced, on average, the best combination of density and hardness properties of all samples investigated.
5. Casting ECAPed pure aluminium-carbon nanotube specimens with minimal agitation was concluded to be ineffective; specimens displayed incomplete melting of ECAP specimens within the pure aluminium matrix, as well as lack of wetting between the matrix aluminium and the ECAP specimens. This indicated that pure aluminium did not wet any of the carbon nanotube surfaces.

Chapter 7

Bibliography

- IIJIMA, S. 1991. Helical microtubules of graphite carbon, Nature, 354: 56-58
- ABBASIPOUR, B., NIROUMAND, B., MONIRVAGHEFI, S. M. and TMS 2012. Mechanical properties of A356-CNT cast nano composite produced by a special compocasting route.
- ABBASIPOUR, B., NIROUMAND, B. & VAGHEFI, S. M. M. 2010. Compocasting of A356-CNT composite. Transactions of Nonferrous Metals Society of China, 20.
- AGARWAL, A., BAKSHI, S.R. & LAHIRI, D. 2011. Nanomaterials and Their Application, Carbon Nanotubes: Reinforced Metal Matrix Composites. CRC Press, 7.
- BACON, R. 1960. Growth, Structure, and properties of graphite whiskers. Journal of Applied Physics, 31, 283-290.
- BAKSHI, S. R., SINGH, V., SEAL, S. & AGARWAL, A. 2009. Aluminum composite reinforced with multiwalled carbon nanotubes from plasma spraying of spray dried powders. Surface & Coatings Technology, 203, 1544-1554.
- BETHUNE, D. S., KIANG, C. H., DEVRIES, M. S., GORMAN, G., SAVOY, R., VAZQUEZ, J. & BEYERS, R. 1993. Cobalt-catalyzed growth of carbon nanotubes with single-atomic layer walls. Nature, 363, 605-607.
- CAMPBELL, J. 1991. New metallurgy of cast metals: Castings. Second Edition. 2nd Edition. Oxford. Elsevier Butterworth-Heinemann.

- CHA, S. I., KIM, K. T., ARSHAD, S. N., MO, C. B. & HONG, S. H. 2005. Extraordinary strengthening effect of carbon nanotubes in metal-matrix nanocomposites processed by molecular-level mixing. Advanced Materials, 17, 1377-+.
- SEE, C. H., HARRIS, A. T. 2007. A review of carbon nanotube synthesis via fluidized-bed chemical vapour deposition. Industrial & Chemistry Research, 46, 997-1012.
- CHOI, H., SHIN, J., MIN, B., PARK, J. & BAE, D. 2009a. Reinforcing effects of carbon nanotubes in structural aluminum matrix nanocomposites. Journal of Materials Research, 24, 2610-2616.
- CHOI, H., SHIN, J., MIN, B., PARK, J. & BAE, D. 2009b. Reinforcing effects of carbon nanotubes in structural aluminum matrix nanocomposites. Journal of Materials Research, 24, 2610-2616.
- CHOI, H. J., KWON, G. B., LEE, G. Y. & BAE, D. H. 2008. Reinforcement with carbon nanotubes in aluminum matrix composites. Scripta Materialia, 59, 360-363.
- COLEMAN, J. N., CADEK, M., BLAKE, R., NICOLOSI, V., RYAN, K. P., BELTON, C., FONSECA, A., NAGY, J. B., GUN'KO, Y. K. & BLAU, W. J. 2004. High-performance nanotube-reinforced plastics: Understanding the mechanism of strength increase. Advanced Functional Materials, 14, 791-798.
- COLEMAN, J. N., KHAN, U., BLAU, W. J. & GUN'KO, Y. K. 2006. Small but strong: A review of the mechanical properties of carbon nanotube-polymer composites. Carbon, 44, 1624-1652.

- DERAKHSHANDEH, R. & JAHROMI, A. J. 2011. An investigation on the capability of equal channel angular pressing for consolidation of aluminum and aluminum composite powder. Materials & Design, 32, 3377-3388.
- DUJARDIN, E., EBBESEN, T. W., HIURA, H. & TANIGAKI, K. 1994. Capillarity and wetting of carbon nanotubes. Science, 265, 1850-1852.
- ESAWI, A. & MORSI, K. 2007. Dispersion of carbon nanotubes (CNTs) in aluminum powder. Composites Part a-Applied Science and Manufacturing, 38, 646-650.
- FAN, Z., WANG, Y., ZHANG, Z. F., XIA, M., LI, H. T., XU, J., GRANASY, L. & SCAMANS, G. M. 2009. Shear enhanced heterogeneous nucleation in some Mg- and Al-alloys. International Journal of Cast Metals Research, 22, 318-322.
- FAN, Z., XIA, M., BIAN, Z., BAYANDORIAN, I., CAO, L., LI, H. & SCAMANS, G. M. 2010. Refinement of Solidification Microstructures by the MCAST Process. In: ROOSZ, A. M. V. B. P. H. C. (ed.) Solidification and Gravity V
- GEORGE, R., KASHYAP, K. T., RAW, R. & YAMDAGNI, S. 2005. Strengthening in carbon nanotube/aluminium (CNT/Al) composites. Scripta Materialia, 53, 1159-1163.
- GOUSSOUS, S., XU, W., WU, X. & XIA, K. 2009. Al-C nanocomposites consolidated by back pressure equal channel angular pressing. Composites Science and Technology, 69, 1997-2001.
- HE, C. N., ZHAO, N. Q., SHI, C. S., DU, X. W., LI, J. J., LI, H. P. & CUI, Q. R. 2007. An approach to obtaining homogeneously dispersed carbon nanotubes

in Al powders for preparing reinforced Al-matrix composites. Advanced Materials, 19, 1128-1132.

- IIJIMA, S. & ICHIHASHI, T. 1993a. Single-shell carbon nanotubes of 1-nm diameter. Nature, 363, 603-605.
- IIJIMA, S. & ICHIHASHI, T. 1993b. Single-shell carbon nanotubes of 1-nm diameter. Nature, 364, 737-737.
- KIM, K. T., IL CHA, S., HONG, S. H. & HONG, S. H. 2006. Microstructures and tensile behaviour of carbon nanotube reinforced Cu matrix nanocomposites. Materials Science and Engineering a-Structural Materials Properties Microstructure and Processing, 430, 27-33.
- KOLLO, L., KALLIP, K., GOMON, J. K. & KOMMEL, L. 2012. Hot Consolidation of Aluminium and Aluminium nano-MMC Powders by Equal Channel Angular Pressing. Materials Science-Medziagotyra, 18, 234-237.
- KRISHNAN, A., DUJARDIN, E., EBBESEN, T. W., YIANILOS, P. N. & TREACY, M. M. J. 1998. Young's modulus of single-walled nanotubes. Physical Review B, 58, 14013-14019.
- KUZUMAKI, T., MIYAZAWA, K., ICHINOSE, H. & ITO, K. 1998. Processing of carbon nanotube reinforced aluminum composite. Journal of Materials Research, 13, 2445-2449.

LAHA, T., CHEN, Y., LAHIRI, D. & AGARWAL, A. 2009. Tensile properties of carbon nanotube reinforced aluminum nanocomposite fabricated by plasma spray forming. Composites Part a-Applied Science and Manufacturing, 40, 589-594.

- LAHIRI, D., BAKSHI, S. R., KESHRI, A. K., LIU, Y. & AGARWAL, A. 2009. Dual strengthening mechanisms induced by carbon nanotubes in roll bonded aluminum composites. Materials Science and Engineering a-Structural Materials Properties Microstructure and Processing, 523, 263-270.
- LI, H., MISRA, A., ZHU, Y., HORITA, Z., KOCH, C. C. & HOLESINGER, T. G. 2009a. Processing and characterization of nanostructured Cu-carbon nanotube composites. Materials Science and Engineering a-Structural Materials Properties Microstructure and Processing, 523, 60-64.
- LI, Q., VIERECKL, A., ROTTMAIR, C. A. & SINGER, R. F. 2009b. Improved processing of carbon nanotube/magnesium alloy composites. Composites Science and Technology, 69, 1193-1199.
- LIM, D. K., SHIBAYANAGI, T. & GERLICH, A. P. 2009. Synthesis of multi-walled CNT reinforced aluminium alloy composite via friction stir processing. Materials Science and Engineering a-Structural Materials Properties Microstructure and Processing, 507, 194-199.
- LIU, Z. Y., XIAO, B. L., WANG, W. G. & MA, Z. Y. 2012. Singly dispersed carbon nanotube/aluminum composites fabricated by powder metallurgy combined with friction stir processing. Carbon, 50, 1843-1852.
- LOURIE, O. & WAGNER, H. D. 1998. Evaluation of Young's modulus of carbon nanotubes by micro-Raman spectroscopy. Journal of Materials Research, 13, 2418-2422.
- MORCOM, M., ATKINSON, K. & SIMON, G. P. 2010. The effect of carbon nanotube properties on the degree of dispersion and reinforcement of high density polyethylene. Polymer, 51, 3540-3550.

- MORSI, K. & ESAWI, A. 2007. Effect of mechanical alloying time and carbon nanotube (CNT) content on the evolution of aluminum (Al)-CNT composite powders. Journal of Materials Science, 42, 4954-4959.
- NURIEL, S., LIU, L., BARBER, A, H. & WAGNER, H, D. 2005. Direct measurement of multiwall nanotube surface tension. Chemical Physics Letters, 404, 263-266.
- PONCHARAL, P., WANG, Z. L., UGARTE, D. & DE HEER, W. A. 1999. Electrostatic deflections and electromechanical resonances of carbon nanotubes. Science, 283, 1513-1516.
- QUANG, P., JEONG, Y. G., YOON, S. C., HONG, S. H. & KIM, H. S. 2007a. Consolidation of 1 vol. % carbon nanotube reinforced metal matrix nanocomposites via equal channel angular pressing. Journal of Materials Processing Technology, 187, 318-320.
- QUANG, P., JEONG, Y. G., YOON, S. C., HONG, S. I., HONG, S. H. & KIM, H. S. 2007b. Carbon nanotube reinforced metal matrix nanocomposites via equal channel angular pressing. Progress in Powder Metallurgy, Pts 1 and 2, 534-536, 245-248.
- RYU, H. J., CHA, S. I. & HONG, S. H. 2003. Generalized shear-lag model for load transfer in SiC/Al metal-matrix composites. Journal of Materials Research, 18, 2851-2858.
- SALVETAT, J. P., BONARD, J. M., THOMSON, N. H., KULIK, A. J., FORRO, L., BENOIT, W. & ZUPPIROLI, L. 1999. Mechanical properties of carbon nanotubes. Applied Physics a-Materials Science & Processing, 69, 255-260.

- SU, H., GAO, W. L., ZHANG, H., LIU, H. B., LU, J. & LU, Z. 2012. Study on preparation of large sized nanoparticle reinforced aluminium matrix composite by solid-liquid mixed casting process. Materials Science and Technology, 28, 178-183.
- SURYANARAYANA, C. 2001. Mechanical alloying and milling. Progress in Materials Science, 46, 1-184.
- TREACY, M. M. J., EBBESEN, T. W. & GIBSON, J. M. 1996. Exceptionally high Young's modulus observed for individual carbon nanotubes. Nature, 381, 678-680.
- UOZUMI, H., KOBAYASHI, K., NAKANISHI, K., MATSUNAGA, T., SHINOZAKI, K., SAKAMOTO, H., TSUKADA, T., MASUDA, C. & YOSHIDA, M. 2008. Fabrication process of carbon nanotube/light metal matrix composites by squeeze casting. Materials Science and Engineering a-Structural Materials Properties Microstructure and Processing, 495, 282-287.
- WONG, E. W., SHEEHAN, P. E. & LIEBER, C. M. 1997. Nanobeam mechanics: Elasticity, strength, and toughness of nanorods and nanotubes. Science, 277, 1971-1975.
- YEH, M. K., TAI, N. H. & LIU, J. H. 2006. Mechanical behaviour of phenolic-based composites reinforced with multi-walled carbon nanotubes. Carbon, 44, 1-9.
- YU, M. F., FILES, B. S., AREPALLI, S. & RUOFF, R. S. 2000a. Tensile loading of ropes of single wall carbon nanotubes and their mechanical properties. Physical Review Letters, 84, 5552-5555.

- YU, M. F., LOURIE, O., DYER, M. J., MOLONI, K., KELLY, T. F. & RUOFF, R. S. 2000b. Strength and breaking mechanism of multiwalled carbon nanotubes under tensile load. Science, 287, 637-640.